DEVELOPMENT AND EVALUATION OF GRAPHENE-BASED ADSORBENTS FOR REMEDIATION OF SOIL CONTAMINANTS

SUPRIYA LATH

School of Agriculture, Food and Wine

The University of Adelaide

This thesis is submitted in fulfilment of the requirements for

the degree of Doctor of Philosophy

September 2018

TABLE OF CONTENTS

TABLE OF CONTENTS III
THESIS ABSTRACT VII
DECLARATION IX
ACKNOWLEDGEMENTS X
LIST OF PUBLICATIONS XI
LIST OF CONFERENCE PRESENTATIONS XII
STRUCTURE OF THE THESIS XIII
CHAPTER 1. Introduction and Literature Review 14
1. Literature Review 15
1.1. Soil contamination and its sources 15
1.2. Fate, bioavailability and toxicity of contaminants 15
1.3. Soil remediation strategies 16
1.4. *In situ* adsorption-based remediation 17
1.5. Graphene's potential as an adsorbent 19
1.6. Application of graphene for soil remediation 20
2. Summary of Research Gaps and Research Framework 21
3. Aims and Objectives 26
4. References 26
CHAPTER 2. Synthesis and Characterisation of Graphene Adsorbents 32
1. Introduction 33
2. Synthesis of Graphene-Based Adsorbents 34
2.1. Synthesis of graphene oxide, GO 34
2.2. Synthesis of iron-oxide-modified reduced-GO composite, FeG 35
3. Sample Preparation for Characterisation of Adsorbents 36
3.1. Electron microscopy techniques 36
3.2. X-Ray diffraction analysis 39
3.3. Fourier transform infrared spectroscopy 40
3.4. Surface zeta potential measurements 41
3.5. Specific surface area measurements 42
4. Summary 44
5. References 45
CHAPTER 3. Mixed-Mode Remediation of Cadmium and Arsenate Ions Using Graphene-Based Materials 46
Abstract 49
1. Introduction 50

2. Materials and Methods 51
2.1. Materials 51
2.2. Synthesis and characterisation of adsorbents 52
2.3. Batch sorption studies 52
2.4. Data analyses 53
3. Results and Discussion 53
3.1. Characterisation of adsorbents 53
3.2. Effect of pH on Cd-sorption by GO and RemB 55
3.3. Effect of pH on As-sorption by FeG and RemB 57
3.4. Sorption as a function of Cd and As concentration 58
3.5. Effect of competing ions 59
3.6. Mixed-mode remediation 61
4. Conclusions 63
5. Acknowledgements 63
6. Conflict of Interest 63
7. References 63
8. Supporting Information 68
CHAPTER 4. Sorptive Remediation of Perfluorooctanoic Acid (PFOA) Using Mixed Mineral and Carbon-Based Materials 82
Abstract 85
1. Introduction 86
2. Materials and Methods 88
2.1. Materials and chemicals 88
2.2. Synthesis and characterisation of adsorbents 88
2.3. Batch sorption studies 88
2.4. Quantitative analyses 89
2.5. Data analyses 90
3. Results and Discussion 90
3.1. Characterisation of prepared graphene-based adsorbents 90
3.2. Batch sorption studies 91
3.3. Desorption experiments 95
3.4. Remediation of a contaminated-site water sample 97
4. Conclusions 98
5. Acknowledgements 99
6. Conflicts of Interest 99
7. References 99

8. Supporting Information 103
CHAPTER 5. Sorption of PFOA onto Different Laboratory Materials: Filter Membranes and Centrifuge Tubes 110
Abstract 113
1. Introduction 114
2. Materials and Methods 115
2.1. Materials 115
2.2. Filter sorption studies 117
2.3. Tube sorption studies 118
2.4. Data and statistical analysis 118
3. Results and Discussion 119
3.1. Filter sorption studies 119
3.1.1. Sorption losses observed on different filter membrane-types 119
3.1.2. Effect of PFOA concentration on PFOA recovery 121
3.2. Tube sorption studies 122
3.2.1. Effect of contact time on recovery of PFOA 122
3.2.2. Effect of solution chemistry on recovery of PFOA 123
3.2.3. Effect of PFOA concentration on recovery of PFOA 125
4. Conclusions and Implications 126
5. Acknowledgements 127
6. References 127
7. Supporting Information 131
CHAPTER 6. Mixed-Mode Mineral, Carbon and Graphene-Based Materials for Simultaneous Remediation of Arsenic, Cadmium, PFOA and PFOS in Soils 133
Abstract 136
1. Introduction 137
2. Materials and Methods 139
2.1. Materials and chemicals 139
2.1.1. Contaminants 139
2.1.2. Other chemicals and materials 139
2.2. Synthesis and characterisation of GO and FeG 140
2.3. Soil 140
2.4. Soil spiking 140
2.5. Soil nitrification tests 141
2.5.1. Experimental setup 141
2.5.2. Nitrate analysis 141

2.5.3. Determination of EC50 values for soil nitrification 141
2.6. Soil remediation trial 142
2.6.1. Experimental setup 142
2.6.2. Assessment of remediation efficacy 142
3. Results and Discussion 143
3.1. Adsorbent properties 143
3.2. Determination of EC50 of As, Cd, PFOA and PFOS towards nitrification 144
3.3. Chemical assessment of remediation efficacy: $CaCl_2$-extractability 144
3.3.1. Arsenic bioaccessibility 147
3.3.2. Cadmium bioaccessibility 148
3.3.3. PFOA and PFOS bioaccessibility 149
3.3.4. Outcomes and implications of bioaccessibility-based assessment 150
3.4. Biological assessment of remediation efficacy: soil nitrification response 151
4. Conclusions 155
5. Acknowledgements 155
6. References 155
7. Supporting Information 160
CHAPTER 7. Summary and Future Research Directions 172
1. Summary of Thesis Outcomes 173
1.1. Synthesis of GBMs and characterisation of adsorbents successfully completed 173
1.2. Successful demonstration of multiple sorption of As and Cd using GBMs 174
1.3. Successful demonstration of sorption of PFOA and other PFASs using GBMs 175
1.4. PFOA sorption-losses observed on laboratory-ware 176
1.5. Successful demonstration of mixed soil remediation of As, PFOA, PFOS 176
2. Future Research Recommendations 178
2.1. Further optimisation of GBMs for improved performance 178
2.2. Identify specific binding mechanisms through molecular techniques 178
2.3. Understand long-term environmental fate of adsorbent-contaminant complexes 179
2.4. Assessment of remediation using other soil ecological endpoints 179

THESIS ABSTRACT

Contaminated soils contain a mix of different contaminant-types; efficient simultaneous *in situ* remediation is challenging as a single process may not suffice. Adsorption is a favourable *in situ* technique. While graphene-based materials (GBMs) have recently been developed as adsorbents for contaminant-removal from water due to their unique functional properties, virtually no studies have investigated their potential in soil. This thesis investigates two prepared GBMs – graphene oxide (GO), and an iron-oxide-modified reduced-GO composite (FeG) – for simultaneous adsorption of 4 model contaminants – arsenate (As; an anionic metalloid), cadmium (Cd; a cationic metal), perfluorooctanoic acid (PFOA) and perfluorooctane sulphonate (PFOS). A 'mixed' mineral and carbon-based adsorbent, RemBind™ (RemB) was also tested for comparison.

Positively-charged FeG showed a strong affinity for binding anionic As, whereas negatively-charged GO showed a strong affinity for binding cationic Cd. An increase in pH promoted Cd sorption and decreased As sorption. Arsenate sorption by FeG was comparable to that by RemB. GO displayed excellent Cd sorption even in acidic conditions, outperforming RemB. Competition by phosphate did not affect As sorption, whereas competition by Ca strongly suppressed Cd sorption. In the case of FeG and RemB, As binding was attributed to ligand-exchange mechanisms with hydroxyl groups on the mineral phases (goethite and alumina, respectively) of the adsorbents. Electrostatic interactions were identified as the main mechanism for Cd sorption by GO and RemB. A mixture of GO and FeG was successful in simultaneous sorption of Cd and As from co-contaminated solutions; amounts sorbed by this mixture were greater than that sorbed by RemB.

Sorption of PFOA by FeG and RemB was much greater than GO. While sorption by GO was hindered at increased pH due to increased repulsion of the PFOA anion, sorption by FeG and RemB were unaffected by variations in pH and ionic strength. In addition to hydrophobic interactions with the carbonaceous phases, the role of combined Fe- and Al-mineral phases in FeG and RemB proved strategic in binding PFOA *via* multiple mechanisms. From an environmental partitioning perspective, precipitation from rainfall events is unlikely to desorb PFOA bound by FeG and RemB. However, leaching of bound PFOA is likely in the presence of polar organic solvent waste at waste disposal or landfill sites. The 'mixed' adsorbents, FeG and RemB, successfully sorbed a range of per- and polyfluoroalkyl substances (PFASs) from a contaminated field sample, demonstrating great potential for use in soil.

During experimental work with ^{14}C-PFOA, sorption losses of the analyte onto common laboratory ware were observed. Losses observed on polypropylene tubes were remarkably higher than on glass, contradictory to the published literature. Filtration was also determined

to be a major source of error, leading to an underestimation of dissolved concentrations. These losses drew attention towards potential analytical bias related to PFASs during routine procedures.

Finally, to test the remediation efficiency of GBMs *in situ* in a soil matrix, using singly-contaminated soils and a 'cocktail'-contaminated soil containing As, Cd, PFOA and PFOS, impacts on contaminant bioaccessibility and microbial soil nitrification were measured. FeG and RemB greatly reduced bioaccessibility of As, PFOA and PFOS (but not Cd) by 89 – 100%, compared to GO (36 – 86%). The mixed-mineral and carbonaceous nature of FeG and RemB offered multiple binding pathways – i.e. hydrophobic interactions with the graphitic plane (for PFOA and PFOS), and ligand-exchange with the goethite or alumina phase (for As, PFOA and PFOS), for FeG and RemB, respectively. Despite the widely-demonstrated success of GO for Cd-removal from water, GO did not bind Cd in the soils. In fact, GO increased Cd-bioaccessibility by 2 fold compared to the unremediated control due to lowered pH (3.5) and concurrent release of calcium ions (Ca^{2+}), which competed with Cd^{2+} for GO's binding sites. Addition of GBMs severely impaired microbial-driven soil nitrification processes (55 – 99% inhibition) due to soil-acidification. While GBMs (particularly FeG) show great promise for reducing bioaccessibility of contaminant-mixtures, their potential to be used for effective *in situ* soil remediation requires that the acidity generated by the materials is neutralised.

In summary, adsorbents (particularly, FeG and RemB) that provided multiple pathways for binding contaminants showed great potential for use as *in situ* soil adsorbents for simultaneous remediation of multiple contaminant-types. For GBMs to be applied efficiently *in situ*, the risk of soil acidification will require management.

DECLARATION

I, Supriya Lath, certify that this work contains no material which has been accepted for the award of any other degree or diploma in my name in any university or other tertiary institution and, to the best of my knowledge and belief, contains no material previously published or written by another person, except where due reference has been made in the text.

In addition, I certify that no part of this work will, in the future, be used in a submission in my name for any other degree or diploma in any university or other tertiary institution without the prior approval of the University of Adelaide.

I acknowledge that copyright of published works contained within this thesis resides with the copyright holder(s) of those works.

I give permission for the digital version of my thesis to be made available on the web, *via* the University's digital research repository, the Library Search and also through web search engines, unless permission has been granted by the University to restrict access for a period of time.

I acknowledge the support I have received for my research through the provision of an Australian Government Research Training Program Scholarship, as well as a top-up Ziltek Soil Science Scholarship.

Supriya Lath Date: 15 September 2018

ACKNOWLEDGEMENTS

Firstly, I would like to thank my supervisors, Mike McLaughlin and Divina Navarro, as well as my co-supervisors, Dusan Losic and Anu Kumar for providing me with the opportunity to work with them. I am grateful for the valuable experiences I have gained, and the continuous mentorship and advice I have received from Mike and Divina, as well as the guidance and support received from Dusan and Anu. Thank you for pushing me to do better and think bigger – you have inspired confidence in me. Your expertise has enabled me to learn broadly from you. I am grateful for the research support I have received through the Australian Government RTP Scholarship, and the Ziltek Soil Science Scholarship, as well as various conference sponsors in terms of travel grants awarded. Attending conferences and networking with peers and leaders made it all the more rewarding.

Thanks are due to many University and CSIRO staff that assisted me with various analytical techniques - Bogumila Tomczak (ICP-OES), Jun Du (PFAS analysis), Mark Raven (XRD), Claire Wright and John Gouzos (ICP-MS and soil characterisation), Cathy Fiebiger and Erinne Stirling (nitrification tests and nitrate analysis). Thanks also to Ashleigh Broadbent, Colin Rivers, Roslyn Baird, Daniel Khajavi, Caroline Johnston, Sonia Grocke, Adelle Craig, Rai Kookana and Melanie Kah who have all provided immense support and advice throughout my candidature. Thank you to Shervin, Ivan, Marijana and Diana for graphene-related conversations and advice. Being a part of the Soils Group has been fantastic. Thanks to Ron Smernik, Tim Cavagnaro, Petra Marschner, Pichu Rengasamy, Cameron Grant, Rodrigo Coqui da Silva, Fien Degryse and Ashlea Doolette – you have all either entertained occasional knocks on your door for soil-science related questions, helped me ease my worries, or encouraged me to go on. The same hold true for all past and current fellow PhD students that I have shared space and time with (there are too many of you to mention) - thank you most of all for your companionship, lunch breaks, ice-cream breaks, and after-work socials. Particular thanks to my office-mates Emma, Chandnee, Shervin, Maarten and Austin for keeping things lively and, on occasion, ensuring I have been fed.

Special thanks are reserved for my family and close friends that have supported me, asked me how it was going, and cheered me on to persist when things got difficult. Thanks to mum and dad for their constant support without which this would not have been possible - you have encouraged me to do my best and make the most of every opportunity. Lastly, thanks to Roshan for supporting me through the highs and the lows, reading my chapters, keeping me company during late-night writing, and making me laugh - you made the journey easier.

LIST OF PUBLICATIONS

Publications arising from this thesis

1. **S Lath**, DA Navarro, D Tran, A Kumar, D Losic, MJ McLaughlin (2018). Mixed-mode remediation of cadmium and arsenate ions using graphene-based materials. CLEAN – Soil, Air, Water, 46, 1800073. https://doi.org/10.1002/clen.201800073.
2. **S Lath**, DA Navarro, D Losic, A Kumar, MJ McLaughlin (2018). Sorptive remediation of perfluorooctanoic acid (PFOA) using mixed mineral and carbon-based materials. Environmental Chemistry *(Submitted; in review; recommended for publication pending minor revisions).*
3. **S Lath**, DA Navarro, A Kumar, D Losic, MJ McLaughlin (2018). Mixed-mode mineral, carbon and graphene-based materials for simultaneous remediation of arsenic, cadmium, PFOA and PFOS in soils. *(Manuscript in preparation for submission to Environmental Chemistry)*.
4. **S Lath**, ER Knight, DA Navarro, R Kookana, MJ McLaughlin (2018). Sorption of PFOA onto different laboratory materials: filter membranes and centrifuge tubes. *(Manuscript in preparation for submission to Environmental Research Letters)*.

Other publications

1. M Markovic, A Kumar, I Andjelkovic, **S Lath**, J Kirby, D Losic, GE Batley, MJ McLaughlin (2018). Ecotoxicology of manufactured graphene oxide nanomaterials and derivation of preliminary guideline values for freshwater environments. Environmental Toxicology and Chemistry, 37: 1340-1348.
2. A Kumar, P Rengasamy, L Smith, H Doan, D Gonzago, A Gregg, **S Lath**, D Oats, R Correl. 2014. Sustainable recycled winery water irrigation based on treatment fit for purpose approach. Report CSL1002. Grape and Wine Research Development Corporation/CSIRO Land and Water, Adelaide, Australia.

LIST OF CONFERENCE PRESENTATIONS

1. 2018 What's in Our Water Symposium (scheduled 29 - 31 Oct 2018), Canberra, Australia.
   Poster presentation: *"In situ remediation of As, Cd, PFOA and PFOS from soil using graphene-based materials".*
2. 2018 Battelle 11th International Conference on Remediation of Chlorinated and Recalcitrant Compounds, Palm Springs, USA.
   Poster presentation: *"Adsorption of Perfluorooctanoic Acid (PFOA) Using Graphene-Based Materials".*
3. CleanUp 2017, 7th International Contaminated Site Remediation Conference, Melbourne, Australia.
   Oral presentation: *"Adsorption of PFOA Using Graphene-Based Materials".*
4. Society of Environmental Toxicology and Chemistry (SETAC) 2017 Australasia Conference, Gold Coast, Australia. *Oral presentation: "Adsorption of PFOA Using Graphene-Based Materials".*
5. SETAC 2016 Australasia Conference, Hobart, Australia.
   Oral presentation: *"Using graphene-based materials for remediation of arsenic and cadmium".*

STRUCTURE OF THE THESIS

This thesis has been presented as a combination of papers that have been published, submitted for publication, or prepared for submission to a journal, in addition to introductory and summary chapters that will not be submitted for publication. .

Chapter 1 provides an introduction and overview of the literature on the use of adsorptive immobilisation for remediation of soil contaminants. The research gaps have been summarised, and the aims, objectives and framework of the thesis have been provided.

Chapter 2 provides a rationale for the choice of adsorbents used in this research, and details the laboratory procedures involved in the synthesis and characterisation of the adsorbents.

Chapter 3 comprises a paper that has been published in *CLEAN – Soil, Air, Water*. It evaluates the sorption performance and behaviour of the adsorbents towards chosen model inorganic contaminants – arsenate (As) and cadmium (Cd). The paper has been reformatted (including referencing style) to maintain consistency with other chapters in this thesis.

Chapter 4 comprises a paper that has been recommended for acceptance for publication in *Environmental Chemistry*, pending minor revisions. It evaluates the sorption behaviour of the adsorbents towards two chosen perfluorinated alkyl substances (PFASs) of current interest – perfluorooctanoic acid (PFOA) and perfluorooctane sulphonate (PFOS) – and highlights the role of 'mixed' adsorbents for improved binding.

Chapter 5 comprises work that is being prepared for submission to *Environmental Research Letters*; a condensed version of the chapter will be submitted for publication. It demonstrates and draws attention towards the occurrence of PFAS-analytical biases as a result of sorption losses onto routine laboratory ware including glass and plastic tubes, and filter-membranes.

Chapter 6 comprises work that has been prepared for submission to *Environmental Chemistry* for publication. It evaluates the use of the 'mixed' mineral and carbon/graphene-based adsorbents for *in situ* remediation of soils contaminated with As, Cd, PFOA and PFOA, as a measure of contaminant bioaccessibility and impact on soil nitrification processes.

Chapter 7 provides a summary of the thesis outcomes, as well as makes recommendations for relevant future research.

CHAPTER 1. Introduction and Literature Review

1. Literature Review

1.1. Soil contamination and its sources

Recent as well as historical development and industrial activities have caused an influx of various contaminants into the environment, to soil, sediments, groundwaters, and surface waters. Accumulation of contaminants in the environment above safe levels can have long-term adverse effects on both human (Inoue et al., 2004, Pan et al., 2010) and ecological (Li, 2009, Planelló et al., 2010, Scheuhammer et al., 2014) health. In addition, contamination can also lead to decline in property value, and affect proposed land use (e.g., commercial or residential) or development of a site. Maintaining and restoring the quality of the environment has thus become one of the greatest challenges of our time. Adequate remediation can restore contaminated sites for different land uses, depending on the level of clean-up achieved.

Soil is a repository for a wide variety of organic and inorganic contaminants, including heavy metals and metalloids, polyaromatic hydrocarbons (PAHs), polychlorinated biphenyls (PCBs), dioxins, brominated and fluorinated flame retardants, etc. (Lambert et al., 1997). These may be released into the environment through various sources. Some common anthropogenic activities that cause contamination include the use of pesticides, fertilizers and leaded paints, vehicular emissions, mining and smelting operations, accidental oil and chemical spills, leakage from landfills, poor waste disposal, as well as burning of wastes and biosolids (Wuana and Okieimen, 2011). For instance, phosphatic fertilizers contain small amounts of cadmium (Cd) and lead (Pb), which can accumulate in soil on recurrent agricultural application. Recycling of urban wastewater biosolids and industrial sludges is common practice in many countries; however, as these can be enriched with a wide variety of persistent contaminants (e.g. PAHs, PCBs, metals), continued land-application can increase contaminant loads over time (Rogers, 1996). In addition to anthropogenic sources, risks can also originate from geogenic sources, i.e., derived from geological sources. For example, elevated concentrations of naturally occurring arsenic (As) have been found in some highly mineralised geological regions, tightly bound to iron (Fe)-based minerals (Juhasz et al., 2007). However, since both As and Fe are redox-sensitive, change in redox conditions can lead to desorption of As from the mineral surfaces, causing increased As-mobility.

1.2. Fate, bioavailability and toxicity of contaminants

The fate of contaminants in the terrestrial environment can vary depending on the nature of the contaminant. For instance, organic contaminants can degrade into products that may be

more or less toxic than the original compound, as a result of breakdown initiated by plant exudates or microbial enzymes (Megharaj et al., 2011). While metals do not undergo similar breakdown processes, they can undergo biogeochemical-induced changes into forms that may be more or less soluble. Soil physiochemical properties also play a major role in controlling fate and mobility of contaminants. Most soils contain organic matter, humic substances, clays, minerals and hydrous oxides of aluminium (Al), Fe and manganese (Mn), which act as natural sinks (adsorbents) for contaminants. Layer silicate clays mainly carry permanent negative charges (McBride, 1994), whereas oxides and hydroxides of Al/Fe/Mn may be variably-charged based on the solution pH and the resultant degree of (de)protonation (Bowden et al., 1977). Soil organic matter (SOM) and humus are usually dominated by negatively charged oxygen-containing carboxylic and phenolic groups (McBride, 1994). These constituents play an important role in the natural attenuation of soil contaminants. For instance, a proportion of the cationic heavy metals in soils are adsorbed to the Fe and Mn oxides (Cowan et al., 1991, Johnson et al., 2007), though there may be competition for the same sorption sites by other commonly occurring alkaline earth metals like calcium (Ca) and magnesium (Mg) (Cowan et al., 1991). Additionally, moisture level, redox potential, and temperature (Wuana and Okieimen, 2011) can also control contaminant mobility.

The toxicity of soil contaminants is influenced by their fate, mobility and bioavailability. Once they enter the soil, contaminants could leach into ground-waters, enter surface runoff waters, or be taken up by soil biota or crop plants, and be passed on through the food chain. Generally, it is the 'bioavailable' or 'bioaccessible' fraction of the total contaminant mass in soils – i.e., the soluble and exchangeable fraction that is actually mobile and available for interaction with receptor organisms (Adriano et al., 2004, Soon and Bates, 1982) – which can directly adversely affect plant, animal or human health. Human exposure to contaminants could be *via* dermal exposure (direct skin contact), inhalation (dust) or ingestion (eating or drinking contaminated food or water). Most regulatory guidelines are based on total contaminant concentrations in the soil, rather than the bioavailable fractions. Thus a bioavailability-based approach needs to be adopted when considering issues of soil management and remediation (McLaughlin et al., 2000).

1.3. Soil remediation strategies

Due to the persistent nature of many soil contaminants, their natural attenuation can be very slow, emphasising the need for development of active remediation technologies. Remediation of soil can be achieved either through degradation or extraction of the contaminants to reduce contaminant loads, or through stabilisation of the contaminants to

reduce mobility and bioavailability (Yeung, 2010). These processes can be carried out either *ex situ*, in which case soil is excavated and transported offsite for treatment, or *in situ*, where treatment is performed on site. Conventional approaches to remediation are based on different strategies:

- physical (disposal to landfill, solidification using cement, electrokinetic separation, soil washing)
- thermal (incineration, vitrification, vapour extraction)
- chemical (solvent extraction, chemical stabilization by adsorption, precipitation, changes in pH and redox potential)
- biological (microbial degradation, phyto-extraction, rhizo-remediation)

While several of the above remediation strategies have been used successfully, they are often invasive, inefficient and require large amounts of water and energy. For instance, processes like vitrification involve the use of very high temperatures and are accompanied by formation of secondary waste products like noxious off-gases (Hillier et al., 2009) which then require further treatment (Mulligan et al., 2001). Residual wastewaters from soil washing and solvent extraction also require further treatment to destroy or remove the contaminants before disposal (Yeung, 2010). Similarly, soil flushing process may mobilise some of the metals that may have otherwise been stabilised by naturally occurring processes (Brown et al., 1998), potentially worsening the situation. Most of these traditional remediation processes are carried out *ex situ*. However, with advances in technology, *in situ* processes are generally favoured as they eliminate extra transport and logistics costs and cause minimum disturbance to soil structure and function.

Soil is a very heterogeneous medium; its chemical, mineralogical and biological complexity makes soil remediation a challenging task. A range of contaminant classes often occur alongside each other, simultaneously, and a single process may not be sufficient for adequate treatment of a site (Wood, 1997). In addition, contaminants may also interact antagonistically or synergistically in the presence of other soil contaminants (Rodea-Palomares et al., 2012). Hence there is a need to develop efficient technologies that can target multiple contaminant classes simultaneously, *in situ*, avoiding the need for multiple remediation attempts at the same site.

1.4. *In situ* adsorption-based remediation

One of the primary strategies for *in situ* remediation of soil contaminants that is considered mild and less invasive than other thermal, physical and chemical methods is immobilisation

via adsorption (Koptsik, 2014). Adsorption involves lowering contaminant mobility and bioavailability, rather than removal or degradation of contaminants. It is achieved by adding reactive amendments to soil so as to control the concentration of contaminants in the soil solution phase, thereby lowering their toxic potential (Lim et al., 2013, Mench et al., 1994). Depending on the site geochemistry, this could serve as a long term remediation solution at the site (McBride, 1994). Adsorption of organic compounds is usually controlled by hydrophobic partitioning onto organic or carbonaceous phases. However, polar organic compounds may be bound *via* charge-based interactions. Binding of inorganic contaminants like metals and metalloids is usually controlled by electrostatic interactions, like ion-exchange, or stronger ligand-exchange mechanisms.

For effective adsorption, an ideal adsorbent typically has large surface area, high porosity, presence of surface charge and functional groups (Kumar, 2010). These properties result in high adsorption capacities and potential affinity towards a wide range of contaminants. Several materials have been used as adsorbents for remediation. Phyllosilicate clays (kaolinite, mica, vermiculite, smectite), zeolites, Al/Fe/Mn-based oxides and hydroxides as well as organic substances like compost, biosolids and sludge have been known for their sorption capacity. Lime and phosphate-based amendments have also been used for metal fixation in soils through formation of precipitates like metal phosphates, carbonates and hydroxides (Lim et al., 2013, Mench et al., 1994). Carbon-based materials such as soot, charcoal, biochar and activated carbon have been used conventionally for adsorption in environmental remediation (Rakowska et al., 2012). However their sorptive capabilities are limited by the low density of surface active sites, their non-specificity in heterogeneous environments and slow kinetics (Mauter and Elimelech, 2008). Such limitations can be overcome by using 'nano'-sized materials; their smaller sizes and large specific surface areas correspond to enhanced reactivity, giving them an edge over the bulk parent materials (Li et al., 2006, Taghizadeh et al., 2013). For example, nano zero-valent Fe can have surface areas up to 30 times greater than larger-size granular Fe powder and up to 10^4 times more reactive (Mueller and Nowack, 2010). Recently, a spectrum of advanced carbonaceous nanomaterials like carbon nanotubes (Chen et al., 2007, Tofighy and Mohammadi, 2011) and graphene-based materials (GBMs) (Chowdhury and Balasubramanian, 2014, Ji et al., 2013) have also been demonstrated for their use in adsorption, due to their high surface area to volume ratio, controlled pore size distribution and tuneable surface chemistry (Mauter and Elimelech, 2008), however, this has predominantly been in water.

1.5. Graphene's potential as an adsorbent

Graphene, a single-atom thick layer of graphite, composed of a 2-dimensional plane of closely packed sp^2 hybridised carbon atoms arranged in a hexagonal pattern, is the latest addition to the nanocarbon family. Ever since its Nobel prize-winning recognition in 2010 (Novoselov et al., 2012), there has been a lot of excitement about graphene. Due to its extraordinary physico-chemical properties, recent research and development has seen graphene emerge as a 'miracle material' being integrated worldwide in electronics, drug delivery, energy storage, bio-sensing, filtration, etc. (Novoselov et al., 2012). However, its use in environmental remediation is still an emerging area of application.

Graphene is an excellent candidate to be utilised as an adsorbent due to its high theoretical specific surface area (2630 $m^2 g^{-1}$) (Niu et al., 2014) and controllable surface functionality (Dreyer et al., 2010). Pristine graphene has been used for the adsorption of organic contaminants such as PAHs (e.g. naphthalene), antibiotics (e.g. tetracycline) and dyes (e.g. methylene blue) (Ersan et al., 2017, Ji et al., 2013) from water; these interactions were attributed to either hydrogen bonding, hydrophobic interactions, or π–π electron donor–acceptor interactions at the hydrophobic graphitic basal plane. The surface of graphene can be functionalised to form different GBMs, allowing for interactions with different types of contaminants. The most common derivative of graphene is graphene oxide (GO), containing a myriad of oxygen functionalities including carbonyl, carboxyl and hydroxyl groups, which confer a negative charge to the carbon surface. Consequently, GO has been used to bind divalent heavy metal cations such as copper (Cu), Cd, Pb and zinc (Zn) from water through coordination and electrostatic interactions (Sitko et al., 2013, Wang et al., 2013). This oxidation of graphene also increases hydrophilicity due to the formation of hydrogen bonds with water (Bandosz, 2006). Graphene oxide functionalised with EDTA has been used successfully to remove Pb^{2+} from contaminated waters by chelate formation (Madadrang et al., 2012). Several graphene/metal oxide composites, mainly Fe- or Mn-based, have also been developed as adsorbents. For instance, magnetite-graphene/GO composites have been successful in adsorbing a variety of PAHs, dyes, and metals from water *via* previously mentioned mechanisms, as well as metalloids like arsenate (As^{V}) and chromate (Cr^{VI}) *via* ligand-exchange and inner-sphere complexation mechanisms (Upadhyay et al., 2014, Zhang et al., 2013). Such control over the surface properties of GBMs offer possible pathways to engineer advanced functionalised materials for remediation of contaminant mixtures in the environment.

1.6. Application of graphene for soil remediation

While several studies have shown successful contaminant management through the application of GBMs in water, the use of GBMs for *in situ* soil remediation remains largely unexplored. Only a handful of accounts have been reported in the published literature using soil as a medium. In one study, two PAHs, phenanthrene (hydrophobic organic) and 1-naphthol (polar organic) were adsorbed using colloidal GO, *via* hydrophobic interactions and hydrogen-bonding, respectively (Qi et al., 2014); however, in saturated soil conditions, significant mobility of the GO-bound naphthol was observed. In a study with Cd-spiked soil this year, addition of GO was reported to reduce the bioavailability and solubility of Cd due to binding *via* electrostatic interactions and surface complexation mechanisms, involving the negatively charged oxygen-functional groups on the GO surface (Xiong et al., 2018). In a natural As-enriched soil, where As was linked to Fe-(hydr)oxides within the soil, the addition of reduced GO in flooding (anaerobic) conditions enhanced the microbial reduction of Fe^{III}/As^{V} precipitates, mobilising Fe^{II} and As^{III} from the soil (Chen et al., 2018), leading to an increase in bioavailable-As. Apart from GO or reduced GO, there are no accounts of other functionalised GBMs for soil remediation. Moreover, simultaneous remediation of multiple contaminant-types hasn't been considered. Overall, the studies with respect to the application of GBMs in soil are scarce, and outcomes are varied.

In addition to reduced contaminant-bioavailability or bioaccessibility, restoration of soil functionality is also an important indicator of soil quality after remediation. It is known that accumulation of contaminants in the soil can disturb biologically mediated soil processes and affect soil microbial communities, which are known to play a vital role in maintaining soil health and function (Pérez-de-Mora et al., 2006, Ramakrishnan et al., 2011). This could be through changes in soil respiration, microbial biomass and soil enzyme activities (Liu et al., 2009, Pan and Yu, 2011), as well as in the structure and diversity of the soil microbial community (Pérez-de-Mora et al., 2006, Xiong et al., 2018). The remediation technique employed is also expected to alter soil function by impacting soil parameters like soil pH and SOM, which are linked to many soil processes (O'Brien et al., 2017). In the previously-mentioned study where the addition of GO reduced Cd-bioavailability from a Cd-contaminated soil, changes in soil microbial parameters were reported – e.g. dehydrogenase enzyme activity was enhanced, but urease activity was inhibited (Xiong et al., 2018). Moreover, the relative abundance of some sensitive functional bacteria which are related to nitrogen (N)-cycling (*Nitrospira*) and carbon-cycling (*Actinobateria*) processes decreased, whereas other dominant phyla increased (Xiong et al., 2018). Such changes in soil function can have a bearing on overall soil health, which is an important consideration during *in situ*

remediation. It has thus been suggested that post-remediation, impacts of remediation strategies on soil function should also be investigated (O'Brien et al., 2017).

2. Summary of Research Gaps and Research Framework

Based on the literature review, we identified a need to develop *in situ* remediation technologies that can efficiently target multiple contaminant types, simultaneously, using a range of mechanisms. The sophisticated nature and versatile surface chemistry of graphene makes it a great candidate to be developed as an adsorbent and offers possible pathways to engineer advanced functionalised materials for remediation of contaminant mixtures in the environment. There are only a handful of studies that have investigated the interactions between GBMs and contaminants in soil. Moreover, no studies have been conducted using contaminant mixtures. In general, mineral-based adsorbents have commonly been employed to immobilise inorganic contaminants (O'Day and Vlassopoulos, 2010), whereas carbon-based materials are used to bind organic contaminants (Rakowska et al., 2012). It was thus anticipated that combining mineral and carbon-phases in adsorbents may prove advantageous in simultaneous remediation of multiple contaminant types (inorganic and organic), *via* multiple binding mechanisms. As both contamination and remediation activities can alter soil function, certain sensitive soil microbial processes can be used as additional indicators of restoration of soil function, in addition to reduction of contaminant-bioaccessibility, providing an integrated view of 'remediation'.

The graphene-based adsorbents chosen for remediation in this study were GO, and an Fe-oxide-modified reduced-GO composite (FeG). The former (GO) was chosen as it has been widely demonstrated for its adsorptive capabilities in aqueous media. The latter (FeG) was chosen as it is a mixed mineral and graphene/carbon-based adsorbent that could potentially offer multiple pathways to bind several contaminants. A non-graphene commercial adsorbent product, RemBind™, which is a powdered mixture of activated-C, amorphous aluminium hydroxide and kaolin clay, was also tested from the same perspective, and used as a benchmark for comparison.

In order to account for different types of contaminants, for the purpose of this thesis, we chose 'model' contaminants from 3 different contaminant classes. These include arsenate (As^{V}; an anionic metalloid), cadmium (Cd; a cationic metal) and two perfluorinated alkyl substances (PFASs) of current interest, perfluorooctanoic acid (PFOA) and perfluorooctane sulphonate (PFOS) – each of these are persistent contaminants that have been shown to accumulate in the food chain. The inorganic contaminants, As and Cd are notorious for posing high health risks to humans through intake of contaminated food and water. The organic contaminants, PFOA and PFOS, are known for their persistence in the environment

and bioaccumulation potential through long-range transport. Adsorptive binding of these contaminants in the environment would limit their mobility and bioaccessibility, hence reducing their toxic potential. Further information relevant to the environmental fate and remediation of As, Cd, PFOA and PFOS, including physiochemical properties is provided in Table 1 below.

*Table 1. Properties of the model contaminants**

Characteristics	**Arsenic (anionic metalloid)**	**Cadmium (cationic metal)**	**PFOA and PFOS (organic)**
Concern	Priority List of Hazardous Substances in US Superfund	Priority List of Hazardous Substances in US Superfund	Stockholm Convention's list of Persistent Organic Pollutants of emerging concern
Anthropogenic sources	Pesticides; wood treatment/preservation; mining, smelting; fuel combustion; application of biosolids; waste incineration (USEPA, 2002)	Metal mining and smelting; impurities in phosphate fertilisers; urban waste biosolids (Singh and McLaughlin, 1999)	Flame retardants; fire-fighting foams; repellent-coatings for fabric and paper; cleaning agents; degradation product of longer PFASs (Buck et al., 2011)
Geogenic sources	3 - 4 mg/kg in earth's crust, associated with volcanic rocks and several minerals (USATSDR, 2007)	0.1 - 0.5 mg/kg in earth's crust, associated with Zn ores and phosphate minerals (USATSDR, 2012)	- n/a -

* *continued on next page*

*Table 1 (continued). Properties of the model contaminants**

Characteristics	Arsenic (anionic metalloid)	Cadmium (cationic metal)	PFOA and PFOS (organic)
Human Exposure pathways	Contaminated drinking water and food intake; dermal exposure and inhalation (USATSDR, 2007)	Contaminated food and food-chain transfer account for > 90% of human Cd uptake (Singh and McLaughlin, 1999, Violante et al., 2002); inhalation from dust and fumes; tobacco smoking (Campbell, 2006)	Bioaccumulation along the higher levels of the food chain; consumption of contaminated food and water (OECD, 2002); breast-feeding
Risk to Human Health	Skin cancer; circulatory system problems (Wuana and Okieimen, 2011); skin lesions; GI-tract irritation; liver and lung cancer (USATSDR, 2007)	Kidney dysfunction due to chronic accumulation; lung cancer; stomach irritation (USATSDR, 2012)	Binds to blood and liver proteins; detected in human blood and fetal cord blood samples (Inoue et al., 2004); inconsistent evidence of links to cancer and heart disease
Environmental risks	Risk mainly through soil acidification and consequent leaching into water sources	Moves along the soil-to-plant pathway through food chain	Long range transport due to polar and amphiphilic nature; bio-accumulative potential. Highly persistent

* *continued on next page*

*Table 1 (continued). Properties of the model contaminants**

Characteristics	**Arsenic (anionic metalloid)**	**Cadmium (cationic metal)**	**PFOA and PFOS (organic)**
Speciation in soil	Oxyanions; predominantly $H_2AsO_4^{--}$ (pH 2.5–6.5) and $HAsO_4^{2-}$ (pH 6.5–12) arsenates [As^V]. Arsenite $H_2AsO_3^-$ in anoxic conditions [As^{III}]	Cationic Cd^{2+} (Lambert et al., 1997) up to pH 8; precipitation > pH 8	Fully fluorinated organic anion $C_8F_{15}O_2^-$ and $C_8F_{17}SO_3^-$; low pKa values
Fate in soil	Redox sensitive. As^{III} and As^V are the common oxidation states. Bound strongly to soil colloids and Fe/Mn oxides, hence relatively immobile (Hudson-Edwards et al., 2004). Mobility and solubility increase in reducing conditions	pH sensitive. Soils with low pH and clay content are at risk of allowing greater Cd-uptake by plants (McLaughlin et al., 2006). Speciation also depends on CEC and content of carbonate minerals and SOM	Resilient to hydrolysis, photolysis and biodegradation. Both hydrophobic and electrostatic interactions may play an important role in its distribution in the environment (Hekster et al., 2003)
Toxicity in soil	As^V predominates in oxidising conditions. As^{III} in reducing conditions. Mobility and toxicity of As^{III} >>As^V	Toxicity depend on concentration of ions in the soluble, exchangeable or mobile fractions of the soil	High mobility and bioavailability due to polar nature; uptake by plants and earthworms

** continued on next page*

Table 1 (continued). Properties of the model contaminants.

Characteristics	Arsenic (anionic metalloid)	Cadmium (cationic metal)	PFOA and PFOS (organic)
Known remediation strategies	Oxidation of As^{III} to less mobile As^{V} using Fe^{III} to form ferric arsenate is the most common approach. Ferrihydrite (FeOOH) and Fe_2O_3 also bind As through adsorption and co-precipitation (Martin and Ruby, 2003) in oxidised soils.	Precipitation of immobile $CdCO_3$ (Lim et al., 2013) by adding lime-based amendments is very common. Lime also raises soil pH, causing increase in net negative charge of soil colloids, leading to increased sorption of Cd onto soil (Lee et al., 2009).	Degradation by high temperature (>800°C) incineration; sorption from water using zeolites, granular activated carbon, boehmite (AlOOH) and ion-exchange resins (Kucharzyk et al., 2017). One soil study used a modified clay adsorbent, matCARE™ (Das et al., 2013).

In addition to measuring remediation efficiency by monitoring contaminant solubility and bioaccessibility, the effects of the adsorbents on a selected microbial indicator – soil nitrification – were also investigated. Nitrification (conversion of ammonium to nitrite, and then into a plant-available form, nitrate), is a key process in nitrogen-cycling in soil, and is controlled by a limited number of specialist soil microorganisms (Leininger et al., 2006, Robertson and Groffman, 2015). As these processes are extremely sensitive, monitoring of nitrification can be used to evaluate the effects of the adsorbents after remediation.

The work described in this thesis is based on a multi-disciplinary approach combining aspects of chemical engineering, environmental chemistry, soil chemistry and ecotoxicology to synthesise and evaluate graphene-based adsorbents that can be used for adsorptive remediation of multiple soil contaminants, thereby reducing their bioaccessibility and toxicity.

3. Aims and Objectives

The primary focus of this research was to investigate the use of GBMs for adsorptive remediation of soil contaminants.

The specific aims and objectives of this thesis were:

1. To develop mixed-mode GBMs with chemical functionalities that facilitate binding of multiple contaminant-types:
   i. Synthesise GBMs and characterise their structural properties;
   ii. Evaluate affinity of GBMs towards binding of As, Cd, PFOA and PFOS and compare performance with a commercial adsorbent;
   iii. Evaluate adsorption in different soil-solution conditions; and
   iv. Understand possible binding mechanisms.
2. To evaluate potential application of GBMs for *in situ* remediation of singly-contaminated and mixed-contaminated soils:
   i. Measure 'bioaccessible' fractions of As, Cd, PFOA and PFOS after remediation; and
   ii. Determine impact of the process on the microbial-nitrification function of soil.

4. References

Adriano DC, Wenzel WW, Vangronsveld J, Bolan NS (2004). Role of assisted natural remediation in environmental cleanup. *Geoderma,* **122,** 121-142.

Bandosz TJ 2006. *Activated carbon surfaces in environmental remediation*, Academic Press.

Bowden J, Posner A, Quirk J (1977). Ionic adsorption on variable charge mineral surfaces. Theoretical charge development and titration curves. *Soil Research,* **15,** 121-136.

Brown RA, Leaby MC, Pyrih RZ (1998). In situ remediation of metals comes of age. *Remediation Journal,* **8,** 81-96.

Buck RC, Franklin J, Berger U, Conder JM, Cousins IT, de Voogt P, Jensen AA, Kannan K, Mabury SA, van Leeuwen SPJ (2011). Perfluoroalkyl and polyfluoroalkyl substances in the environment: Terminology, classification, and origins. *Integrated Environmental Assessment and Management,* **7,** 513-541.

Campbell PGC (2006). Cadmium - A priority pollutant. *Environmental Chemistry,* **3,** 387-388.

Chen W, Duan L, Zhu D (2007). Adsorption of polar and nonpolar organic chemicals to carbon nanotubes. *Environmental Science & Technology,* **41,** 8295-8300.

Chen Z, Li H, Ma W, Fu D, Han K, Wang H, He N, Li Q, Wang Y (2018). Addition of graphene sheets enhances reductive dissolution of arsenic and iron from arsenic contaminated soil. *Land Degradation & Development,* **29,** 572-584.

Chowdhury S, Balasubramanian R (2014). Recent advances in the use of graphene-family nanoadsorbents for removal of toxic pollutants from wastewater. *Advances in Colloid and Interface Science,* **204,** 35-56.

Cowan CE, Zachara JM, Resch CT (1991). Cadmium adsorption on iron oxides in the presence of alkaline-earth elements. *Environmental Science & Technology,* **25,** 437-446.

Das P, Kambala V, Mallavarapu M, Naidu R (2013). Remediation of perfluorooctane sulfonate in contaminated soils by modified clay adsorbent—a risk-based approach. *Water, Air, & Soil Pollution,* **224,** 1-14.

Dreyer DR, Park S, Bielawski CW, Ruoff RS (2010). The chemistry of graphene oxide. *Chemical Society Reviews,* **39,** 228-240.

Ersan G, Apul OG, Perreault F, Karanfil T (2017). Adsorption of organic contaminants by graphene nanosheets: A review. *Water Research,* **126,** 385-398.

Hekster F, Laane RPM, de Voogt P 2003. Environmental and toxicity effects of perfluoroalkylated substances. *Reviews of Environmental Contamination and Toxicology.* Springer New York.

Hillier N, Gennissen J, Pickering B, Smolenski R, with an introduction by Paul B (2009). Our battle with hexachlorobenzene: Citizen perspectives on toxic waste in Botany. *Journal of Environmental Management,* **90,** 1605-1612.

Hudson-Edwards K, Houghton S, Osborn A (2004). Extraction and analysis of arsenic in soils and sediments. *TrAC Trends in Analytical Chemistry,* **23,** 745-752.

Inoue K, Okada F, Ito R, Kato S, Sasaki S, Nakajima S, Uno A, Saijo Y, Sata F, Yoshimura Y (2004). Perfluorooctane sulfonate (PFOS) and related perfluorinated compounds in human maternal and cord blood samples: assessment of PFOS exposure in a susceptible population during pregnancy. *Environmental Health Perspectives***,** 1204-1207.

Ji L, Chen W, Xu Z, Zheng S, Zhu D (2013). Graphene nanosheets and graphite oxide as promising adsorbents for removal of organic contaminants from aqueous solution. *Journal of Environmental Quality,* **42,** 191-198.

Johnson RL, Anschutz AJ, Smolen JM, Simcik MF, Penn RL (2007). The adsorption of perfluorooctane sulfonate onto sand, clay, and iron oxide surfaces. *Journal of Chemical & Engineering Data,* **52,** 1165-1170.

Juhasz AL, Smith E, Weber J, Rees M, Rofe A, Kuchel T, Sansom L, Naidu R (2007). In vitro assessment of arsenic bioaccessibility in contaminated (anthropogenic and geogenic) soils. *Chemosphere,* **69,** 69-78.

Koptsik GN (2014). Modern approaches to remediation of heavy metal polluted soils: A review. *Eurasian Soil Science,* **47,** 707-722.

Kucharzyk KH, Darlington R, Benotti M, Deeb R, Hawley E (2017). Novel treatment technologies for PFAS compounds: A critical review. *Journal of Environmental Management,* **204,** 757-764.

Kumar CS 2010. *Biomimetic and bioinspired nanomaterials*, John Wiley & Sons.

Lambert M, Pierzinski G, Erickson L, Schnoor J 1997. Remediation of lead-, zinc-and cadmium contaminated soils. *In:* Hester, RE & Harrison, RM (eds.) *Issues in Environmental Science and Technology.* Cambridge, United Kingdom: Royal Society of Chemistry.

Lee S-H, Lee J-S, Jeong Choi Y, Kim J-G (2009). In situ stabilization of cadmium-, lead-, and zinc-contaminated soil using various amendments. *Chemosphere,* **77,** 1069-1075.

Leininger S, Urich T, Schloter M, Schwark L, Qi J, Nicol GW, Prosser JI, Schuster SC, Schleper C (2006). Archaea predominate among ammonia-oxidizing prokaryotes in soils. *Nature,* **442,** 806-9.

Li MH (2009). Toxicity of perfluorooctane sulfonate and perfluorooctanoic acid to plants and aquatic invertebrates. *Environmental Toxicology,* **24,** 95-101.

Li X-q, Elliott DW, Zhang W-x (2006). Zero-valent iron nanoparticles for abatement of environmental pollutants: materials and engineering aspects. *Critical Reviews in Solid State and Materials Sciences,* **31,** 111-122.

Lim JE, Ahmad M, Lee SS, Shope CL, Hashimoto Y, Kim K-R, Usman ARA, Yang JE, Ok YS (2013). Effects of lime-based waste materials on immobilization and phytoavailability of cadmium and lead in contaminated soil. *CLEAN – Soil, Air, Water,* **41,** 1235-1241.

Liu F, Ying G-G, Tao R, Zhao J-L, Yang J-F, Zhao L-F (2009). Effects of six selected antibiotics on plant growth and soil microbial and enzymatic activities. *Environmental Pollution,* **157,** 1636-1642.

Madadrang CJ, Kim HY, Gao G, Wang N, Zhu J, Feng H, Gorring M, Kasner ML, Hou S (2012). Adsorption behavior of EDTA-graphene oxide for Pb (II) removal. *ACS Applied Materials & Interfaces,* **4,** 1186-1193.

Martin TA, Ruby MV (2003). In situ remediation of arsenic in contaminated soils. *Remediation Journal,* **14,** 21-32.

Mauter MS, Elimelech M (2008). Environmental applications of carbon-based nanomaterials. *Environmental Science & Technology,* **42,** 5843-5859.

McBride MB 1994. *Environmental chemistry of soils*, Oxford university press.

McLaughlin MJ, Hamon R, McLaren R, Speir T, Rogers S (2000). Review: A bioavailability-based rationale for controlling metal and metalloid contamination of agricultural land in Australia and New Zealand. *Soil Research,* **38,** 1037-1086.

McLaughlin MJ, Whatmuff M, Warne M, Heemsbergen D, Barry G, Bell M, Nash D, Pritchard D (2006). A field investigation of solubility and food chain accumulation of biosolid-cadmium across diverse soil types. *Environmental Chemistry,* **3,** 428-432.

Megharaj M, Ramakrishnan B, Venkateswarlu K, Sethunathan N, Naidu R (2011). Bioremediation approaches for organic pollutants: A critical perspective. *Environment International,* **37,** 1362-1375.

Mench MJ, Didier VL, Löffler M, Gomez A, Masson P (1994). A mimicked in-situ remediation study of metal-contaminated soils with emphasis on cadmium and lead. *Journal of Environmental Quality,* **23,** 58-63.

Mueller NC, Nowack B (2010). Nanoparticles for remediation: solving big problems with little particles. *Elements,* **6,** 395-400.

Mulligan CN, Yong RN, Gibbs BF (2001). Remediation technologies for metal-contaminated soils and groundwater: an evaluation. *Engineering Geology,* **60,** 193-207.

Niu Z, Liu L, Zhang L, Chen X (2014). Porous graphene materials for water remediation. *Small,* **10,** 3434-3441.

Novoselov KS, Falko VI, Colombo L, Gellert PR, Schwab MG, Kim K (2012). A roadmap for graphene. *Nature,* **490,** 192-200.

O'Day PA, Vlassopoulos D (2010). Mineral-based amendments for remediation. *Elements,* **6,** 375-381.

O'Brien PL, DeSutter TM, Casey FXM, Wick AF, Khan E (2017). Evaluation of soil function following remediation of petroleum hydrocarbons—a review of current remediation techniques. *Current Pollution Reports,* **3,** 192-205.

OECD (2002). Hazard assessment of perfluorooctane sulfonate (PFOS) and its salts. Paris: OECD Publishing.

Pan J, Plant JA, Voulvoulis N, Oates CJ, Ihlenfeld C (2010). Cadmium levels in Europe: implications for human health. *Environmental Geochemistry and Health,* **32,** 1-12.

Pan J, Yu L (2011). Effects of Cd or/and Pb on soil enzyme activities and microbial community structure. *Ecological Engineering,* **37,** 1889-1894.

Pérez-de-Mora A, Burgos P, Madejón E, Cabrera F, Jaeckel P, Schloter M (2006). Microbial community structure and function in a soil contaminated by heavy metals: effects of

plant growth and different amendments. *Soil Biology and Biochemistry,* **38,** 327-341.

Planelló R, Martínez-Guitarte J, Morcillo G (2010). Effect of acute exposure to cadmium on the expression of heat-shock and hormone-nuclear receptor genes in the aquatic midge *Chironomus riparius*. *Science of the Total Environment,* **408,** 1598-1603.

Qi Z, Hou L, Zhu D, Ji R, Chen W (2014). Enhanced transport of phenanthrene and 1-naphthol by colloidal graphene oxide nanoparticles in saturated soil. *Environmental Science & Technology,* **48,** 10136-10144.

Rakowska M, Kupryianchyk D, Harmsen J, Grotenhuis T, Koelmans A (2012). In situ remediation of contaminated sediments using carbonaceous materials. *Environmental Toxicology and Chemistry,* **31,** 693-704.

Ramakrishnan B, Megharaj M, Venkateswarlu K, Sethunathan N, Naidu R 2011. Mixtures of environmental pollutants: effects on microorganisms and their activities in soils. *In:* Whitacre, DM (ed.) *Reviews of Environmental Contamination and Toxicology Volume 211.* New York, NY: Springer New York.

Robertson GP, Groffman PM 2015. Nitrogen transformations *In:* Paul, EA (ed.) *Soil microbiology, ecology and biochemistry (Fourth edition).* Boston: Academic Press.

Rodea-Palomares I, Leganés F, Rosal R, Fernández-Piñas F (2012). Toxicological interactions of perfluorooctane sulfonic acid (PFOS) and perfluorooctanoic acid (PFOA) with selected pollutants. *Journal of Hazardous Materials,* **201,** 209-218.

Rogers HR (1996). Sources, behaviour and fate of organic contaminants during sewage treatment and in sewage sludges. *Science of The Total Environment,* **185,** 3-26.

Scheuhammer A, Braune B, Chan HM, Frouin H, Krey A, Letcher R, Loseto L, Noël M, Ostertag S, Ross P (2014). Recent progress on our understanding of the biological effects of mercury in fish and wildlife in the Canadian Arctic. *Science of the Total Environment*.

Singh BR, McLaughlin J 1999. *Cadmium in soils and plants*, Springer Netherlands.

Sitko R, Turek E, Zawisza B, Malicka E, Talik E, Heimann J, Gagor A, Feist B, Wrzalik R (2013). Adsorption of divalent metal ions from aqueous solutions using graphene oxide. *Dalton Transactions,* **42,** 5682-5689.

Soon YK, Bates TE (1982). Chemical pools of cadmium, nickel and zinc in polluted soils and some preliminary indications of their availability to plants. *Journal of Soil Science,* **33,** 477-488.

Taghizadeh M, Kebria DY, Darvishi G, Kootenaei FG (2013). The use of nano zero valent iron in remediation of contaminated soil and groundwater. *International Journal of Scientific Research in Environmental Sciences,* **1,** 152-157.

Tofighy MA, Mohammadi T (2011). Adsorption of divalent heavy metal ions from water using carbon nanotube sheets. *Journal of Hazardous Materials,* **185,** 140-147.

Upadhyay RK, Soin N, Roy SS (2014). Role of graphene/metal oxide composites as photocatalysts, adsorbents and disinfectants in water treatment: a review. *RSC Advances,* **4,** 3823-3851.

USATSDR (2007). Toxicological profile for arsenic. Agency for Toxic Substances and Disease Registry (US), Atlanta (Georgia).

USATSDR (2012). Toxicological profile for cadmium. Agency for Toxic Substances and Disease Registry (US), Atlanta (Georgia).

USEPA (2002). Arsenic treatment technologies for soil, waste, and water. EPA Document Number: 542-R-02-004. Washington, D C.

Violante A, Bollag J-M, Gianfreda L, Huang P 2002. *Ecological significance of the interactions among clay minerals, organic matter and soil biota*, Elsevier.

Wang S, Sun H, Ang H-M, Tadé M (2013). Adsorptive remediation of environmental pollutants using novel graphene-based nanomaterials. *Chemical Engineering Journal,* **226,** 336-347.

Wood PA 1997. Remediation methods for contaminated sites. *In:* Hester, RE & Harrison, RM (eds.) *Contaminated Land and its Reclamation.* The Royal Society of Chemistry.

Wuana RA, Okieimen FE (2011). Heavy metals in contaminated soils: a review of sources, chemistry, risks and best available strategies for remediation. *ISRN Ecology,* **2011**.

Xiong T, Yuan X, Wang H, Leng L, Li H, Wu Z, Jiang L, Xu R, Zeng G (2018). Implication of graphene oxide in Cd-contaminated soil: A case study of bacterial communities. *Journal of Environmental Management,* **205,** 99-106.

Yeung AT 2010. Remediation technologies for contaminated sites. *Advances in Environmental Geotechnics.* Springer.

Zhang W, Shi X, Zhang Y, Gu W, Li B, Xian Y (2013). Synthesis of water-soluble magnetic graphene nanocomposites for recyclable removal of heavy metal ions. *Journal of Materials Chemistry A,* **1,** 1745-1753.

CHAPTER 2. Synthesis and Characterisation of Graphene Adsorbents

1. Introduction

Since 2010, when two researchers from the University of Manchester – Andre Geim and Kostya Novoselov – were awarded the Nobel Prize for isolating a single layer of graphene by mechanical exfoliation of graphite using Scotch-tape, it has been the subject of intense research for application in several fields (Zhu et al., 2010). Graphene is the building block of graphite and other graphitic materials, and is described as an arrangement of a monolayer of carbon atoms in a two-dimensional honeycomb lattice structure (Novoselov et al., 2012). Due to its unique properties, including superior mechanical stiffness, strength and elasticity, high surface area, as well as excellent thermal and electrical conductivity, graphene has been perceived as one of the most versatile and promising materials discovered (Novoselov et al., 2012, Zhu et al., 2010).

Synthesis of graphene and graphene-based materials (GBMs) has been a major area of focus, given the demand for these materials. Apart from mechanical exfoliation, chemical vapour deposition is commonly used for the synthesis of pristine graphene, however these methods are suited to small-scale production (Marcano et al., 2010). Other chemical methods of production of graphene have involved chemical exfoliation using surfactants, or through oxidation-reduction of graphite, commonly involving the use of strong oxidising agents to form graphene oxide (GO), followed by reduction (Zhu et al., 2010).

Graphene oxide is the most common derivative of graphene. While graphene itself tends to be inert to reaction, GO has a versatile surface chemistry – the oxygen functional groups provide pathways for functionalisation with different groups or moieties to form different GBMs (Dreyer et al., 2010, Georgakilas et al., 2012). As a result, chemical modification of the graphene surface *via* a variety of reactive pathways is what lends GBMs a competitive edge over other materials. From the perspective of use as an adsorbent for contaminant-remediation, the presence of functional groups on the surface is advantageous as they can act as binding sites for a variety of contaminants (Georgakilas et al., 2012). As a result, GO was chosen as one of the adsorbents, along with an iron (Fe)-oxide-modified reduced-GO composite (henceforth referred to FeG), to be tested for the adsorption of the four model contaminants – arsenate (As), cadmium, perfluorooctanoic acid (PFOA) and perfluorooctane sulphonate (PFOS).

The host of different negatively charged oxygen groups (alcohol, carbonyl, carboxyl, epoxy) on the surface of GO presented an opportunity for sorption of heavy metals like Cd which primarily exists in its free cationic from in the environment. An iron-based modification was planned for binding As, which occurs in the environment as negatively charged arsenate ions, commonly associated with Fe-based minerals (e.g. ferrihydrite, hematite). The organic

contaminants, PFOA and PFOS, interestingly, are both hydrophobic and polar at the same time, and were expected to associate with the carbonaceous phases of GO and FeG.

Both GO and FeG were synthesised in the lab using raw graphite as the starting material, based on methods described in the published literature. Natural graphite flakes were sourced from the Uley graphite mines in the Eyre Peninsula (South Australia). The synthesis and characterisation of the graphene-based adsorbents, GO and FeG, have been discussed below. The commercial adsorbent, RemBind™ (RemB) supplied by Ziltek Pty. Ltd., was also characterised.

2. Synthesis of Graphene-Based Adsorbents

2.1. Synthesis of graphene oxide, GO

A top-down synthetic approach based on an improved Hummer's method (Marcano et al., 2010) involving strong oxidation of natural graphite was used to synthesise graphene oxide. For synthesis, a 9:1 mixture of concentrated sulphuric acid and phosphoric acid (H_2SO_4:H_3PO_4; 360:40 mL) is added to a mixture of graphite flakes (3 g) and potassium permanganate, ($KMnO_4$; 18 g), producing a green-coloured reaction mixture, with a slight exotherm of 35-40°C. This mixture of strong oxidising acids and chemicals plays an important role in the simultaneous oxidation and exfoliation of graphite (Marcano et al., 2010). The acids intercalate into the graphite layers to expand and separate stacked sheets of graphite (Dimiev and Tour, 2014, Zhu et al., 2010). The $KMnO_4$ and H_2SO_4 react to form diamanganese heptoxide (Mn_2O_7), which imparts a green colour.

The mixture is then heated over a magnetic heater-stirrer device at 50°C in a glass reaction vessel over a silicone oil-bath, and stirred for 24 hours. As silicone oil has a high boiling point (>140°C) and distributes heat evenly, it is ideal for use in a heating bath for overnight reactions. Mn_2O_7 is an active oxidizing species, which enables formation of polar oxygen-based functional groups on the graphitic surface; the carbon lattice is interrupted by epoxides, alcohols, carbonyls and carboxylic groups (Marcano et al., 2010). As the Mn_2O_7 is consumed, the green colour slowly disappears, leaving behind a thick brownish-purple slurry of highly oxidised and exfoliated GO. The purple colour is a result of unreacted $KMnO_4$.

The reaction mixture is then cooled to room temperature and poured onto ice (400 g) and hydrogen peroxide (30% H_2O_2; 3 mL). The addition of peroxide aids the conversion of unreacted manganese by-products to colourless $MnSO_4$, leaving behind a thick paste of golden-yellow GO product in suspension, requiring washing and separation (Dimiev and Tour, 2014). The mixture is then centrifuged (4000 g, 1 hour), and the supernatant decanted away. The remaining material in the centrifuge tubes is then washed in succession by re-

suspending in a washing liquid and repeating the 'centrifuge-decant-wash' steps. A series of washings are performed with hydrochloric acid (30% HCl; twice), followed by deionised water (6 – 8 times). The HCl removes the metal and acid residues, while water is used to remove excess acid (Marcano et al., 2010). The material remaining after this multiple wash process was then transferred to open Petri dishes and placed in an oven (35 °C, 36 hours) till dry; a yield of around 5.8 g of the GO was usually obtained through this reaction.

2.2. Synthesis of iron-oxide-modified reduced-GO composite, FeG

Based on a method elucidated by Cong et al. (2012), the GO-product (as synthesised above) was further modified by adding an Fe-salt. First, a stable suspension of well-exfoliated GO (2 mg/mL) was prepared by adding 400 mg of GO in 200 mL deionised water, stirring magnetically for 12 hours, and then placing in a sonicating bath for 1 hour. Due to the negatively charged functional groups on the GO surface, a uniform suspension is formed. Care was taken to ensure no lumps were formed. Ferrous sulphate heptahydrate ($FeSO_4.7H_2O$; 5.5 grams – approximately 20 mmol) was then added to the suspension and stirred for 10 minutes, until dissolved.

After adjusting the pH to ~ 3.5 using ammonia, the suspension was poured into sealed glass reaction vessels. These were then placed in silicone-oil baths at 90 °C for 6 hrs without stirring, and subjected to hydrothermal reduction. The ferrous ions (Fe^{2+}) act as reducing agents to reduce the oxygen-functional groups on the GO sheets (Cong et al., 2012). As the GO starts reducing, the dispersability of the suspended sheets decreases, resulting in a 'stacking' or self-assembly of reduced-GO sheets to form a 3-dimensional interconnected network. This is accompanied by simultaneous *in situ* deposition of Fe-oxide nanoparticles (i.e., α-FeOOH nanorods; goethite) on the graphene sheets (Cong et al., 2012). In a time-dependent manner, the aggregated sheets float towards the top of the water level in the reaction vessel, until a black FeG hydrogel monolith is formed, leaving behind a transparent solution. The hydrogel was then separated, washed, and freeze dried to form an aerogel of FeG, which was crushed and used as a powdered product.

Following the synthesis of GO and FeG (illustrated schematically below), the two GBMs were characterised along with RemB to determine their structural properties based on various microscopic and spectroscopic techniques, as described in the following sections. Surface charge (zeta potential) and surface charge were also determined.

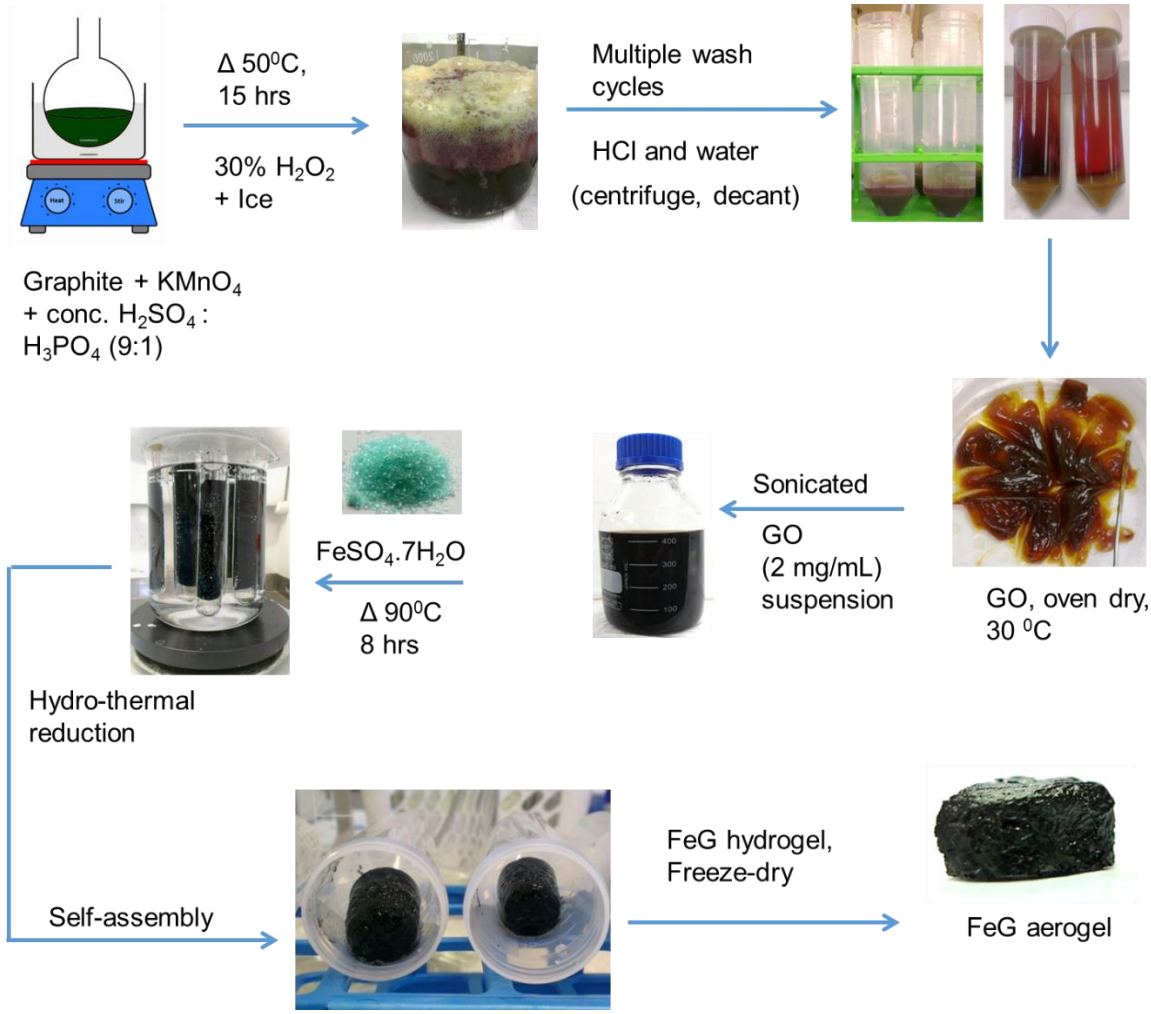

Schematic Illustration: A step-by-step schematic and pictorial illustration of the process of synthesis of the two chosen graphene-based adsorbents – graphene oxide (GO), and (b) an Fe-oxide-modified reduced-GO (FeG) composite.

3. Sample Preparation for Characterisation of Adsorbents

3.1. Electron microscopy techniques

All adsorbents – GO, FeG and RemB – were imaged *via* scanning electron microscopy (SEM; Philips XL20, Waite Microscopy) to determine the structural morphology of the adsorbents. The microscope was coupled with an energy dispersive X-ray (EDX) detector to provide elemental identification and composition of the adsorbents. Higher resolution imaging was conducted for GO and FeG using transmission electron microscopy (TEM; Philips CM100, Waite Microscopy). SEM-EDAX samples were prepared by applying the dried adsorbents directly onto aluminium stubs covered with adhesive carbon tape. Images were obtained using a spot size of 3, and an accelerating voltage of 10 kV. For TEM,

adsorbents were ultra-sonicated in ethanol (20 min), after which the suspensions were drop-casted onto a Lacey copper grid and dried for a few hours before imaging at an accelerating voltage of 100 kV. The SEM and TEM images are shown in Figure 1.

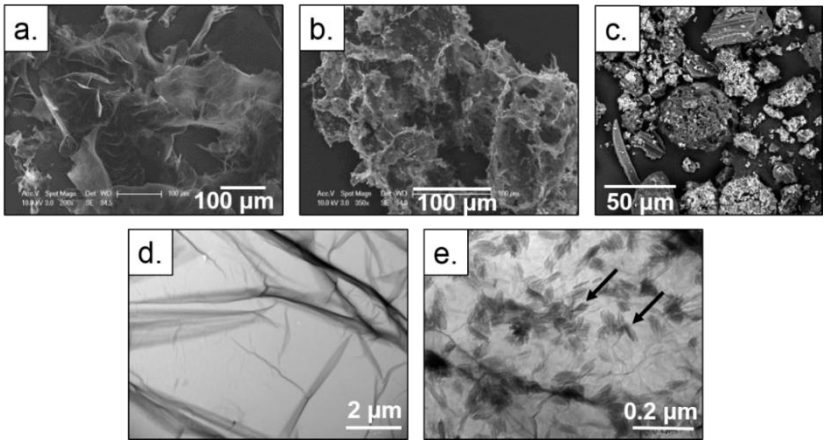

Figure 1. SEM images of (a) graphene oxide (GO), (b) Fe-oxide-modified reduced-GO (FeG), and (c) RemBind™. TEM images of (d) GO, and (e) FeG. Dark spots in 1(e) confirm the attachment of Fe-based nanoparticles.

Oxidation of raw graphite in the presence of strong acids resulted in the formation of thin GO sheets (Figure 1a and 1d) due to the exfoliation and separation of stacked graphitic layers. Hydrothermal reduction of GO with Fe^{2+} led to the formation of FeG (Figure 1b and 1e); attached Fe-oxide-based nanoparticles are seen as dense spots (50 - 100 nm) on the surface (Figure 1d). The commercial adsorbent, RemB (Figure 1c), is a powdered mixture of activated carbon, amorphous Al-hydroxide, kaolin clay and other proprietary additives (Ziltek Pty. Ltd.).

EDX spectra confirmed the elemental composition of the adsorbents (Figure 2 and Table 1), all of which exhibited the presence of C and O – these are indicative of the carbonaceous nature of all adsorbents. No other elements were detected in the case of GO. On the other hand, FeG displayed an additional signal for Fe, confirming the attachment of Fe-based particles following hydrothermal reduction of GO with $FeSO_4.7H_2O$. The Fe-based nanoparticles were determined to be in the size range of 50 – 100 nm. Similarly, RemB displayed additional signals for Al and Si, corroborating the presence of clay and Al-based components in the composite mixture. Thus, GO was determined to be a purely carbonaceous adsorbent, while FeG and RemB were confirmed to be 'mixed' adsorbents with multiple components.

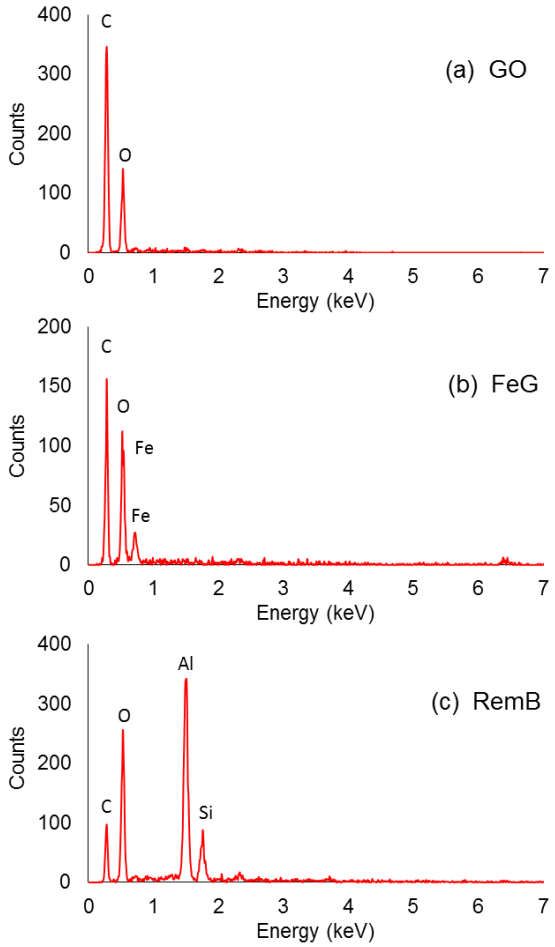

Figure 2. Energy dispersive X-ray (EDX) spectra collected for adsorbents GO, FeG and RemBind™ (RemB).

Table 1. Energy dispersive X-ray (EDX) elemental composition of GO, FeG and RemB.

Adsorbent	Element (series)	Weight %	Atomic %
GO	C (K)	65.88	72.01
	O (K)	34.12	27.99
FeG	C (K)	37.19	56.39
	O (K)	28.48	32.42
	Fe (K)	34.34	11.20
RemB	C (K)	22.42	34.37
	O (K)	27.70	31.89
	Si (K)	38.63	26.36
	Al (K)	11.26	7.38

3.2. X-Ray diffraction analysis

X-ray diffraction (XRD) analysis was performed for phase-identification and determination of crystallinity of the adsorbents. XRD patterns were recorded with a PANalytical X'Pert Pro Multi-purpose Diffractometer using Fe-filtered Co-Kα radiation, automatic divergence slit, 2° anti-scatter slit and fast X'Celerator Si strip detector. Patterns were recorded from 3 to 80° in steps of 0.017° 2 theta with a 0.5 second counting time per step for an overall counting time of approximately 35 minutes. Qualitative analysis was performed on the XRD data using XPLOT and commercial HighScore Plus (from PANalytical) search/match software using the PDF-4+ database of organic and inorganic compounds from the International Centre for Diffraction Data (ICDD). The composition of the samples are shown in Figures 3a, 3b and 3c. The unidentified peaks in the graphene oxide sample at 7.16Å, 3.58Å, 2.38Å and 1.79Å (Figure 3a) also indicate an oriented platy phase with a basal (in the direction of orientation) unit cell of ~7.16Å. The regular d-spacings are 7.16Å divisible by 1, 2, 3 and 4 respectively. Goethite was the only identified crystalline phase in the FeG sample (Figure 3b). The dominant amorphous content in the RemB sample (Figure 3b) is indicative of activated carbon, with peaks for minor quartz, trace kaolin and, muscovite and hematite.

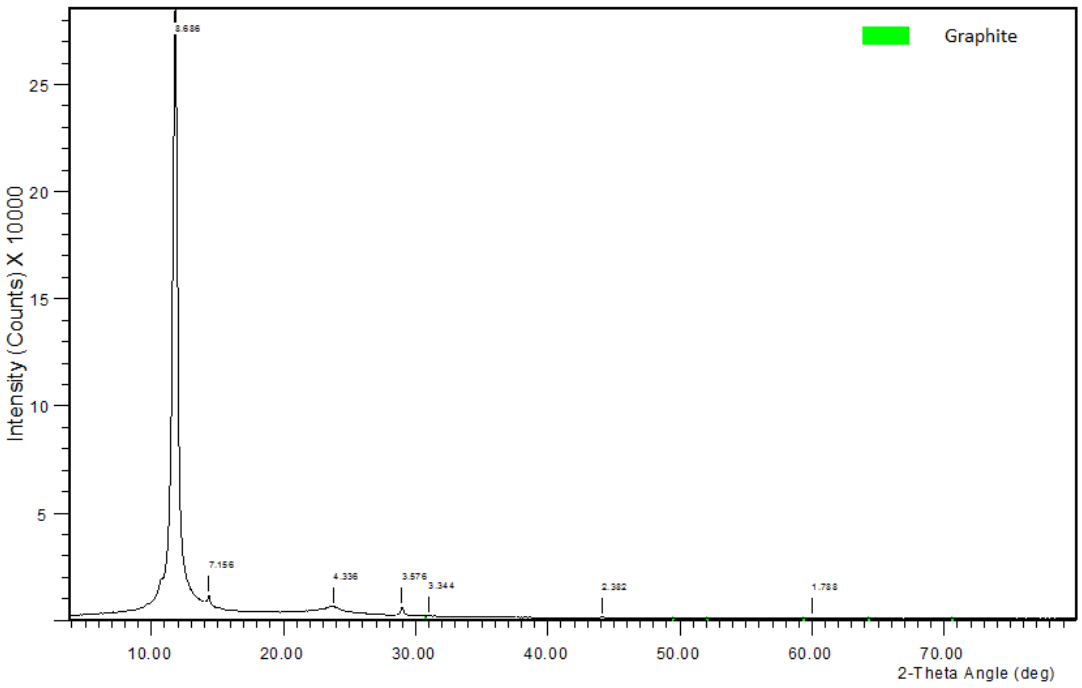

Figure 3a. X-ray diffraction (XRD) spectra of graphene oxide (GO).

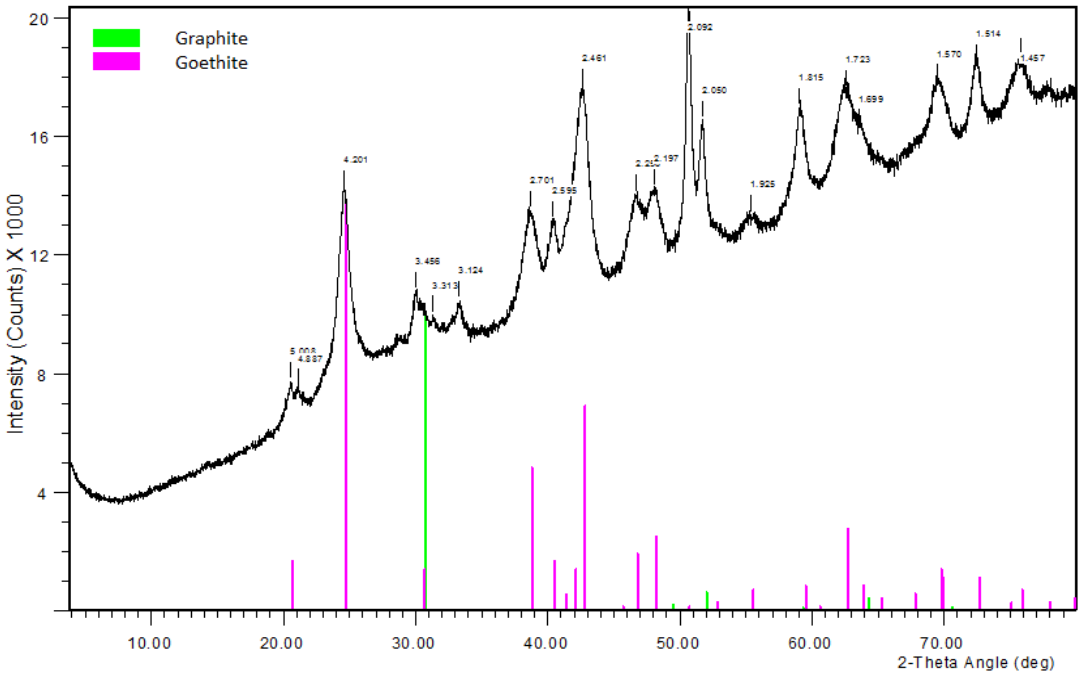

Figure 3b. X-ray diffraction (XRD) spectra of iron-oxide-modified reduced-GO (FeG).

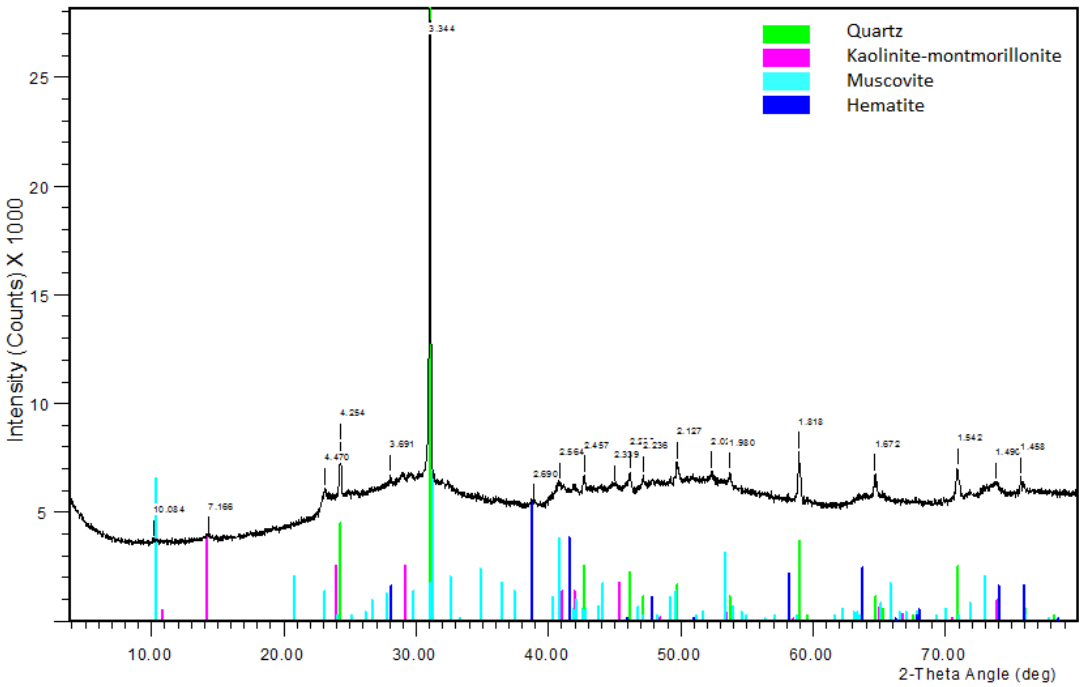

Figure 3c. X-ray diffraction (XRD) spectra of mixed adsorbent, RemBind™ (RemB).

3.3. Fourier transform infrared spectroscopy

To obtain further information about the specific bonds and functional groups, Fourier transform infrared (FTIR; Nicolet 6700 Thermo Fisher) spectroscopy was perfo rmed using

powdered samples of all adsorbents. Spectra were recorded at wavelengths ranging from 400 - 4000 cm^{-1} in transmission mode, using the OMNIC™ Specta Software (Thermo Scientific). FTIR spectra (Figure 4) revealed characteristic peaks of GO including the CO_2H stretching (1725 cm^{-1}) and COH bending vibrations (1220 cm^{-1}) (Marcano et al., 2010), indicating the presence of carboxylic and alcohol groups capable of binding cations. Additional peaks associated with Fe-OH bending (768 and 871 cm^{-1}), and Fe-O stretching vibrations (575 cm^{-1}) (Cong et al., 2012) on FeG confirm the attachment of goethite minerals.

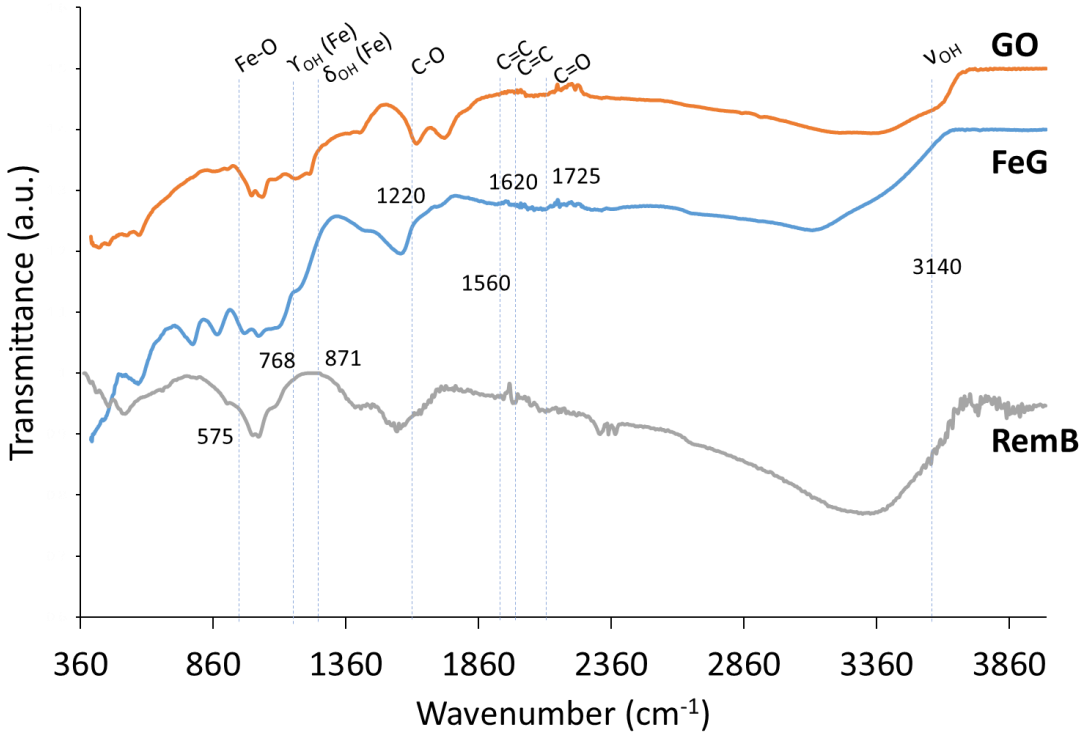

Figure 4. Fourier-transform infrared (FTIR) spectra of adsorbents graphene oxide (GO), Fe-oxide-modified reduced-GO (FeG) and RemBindTM (RemB).

3.4. Surface zeta potential measurements

Surface charge properties and point of zero charge (PZC) were determined by measuring zeta potential of the adsorbents across a pH gradient using dynamic light scattering (Malvern Zetasizer NanoZS). Suspensions of adsorbents were prepared in Milli-Q water (0.1 % w/v); pH values were adjusted using sodium hydroxide (NaOH) or HCl. The suspensions were allowed to equilibrate by magnetically stirring for 48 hours, after which aliquots (in triplicate) were transferred to folded capillary cells for measurement *via* dynamic light scattering (DLS).

Surface charge for FeG and RemB varied notably with pH (Figure 5), with their PZC (pH at which zeta potential is zero) measured at 7.1 and 5.7, respectively. At pH values above the PZC, these adsorbents display a net negative surface charge, whereas at pH below the pZC, they exhibit a net positive surface charge. Iron and Al-based oxide and hydroxide minerals are known to have an amphoteric nature (Kasprzyk-Hordern, 2004); their surface charge properties are dependent on pH. The Fe- and Al-mineral components in FeG and RemB may play a dominant role in controlling the zeta potential of the surface. Conversely, GO maintained a highly negative charge across the pH range, even in low pH conditions; with a greater magnitude of negative charge at higher pH. The net negative charge of GO can be attributed to the negatively charged oxygen-functional groups on the surface as identified *via* FTIR spectra.

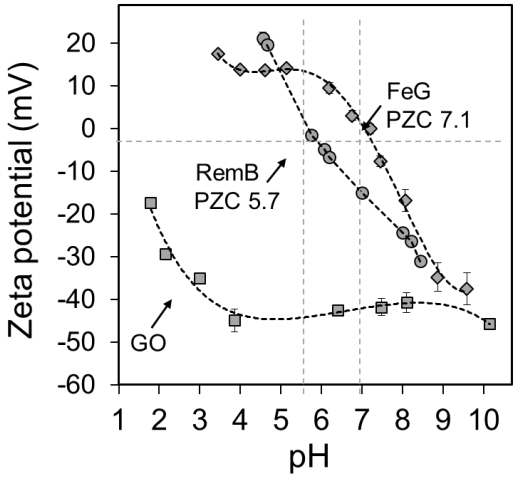

Figure 5. Surface zeta potential measurements of GO, FeG and RemB across a pH gradient (pH 2 – 10) at 25 °C.

3.5. Specific surface area measurements

Specific surface area (SSA) of adsorbents were measured using the methylene blue (MB) dye-absorption method (Montes-Navajas et al., 2013) commonly used for carbonaceous materials. 15 mg of each adsorbent was added to 150 mL of 20 mg/L MB solutions and shaken for 60 h at 100 rpm to allow the solutions to attain equilibrium and maximum absorption. After centrifugation, supernatants were analysed using UV-vis spectrophotometry (at 664 nm) and compared to controls to determine the amount of MB absorbed. The MB concentrations were calculated using a calibration curve (Figure 6) of absorbance measured using standard solutions of known concentrations (0 – 10 mg/L).

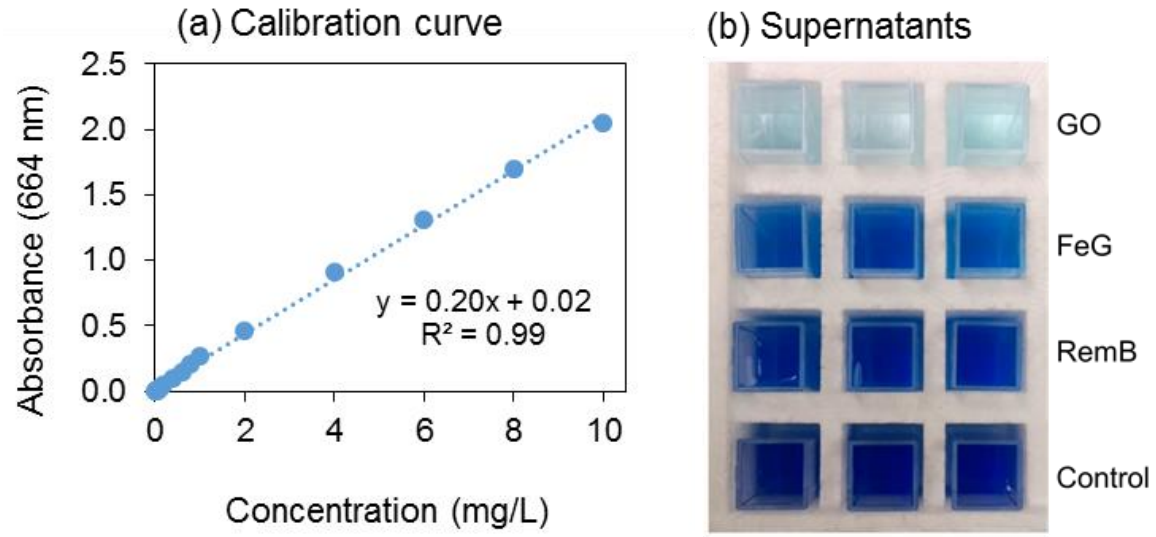

Figure 6. (a) Methylene blue standard calibration curve (664 nm) using standard solutions of known concentrations (0 – 10 mg/L, at 25 °C), and (b) image of supernatants after sorption of methylene blue by GO, FeG and RemB, compared to the control solution where no adsorbent was added.

The SSA was then calculated using the following equation:

$$\mathrm{SSA} = \frac{N_\mathrm{A}\, A_\mathrm{MB}\, (C_\mathrm{i} - C_\mathrm{e})\, V}{M_\mathrm{MB}\, m_\mathrm{s}}$$

where N_A represents the Avogadro number (6.023×10^{23} molecules/mole), A_{MB} is the area covered per MB molecule (1.35 nm^2), C_i and C_e are the initial and equilibrium MB concentrations, respectively, V is the volume of MB solution, M_{MB} is the molecular mass of MB, and m_s is the mass of the adsorbent. Calculations are presented in Table 2 below.

Surface areas of GO, FeG and RemB were determined to be 434.6, 242.4 and 123.4 m^2/g, respectively. The degree of exfoliation as well as the oxidation level of the graphene layers during the synthesis of GO from graphite determines its surface area (Montes-Navajas et al., 2013). On hydrothermal reduction to form FeG, the loss of oxygen functional groups leads to agglomeration of the graphene-sheets (Cong et al., 2012), resulting in a decrease in the surface area. The deposition of Fe-oxide nanoparticles on the surface of reduced GO may also impact surface area, but the overall reduction in the case of FeG can be attributed to the self-assembly of the graphene sheets during the formation of the hydrogel monolith. Yet, both GBMs displayed a high surface area, compared to RemB, which is composed mainly of activated carbon, kaolinite and Al-hydroxide. Kaolinite clay is known to have a surface area

of around 25 m^2/g (Avena et al., 2001), indicating that the other components of RemB help increase the surface area.

Table 2. Equilibrium methylene blue concentration measured after sorption by GO, FeG and RemB, and calculated specific surface areas.

Sample ID (triplicate)	Absorbance measured (at 664 nm)	Equilibrium concentration C_e, mg/L	Average Ce mg/L	Amount of MB absorbed (C_i - C_e) mg/L	Specific Surface Area SSA, m^2/g
Control	2.018	19.14	19.23 (C_i)	na	na
Control	2.008	19.04			
Control	2.057	19.51			
GO	0.045	0.12	0.21	19.02	434.57
GO	0.091	0.34			
GO	0.057	0.18			
FeG	1.883	8.92	8.62	10.61	242.35
FeG	2	9.48			
FeG	1.579	7.47			
RemB	1.453	13.73	13.83	5.40	123.38
RemB	1.449	13.69			
RemB	1.49	14.08			

4. Summary

Two different types of GBMs were synthesised in the laboratory and successfully characterised for use as adsorbents – GO (an oxidised GBM), and FeG (and Fe-oxide modified reduced GO). A commercial adsorbent, RemB was also chosen to compare sorption performance and behaviour. Due to their different surface and charge properties, all 3 adsorbents were expected to interact differently to bind As, Cd, PFOA and PFOS *via* a variety of mechanisms. While GO was primarily a carbonaceous adsorbent, FeG and RemB were mixed-mode adsorbents, comprised of both mineral and carbonaceous phases, potentially offering multiple binding sites.

5. References

Avena MJ, Valenti LE, Pfaffen V, De Pauli CP (2001). Methylene blue dimerization does not interfere in surface-area measurements of kaolinite and soils. *Clays and Clay Minerals,* **49,** 168-173.

Cong H-P, Ren X-C, Wang P, Yu S-H (2012). Macroscopic multifunctional graphene-based hydrogels and aerogels by a metal ion induced self-assembly process. *ACS Nano,* **6,** 2693-2703.

Dimiev AM, Tour JM (2014). Mechanism of graphene oxide formation. *ACS Nano,* **8,** 3060-3068.

Dreyer DR, Park S, Bielawski CW, Ruoff RS (2010). The chemistry of graphene oxide. *Chemical Society Reviews,* **39,** 228-240.

Georgakilas V, Otyepka M, Bourlinos AB, Chandra V, Kim N, Kemp KC, Hobza P, Zboril R, Kim KS (2012). Functionalization of graphene: covalent and non-covalent approaches, derivatives and applications. *Chemical Reviews,* **112,** 6156-6214.

Kasprzyk-Hordern B (2004). Chemistry of alumina, reactions in aqueous solution and its application in water treatment. *Advances in Colloid and Interface Science,* **110,** 19-48.

Marcano DC, Kosynkin DV, Berlin JM, Sinitskii A, Sun Z, Slesarev A, Alemany LB, Lu W, Tour JM (2010). Improved synthesis of graphene oxide. *ACS Nano,* **4,** 4806-4814.

Montes-Navajas P, Asenjo NG, Santamaría R, Menéndez R, Corma A, García H (2013). Surface area measurement of graphene oxide in aqueous solutions. *Langmuir,* **29,** 13443-13448.

Novoselov KS, Falko VI, Colombo L, Gellert PR, Schwab MG, Kim K (2012). A roadmap for graphene. *Nature,* **490,** 192-200.

Zhu Y, Murali S, Cai W, Li X, Suk JW, Potts JR, Ruoff RS (2010). Graphene and graphene oxide: synthesis, properties, and applications. *Advanced Materials,* **22,** 3906-24.

CHAPTER 3. Mixed-Mode Remediation of Cadmium and Arsenate Ions Using Graphene-Based Materials

The work contained in this chapter has been published in *CLEAN – Soil, Air, Water.*

RESEARCH PAPER

CLEAN Soil Air Water

www.clean-journal.com

Mixed-Mode Remediation of Cadmium and Arsenate Ions Using Graphene-Based Materials

Supriya Lath, Divina Navarro, Diana Tran, Anu Kumar, Dusan Losic, and Michael J. McLaughlin*

First published: 14 July 2018
https://doi.org/10.1002/clen.201800073

Volume46, Issue9, 1800073, September 2018

Statement of Authorship

Title of Paper	Mixed-mode remediation of cadmium and arsenate ions using graphene-based materials
Publication Status	☐ Published; ☑ Accepted for publication; ☐ Submitted for publication; ☐ Unpublished and unsubmitted work prepared in manuscript style for publication
Publication Details	CLEAN – Soil, Air, Water; DOI: 10.1002/clen.201800073

Principal Author

Name (Candidate)	Supriya Lath		
Contribution to the Paper	Experimental development; set-up and performed experiments; data analysis and critical interpretation; wrote the manuscript; acted as corresponding author.		
Overall percentage (%)	85%		
Certification:	This paper reports on original research I conducted during the period of my Higher Degree by Research candidature and is not subject to any obligations or contractual agreements with a third party that would constrain its inclusion in this thesis. I am the primary author of this paper.		
Signature		Date	3 Sept 2018

Co-Author Contributions

By signing the Statement of Authorship, each author certifies that: the candidate's stated contribution to the publication is accurate (as detailed above); permission is granted for the candidate in include the publication in the thesis; and the sum of all co-author contributions is equal to 100% less the candidate's stated contribution.

Divina A. Navarro	Assisted with project development; experimental design; data interpretation; manuscript evaluation.		
Signature		Date	28Aug 2018

Diana N. H. Tran	Advised in synthesis and characterisation aspects of graphene-based materials.		
Signature		Date	30/08/2018

Anu Kumar	Assisted in project planning; experimental design; manuscript evaluation.		
Signature		Date	28 Aug 2018

Dusan Losic	Assisted in project planning; advised on graphene-materials; manuscript evaluation.		
Signature		Date	30/08/2018

Michael J. McLaughlin	Supervised project development; experimental design; data interpretation; manuscript evaluation.		
Signature		Date	3rd Sept 2018

Mixed-mode remediation of cadmium and arsenate ions using graphene-based materials

Supriya Lath [*, 1], Divina Navarro [1, 2], Diana Tran [3], Anu Kumar [2], Dusan Losic [3], Michael J. McLaughlin [1, 2]

[1] School of Agriculture Food and Wine, The University of Adelaide, PMB 1 Glen Osmond, SA 5064, Australia.

[2] CSIRO Land and Water, PMB 2 Glen Osmond, SA 5064, Australia.

[3] School of Chemical Engineering, The University of Adelaide, Adelaide, SA 5005, Australia.

* Corresponding author (email: supriya.lath@adelaide.edu.au)
Ms. Supriya Lath, School of Agriculture Food and Wine, The University of Adelaide, PMB 1 Glen Osmond, SA 5064, Australia.

Abstract

Cadmium (Cd) and arsenate (As) are notorious environmental contaminants, and co-contamination usually requires opposing treatment strategies due to their differing physico-chemical properties. Developing adsorbents that can bind both contrasting contaminants simultaneously is desirable. Two prepared graphene materials, graphene oxide (GO) and iron-oxide-modified reduced-GO (FeG), were evaluated for Cd- and As-sorption, and performance was compared to a mixed-mode commercial adsorbent. Negatively-charged GO showed affinity towards cationic Cd, and positively-charged FeG showed affinity towards anionic As. Sorption was pH dependent: increase in pH promoted Cd-sorption and decreased As-sorption. GO displayed excellent Cd-sorption even in acidic conditions. The maximum amounts adsorbed by GO and FeG, were 782 µmol Cd/g and 408 µmol As/g, respectively. Competition by calcium strongly suppressed Cd-sorption, whereas competition by phosphate did not hinder As-sorption. A mixture of GO and FeG demonstrated successful simultaneous sorption of Cd and As from co-contaminated solutions, including a natural water sample, displaying greater sorption than the commercial adsorbent. Data highlight the potential application of graphene materials in effective mixed-mode remediation of multiple contaminants (cations and anions).

Keywords: arsenic; cadmium; graphene; mixed-mode remediation; sorption.

1. Introduction

Extensive industrial activities have caused contaminants to accumulate in the environment above safe levels. A variety of contaminants with different physico-chemical properties often co-exist, and remediation requires complex multi-treatment processes like chemical treatment or physical removal (Koptsik, 2014), which can be costly and energy-intensive. In this regard, adsorption has been applied widely as a simple and efficient technique in water (Arai et al., 2005) and soils to mitigate risks by reducing contaminant-mobility and availability (Koptsik, 2014, Lim et al., 2013).

Recently, advanced nanomaterials such as carbon nanotubes (CNTs) and graphene-based materials (GBMs) have been used for sorption (Smith and Rodrigues, 2015). Graphene, a single-atom thick layer of graphite (Novoselov et al., 2012), has been being explored for use in several applications due to its unique properties (Novoselov et al., 2012), and is an excellent candidate for use as an adsorbent due to its high surface area (Niu et al., 2014). Its most common derivative, graphene oxide (GO), contains negative oxide functionalities including epoxides, carbonyls, carboxyls and hydroxyls, which make it possible to attract cations (Sitko et al., 2013, Zhao et al., 2011), and lend it a versatile surface chemistry for further modifications (Dreyer et al., 2010, Marcano et al., 2010). Such control over the surface properties of GBMs allows for interaction with different types of contaminants *via* multiple mechanisms, offering opportunities for effective mixed-mode remediation (Chowdhury and Balasubramanian, 2014).

Cadmium (Cd) and arsenic (As), released into the environment *via* mining operations and application of fertilisers and sewage sludge, are notorious for posing human health risks through intake of contaminated food and water (Hughes, 2002, Lim et al., 2013). Dissolved concentrations of up to 122 ng/L Cd and 1000 µg/L As have been reported in contaminated surface waters (Nriagu et al., 2007, Stephenson and Mackie, 1988). Total concentrations of up to 1000 mg/kg or greater have been reported in contaminated soils (Buchauer, 1973, Wenzel et al., 2002), while the more relevant 'labile' fractions (e.g. soil solution) may contain Cd or As in the range of 10 – 300 µg/L (Wenzel et al., 2002). In the environment, Cd is mainly present in its free cationic form, Cd^{2+} (Lambert et al., 1997). Arsenic can occur in organic and inorganic forms, however the pentavalent arsenate anion (described henceforth as 'As' in this study) predominates in normal oxidising environments, primarily as $H_2AsO_4^-$ (pH 2.5 – 6.5) and $HAsO_4^{2-}$ (pH 6.5 – 12) (Hughes, 2002). Adsorption and precipitation using lime and Fe-oxide based materials are common techniques used to bind Cd and As, respectively (Lambert et al., 1997, Manceau, 1995, Warren et al., 2003). Recently, more novel materials like MnO_2-functionalised CNTs, magnetic Fe-oxide microspheres, as well as

GO have been demonstrated for their Cd-sorption potential (Jia et al., 2013, Luo et al., 2013). Likewise, nano zero-valent Fe (nZVI), magnetite and other Fe-based graphene composites have been used for enhanced As-sorption (Andjelkovic et al., 2014, Chandra et al., 2010, Zhu et al., 2009).

Co-contamination with Cd and As is common in some countries where exposure due to consumption of rice staples from mine-impacted farmlands is a matter of concern (Arao et al., 2009). However, due to their contrasting physico-chemical properties, Cd and As require different strategies for their management. E.g., while Fe-oxide based amendments can effectively immobilise As in soil, some of them were found to increase leachability of heavy metals cations (Hartley et al., 2004). Similarly, increase in pH due to lime-application for Cd-management in soils may concurrently mobilise other negatively-charged contaminants (Lim et al., 2013). Diammonium phosphate, which was found to be highly effective for reducing leachability and transport of Cd, zinc and lead from a contaminated smelter soil, was also shown to increase leachability of arsenic from the same soils (Basta and McGowen, 2004). To avoid such counter-productive treatment processes and improve efficiency, it is crucial to develop adsorbents that target both contaminants simultaneously.

In this work, two GBMs, GO and an Fe-oxide-modified reduced-GO (described henceforth as FeG), were prepared to bind Cd and As, respectively, using different surface chemistry and active sorption sites. The oxygen groups on GO were expected to show affinity towards Cd, and the Fe-active sites on FeG to display affinity towards As. The influence of different pH conditions, concentrations, and presence of relevant competing ions on sorption were investigated, and performance compared with a commercial adsorbent, RemBind™ (RemB), which is capable of binding a range of contaminants simultaneously. A combination of GO and FeG was then tested for simultaneous sorption of Cd and As. Sorption was also tested in a natural water sample to evaluate the potential use of GBMs as mixed-mode adsorbents. The significance of this work is to gain better fundamental understanding of key parameters affecting sorption by GBMs and to design advanced adsorbents with multiple functions for simultaneous sorption of multiple heavy metal contaminants.

2. Materials and Methods

2.1. Materials

Natural graphite flakes were obtained from the Uley graphite mine (South Australia). All chemicals including potassium permanganate, sulfuric acid, phosphoric acid, hydrogen peroxide, ferrous sulphate heptahydrate, hydrochloric acid (HCl), sodium hydroxide (NaOH), cadmium nitrate tetrahydrate, sodium arsenate dibasic heptahydrate, calcium nitrate tetrahydrate and sodium phosphate dibasic dihydrate were of analytical grade. The

commercial adsorbent RemBind™ was supplied by an environmental remediation company (Ziltek Pty Ltd, South Australia).

2.2. Synthesis and characterisation of adsorbents

Two adsorbents were synthesised using graphite as the base material. Briefly, strong oxidative exfoliation of graphite was performed to prepare GO (Marcano et al., 2010), which was used as flakes. The GO was then hydrothermally reduced in the presence of Fe^{2+} (Cong et al., 2012), to form an Fe-oxide-modified reduced-GO powder (FeG). Morphology of the adsorbents was examined by scanning electron microscopy (SEM, Philips-XL20) and transmission electron microscopy (TEM, Philips-CM100). An energy dispersive X-ray (EDX) detector coupled to the SEM elucidated elemental composition. X-ray diffraction (XRD, PANalytical X'Pert Pro MPD) and Fourier-transform infrared (FTIR, Nicolet 6700, Thermo Fisher) spectra provided structural and functional information. Surface area was determined by the methylene blue adsorption method. Surface charge (reported as zeta potential) and point of zero charge (PZC) were measured using a Malvern Zetasizer NanoZS. Detailed methods are provided in the supporting information.

2.3. Batch sorption studies

Cadmium nitrate and sodium arsenate salts were used to prepare contaminated solutions. Batch sorption tests were carried out by mixing 15 mg adsorbent with 45 mL of the Cd and As-solutions, under constant agitation on an orbital shaker (100 rpm, 25 °C) for 24 hrs to attain equilibrium. Solutions were then centrifuged and filtrates (0.45 µm syringe filters) collected. Concentrations of As, calcium (Ca), Cd and phosphorus (P) in filtrates were measured by inductively-coupled plasma optical emission spectroscopy (ICP-OES); detection limits were 0.009, 0.010, 0.003 and 0.005 mg/L, respectively.

The influence of pH on sorption was investigated for Cd and As solutions of different concentrations (0, 100, 250, 500 and 1000 µM), across pH ranging from 3 to 8. Test solutions were prepared in a background of 5 mM KNO_3 to minimise effects of ionic strength variability. Minimal volumes (< 100 µL) of 1M HCl or NaOH were used to adjust pH. The effect of soluble Ca and inorganic phosphates (described henceforth as P) as competing ions on Cd and As-sorption, respectively, were tested at a fixed pH (5.5 ± 0.03). Soluble Ca salts are usually present in the environment at much higher concentrations compared to heavy metals (Tiller et al., 1979), whereas P-concentrations in soil solutions rarely exceed 10 µM (Schachtman et al., 1998). Concentrations of Ca and P ions were thus chosen to reflect realistic environmental conditions. Sorption of 250 µM solutions of Cd and As was investigated in the presence of varying concentrations of Ca (0 - 50 mM) and P (0 - 25 µM) solutions, respectively.

To assess the potential of GO and FeG for mixed-mode sorption, a 1:1 weight ratio of GO and FeG was combined (GO+FeG) and mixed with co-contaminated solutions of Cd and As at a fixed pH of 5.5. Contaminant mixture concentrations ranged from 100 µM Cd + 100 µM As to 600 µM Cd + 600 µM As. Sorption was also tested in a natural water sample collected from a dam in Urrbrae, South Australia (pH 7.9), spiked with Cd (5.9 µM) and As (5.1 µM), to assess efficiency in a real environmental matrix.

2.4. Data analyses

The amount of contaminant adsorbed was calculated as the difference between concentrations in solution before and after sorption equilibrium. Performance of adsorbents was expressed as the amount adsorbed per gram of adsorbent (µmol/g). Experiments were performed in triplicate; analysis of variance was used to determine if treatments were significantly different ($p \leq 0.05$) from control groups.

Freundlich (Equation 1) and Langmuir (Equation 2) isotherm models were used to fit the sorption data:

$$q_e = K_F\, C_e^n \qquad \text{..... (1)}$$

$$q_e = q_m\, K_L\, C_e \,/\, (1 + K_L\, C_e) \qquad \text{..... (2)}$$

where, q_e (µmol/g) is the amount adsorbed per unit mass of adsorbent at equilibrium, and C_e (µM) is the equilibrium solution concentration of the adsorbate. The Freundlich constant, K_F (L/g), relates to sorption strength, and n describes how sorption varies with solution concentration (Deng et al., 2010), with values usually ranging from 0 to 1 for saturable sorption, and $n > 1$ indicates cooperative sorption (e.g. precipitation) (Hameed et al., 2007). The Langmuir constant, K_L (L/µmol), is the equilibrium constant, and q_m is the maximum monolayer sorption capacity (µmol/g).

3. Results and Discussion

3.1. Characterisation of adsorbents

The morphology of GO and FeG were examined using SEM and TEM imaging (Figure 1). Oxidative exfoliation of graphite resulted in the formation of thin GO sheets (Figure 1a and 1d). Hydrothermal reduction of GO with Fe^{2+} led to the formation of an Fe-oxide-modified reduced-GO composite, FeG (Figure 1b and 1e); attached Fe-oxide-based nanoparticles are seen as dense spots (50 - 100 nm) on the surface (Figure 1d). The commercial adsorbent, RemB (Figure 1c), is a powdered mixture of activated carbon, amorphous Al-hydroxide, kaolin clay and other proprietary additives. EDX spectra confirmed the elemental composition of the adsorbents (Table S1 and Figure S1), all of which exhibited the presence

of carbon and oxygen. FeG displayed an additional signal for Fe, and RemB for Al and silicon.

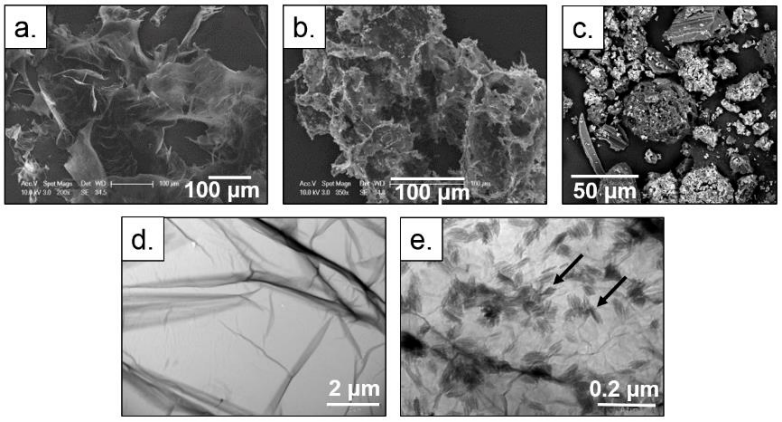

Figure 1. SEM images of (a) graphene oxide (GO), (b) Fe-oxide-modified reduced-GO (FeG), and (c) RemBind™. TEM images of (d) GO, and (e) FeG. Dark spots in 1(e) confirm the attachment of Fe-based nanoparticles (50 - 100 nm).

The structure and mineralogical phase of the adsorbents were confirmed by XRD (Figure S2). GO displayed an oriented 'platy' phase with a unit cell of 7.16Å, consistent with monolayer spacings typically observed for GO (Marcano et al., 2010). Goethite (α-FeOOH) mineral, known for its affinity towards As, was detected as the crystalline phase in FeG, confirming the identity of the Fe-oxide nanoparticles. A dominant amorphous activated carbon phase was detected in RemB, along with aluminosilicate clays, kaolinite and muscovite, demonstrating its potential to bind a variety of contaminants. FTIR spectra (Figure S3) revealed characteristic peaks of GO including the CO_2H stretching (1725 cm^{-1}) and COH bending vibrations (1220 cm^{-1}) (Marcano et al., 2010), indicating the presence of carboxylic and alcohol groups capable of binding cations. Additional peaks associated with Fe-OH bending (768 cm^{-1} and 871 cm^{-1}), and Fe-O stretching vibrations (575 cm^{-1}) (Cong et al., 2012) on FeG confirm the attachment of goethite minerals.

The surface area and charge properties play an important role in adsorbent-adsorbate interactions. Surface areas of GO, FeG and RemB were determined to be 434.6, 242.4 and 123.4 m^2/g respectively (Figure S4). Surface charge for FeG and RemB varied notably with pH (Figure 2), with their PZC (pH at which zeta potential is zero) at 7.1 and 5.7 respectively. Conversely, GO maintained a highly negative charge across the pH range. The negative charge of GO can be attributed to the carboxylate and hydroxyl functional groups on the surface as identified *via* FTIR spectra. The modification of GO in the presence of $FeSO_4$ at low pH to synthesise FeG is accompanied by the reduction of the negative functional oxygen

groups and simultaneous oxidation of ferrous ions (Fe^{2+}) into ferric ions (Fe^{3+}) (Cong et al., 2012), imparting a slight positive charge on the FeG surface in those conditions. Consistent with these charge properties, preliminary sorption tests confirmed that negatively-charged GO showed no affinity towards As, and positively-charged FeG displayed no affinity towards Cd (data not shown). Thus, subsequent batch tests compared Cd-sorption of GO with RemB, and As-sorption of FeG with RemB.

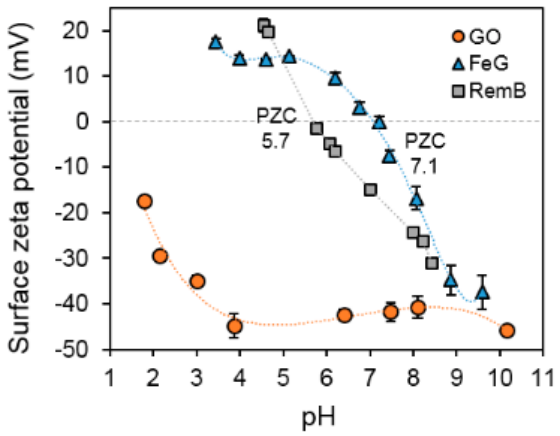

Figure 2. Surface zeta potential measurements of graphene oxide (GO), Fe-oxide-modified reduced-GO (FeG) and a commercial adsorbent, RemBind™ (RemB), as a function of pH (25 °C) to determine point of zero charge (PZC).

3.2. Effect of pH on Cd-sorption by GO and RemB

Amounts of Cd adsorbed by GO and RemB across a pH range of 3 – 8, calculated at different initial Cd-concentrations, are summarised in Table S2. Sorption of Cd was pH-dependent; greater sorption occurred as pH increased (Figure 3). This trend is in agreement with that demonstrated in previous research using GO and CNT-based materials (Bian et al., 2015, Luo et al., 2013, Sitko et al., 2013, Zhao et al., 2011), where, increased pH increases the negative surface charge of the adsorbents, leading to greater retention of Cd. There was a marked difference in Cd-sorption by GO and RemB; the amount adsorbed by GO was superior to that by RemB, regardless of pH or concentration. For instance, at an initial Cd-concentration of 1000 µM and a pH of 6.1, Cd-sorption by GO (760 µmol/g) was 6 times greater than RemB (120 µmol/g). For the same concentration, even at a low pH of 3.7, GO displayed remarkable Cd-sorption (490 µmol/g). Such high Cd-sorption at low pH is unlike that observed with typical adsorbents like lime-based materials, which rely on raising pH to immobilise Cd (Lim et al., 2013). This could be particularly beneficial in situations where Cd-

contaminated sites have acidic conditions due to the application of wastewater or industrial effluents. The results can be explained by considering the zeta potential of the adsorbents. It is known that Cd exists as a free cation up to pH 8 (Lambert et al., 1997). Since GO maintained a high negative charge across this pH range, it is able to successfully retain cationic Cd (Figure 3a). RemB, however, exhibits only a slight negative charge above pH 5.7, and hence, adsorbed minimal amounts of Cd even above the PZC (Figure 3b). Previous studies have demonstrated the role of GO's oxygenated functional groups in sorption of multivalent heavy metals such as lead and Cd through strong surface complexation and ion-exchange mechanisms (Bian et al., 2015, Zhao et al., 2011). Given the strong dependence on pH, electrostatic interactions between the negative functional groups of GO and positive Cd ions are likely the main mechanisms controlling sorption by GO. The greater sorption observed with GO could also be attributed to its high surface area, which was 4 times greater than RemB.

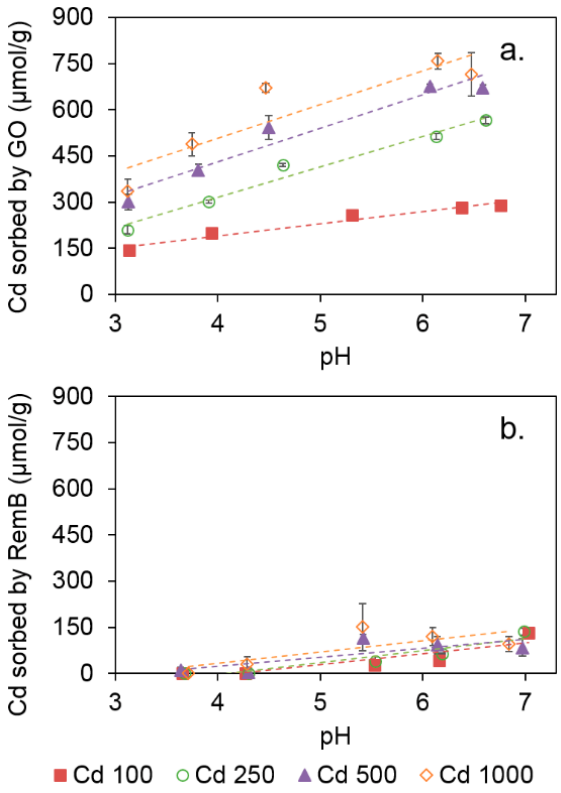

Figure 3. Effect of pH on amount of Cd sorbed by (a) graphene oxide (GO), and (b) RemBind™ (RemB). Initial concentration of Cd added was 0 - 1000 µM at pH 3 - 7 (25 °C). Lines show effect of increasing pH on amount of Cd sorbed per gram of adsorbent.

3.3. Effect of pH on As-sorption by FeG and RemB

Amounts of As adsorbed by FeG and RemB across a pH range of 3 – 8, calculated at different initial As-concentrations, are summarised in Table S3. Both FeG and RemB displayed similar sorption behaviour towards As, with sorption increasing as solution pH decreased (Figure 4). At an initial As-concentration of 250 µM, as pH dropped from 7.3 to 3.5, As-sorption by FeG increased from 95 to 300 µmol/g, and by RemB increased from 95 to 160 µmol/g. These results are consistent with previous reports of enhanced As-sorption at lower pH (Chandra et al., 2010, Zhu et al., 2009). For example, As-sorption by an activated carbon-nZVI complex increased by almost 100% when pH decreased from 12 to 3 (Zhu et al., 2009). Similarly, As-sorption by a magnetite-based graphene composite increased from 13 to 160 µmol/g on decreasing pH from 10 to 4 (Chandra et al., 2010). The pH-dependent As-sorption can partially be explained by the zeta potential of the adsorbents. Below their PZC of 7.1 and 5.7, respectively, FeG and RemB are positively-charged, enabling electrostatic interactions with the negative As ions. At pH values above the PZC, the increase in negatively-charged sites should result in reduced affinity for As due to increased repulsion (Guo and Chen, 2005). While a decrease in sorption was evident, reasonable amounts of As were nevertheless adsorbed by both adsorbents above their PZC (Figure 4), indicating the involvement of additional adsorptive mechanisms. Previous studies have shown that As-ions can be retained on Fe-oxyhydroxide minerals through inner-sphere ligand-exchange mechanisms (Jain et al., 1999, Manceau, 1995) with hydroxyl groups at the mineral surface (Jain et al., 1999, Jia et al., 2013). XRD spectra of FeG revealed the presence of goethite (α-FeOOH) in its structure. Hence, the As-sorption by FeG (Figure 4a) at pH > 7.1 could be attributed to ligand-exchange, promoted by the goethite mineral phase. XRD analysis of FeG after As-sorption revealed no changes to the goethite crystalline phase (Figure S5); no new phases (e.g. Fe-As precipitates like scorodite) were formed. Similarly, sorption by RemB (Figure 4b) at pH > 5.7 could be driven by other mechanisms. The kaolinite (aluminosilicate clay) component of RemB can participate in ligand-exchange between As and surface-coordinated hydroxyl and silicate ions – the same mechanism reported for As-sorption at the allophane-water interface (Arai et al., 2005). Another process likely to facilitate As-binding by RemB is precipitation. Substantial dissolution of the amorphous Al-hydroxide component of RemB was observed at pH values below 5 and above 7 (Figure S6). Once in solution, Al can form an insoluble amorphous Al-arsenate (K_{sp}=10^{-15}-10^{-18}) precipitate with As (Pantuzzo et al., 2014). Thus some of the As-removal at low pH could also be attributed to precipitation with dissolved Al.

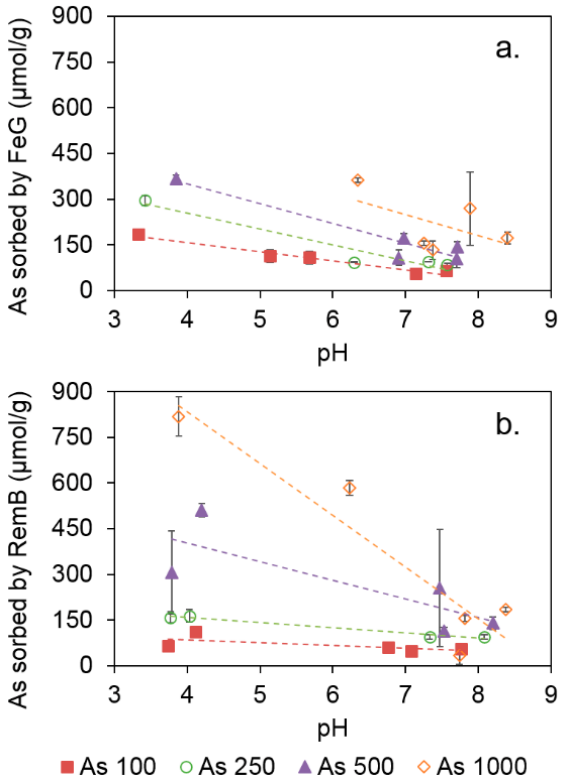

Figure 4. Effect of pH on amount of As sorbed by (a) Fe-oxide-modified reduced-GO (FeG), and (b) RemBind™ (RemB). Initial concentration of As added was 0 - 1000 µM at pH 3 - 8 (25 °C). Lines show effect of increasing pH on amount of As sorbed per gram of adsorbent. Note, due to the high buffering capacity of concentrated As-solutions, there was a shift in solution pH towards the alkaline range.

Overall, GO and FeG were promising adsorbents for Cd and As; the maximum amounts adsorbed by GO and FeG, were 782 µmol Cd/g (Figure 3) and 408 µmol As/g (Figure 4), respectively. Their performance was compared with other novel adsorbents reported in the literature (Table S4) by comparing experimentally observed maximum amounts of Cd and As adsorbed. GO exhibited a greater level of Cd-sorption when compared with other adsorbents like MnO_2-coated multi-walled CNTs and hexafluorophosphate-functionalised graphene (Deng et al., 2010, Luo et al., 2013). The performance of FeG in As-sorption was comparable to other adsorbents described in the literature, including GBMs modified with Fe and Mn-based nanomaterials (Andjelkovic et al., 2015, Luo et al., 2012). Hence GO and FeG are excellent candidates to develop a mixed-ion remediation material.

3.4. Sorption as a function of Cd and As concentration

Sorption data as a function of contaminant concentrations are presented in Figure S7. Predictably, the amounts of Cd and As adsorbed per gram of adsorbent increased with

increase in concentration. The Freundlich and Langmuir models were used to fit the sorption data (Figure S8; model parameters listed in Table S5). Based on correlation coefficient (r^2) values, the Langmuir isotherm was a better fit for the Cd-sorption data, while the Freundlich model was a better fit for the As-sorption data. The Langmuir model assumes homogeneity of the adsorptive surface sites, resulting in monolayer sorption (Masel, 1996). However, it is well-accepted that GO is far from homogeneous, as its surface is interrupted by a multitude of oxygen functionalities (Dreyer et al., 2010). Additionally, RemB, being a composite mixture is also heterogeneous. Consequently, in this work, the Freundlich model was considered appropriate in describing the sorption data, as it takes into account multi-site sorption on heterogeneous surfaces (Masel, 1996).

For Cd and As-sorption by GO and FeG, the values of the Freundlich parameter, *n*, were less than 1 across the pH range, indicating that sorption strength decreased with solution concentration, suggesting an electrostatic bonding mechanism. The same was the case for Cd and As-sorption by RemB at pH 5 - 8. However, at lower pH of 3 - 4, the *n*-values were greater than 1, indicating cooperative sorption mechanisms. This supports the previous speculation that part of the As-removal at low pH by RemB could be due to Al-arsenate precipitation.

3.5. Effect of competing ions

Both Ca and Cd exist in solution as divalent cations, and have similar charge/radius ratios (Ca^{2+} = 2.02 e/Å, Cd^{2+} = 2.06 e/Å), which can favour their competition for soil binding sites (Choong et al., 2014). Increased concentrations of free Ca^{2+} ions have been reported to significantly reduce Cd retention by soil (Temminghoff et al., 1995). It is also well known that As and P ions share similar physico-chemical properties. Previous studies have demonstrated that P-fertiliser application in As-contaminated soils can mobilise As, potentially by competing for reaction sites on the surface of Fe-based minerals in soil (Woolson, 1973), making As more bioavailable. Cadmium and As-sorption by the adsorbents was evaluated in presence of environmentally relevant Ca and P concentrations to gain an insight into their potential performance in soil or water remediation. Data suggest that Ca suppressed Cd-sorption onto GO but did not affect binding on RemB, and P had little effect on As-sorption onto both FeG and RemB (Figure 5).

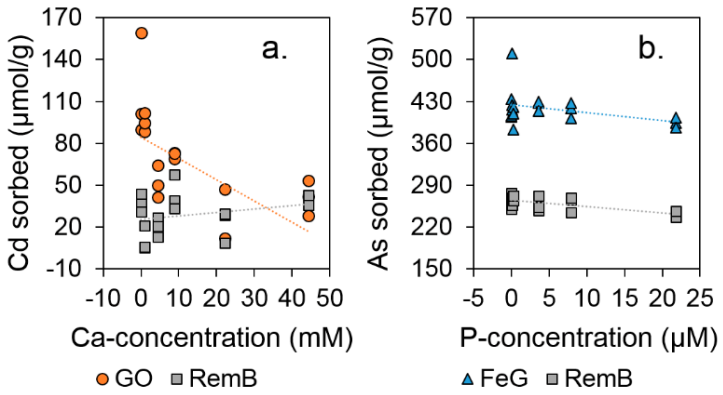

Figure 5. Effects of (a) Ca-competition on Cd-sorption by graphene oxide (GO) and RemBind™ (RemB), and (b) P-competition on As-sorption by Fe-oxide-modified reduced-GO (FeG) and RemB, at fixed solution pH (5.5 ± 0.03). 250 µM Cd and As solutions were tested with 0 - 50 mM for Ca-solution, and 0 - 25 µM P-solutions. Lines represent the relationship between amounts of competing ions added, and amounts of contaminant sorbed.

Competition between Ca and Cd is apparent in the sorption data, particularly in their sorption onto GO (Figure 5a). In presence of environmentally relevant concentrations of Ca (0 - 50 mM), Cd-sorption by GO reduced by up to 90%. This decrease was concentration dependent; greater Ca-concentrations resulted in greater reductions in Cd-sorption. However, no clear trend was observed for the effect of Ca-competition on the performance of RemB. Other studies have also shown that Ca inhibits Cd-sorption. For instance, Uwamariya et al. (2016) showed that Ca competed with Cd for sorption sites on Fe-oxide-coated sand, as well as on granular ferric hydroxide. Similar results were observed during Cd-sorption on chitin (Benaissa and Benguella, 2004). Jia et al. reported that Ca did not affect Cd-sorption on hollow magnetic porous Fe_3O_4/α-FeOOH microspheres (Jia et al., 2013), however, this was likely due to the relatively low Ca-concentration (< 1 mM) used.

At typical environmental concentrations, P-competition did not significantly reduce As-sorption onto FeG and RemB ($p = 0.190$ and 0.069, respectively; Figure 5b). The results suggest As and P did not compete for the same sorption sites. Other studies have however reported that P-competition hindered As-sorption on sorbents like nZVI-activated carbon composite and goethite (Manning and Goldberg, 1996, Zhu et al., 2009). Studies that tested equimolar As + P solution mixtures presented evidence that As and P competed for similar binding sites on the surface of goethite and gibbsite minerals (Manning and Goldberg, 1996), while also proposing that some sites were uniquely available to either As or P. Nevertheless, under typical environmental conditions (up to 25 µM P and pH 5.5), As remained strongly sorbed by FeG.

Results from this study suggest that competitive effects on sorption are dependent on the concentration of competing ions – effects are less apparent at lower concentrations. These results imply that increased concentrations of soluble Ca in the environment (e.g. in agricultural lands, alkaline soils, or hard waters) can potentially hinder Cd-sorption on GO. Thus, the competing effects of background ions must be taken into account when considering remediation strategies.

3.6. Mixed-mode remediation

Due to their differing physico-chemical properties, management of sites or waters co-contaminated with Cd and As would necessitate opposing strategies (high pH or cation exchange for Cd, and low pH or anion exchange for As). Immobilisation of one contaminant may potentially mobilise the other. Although GO and FeG were separately successful at binding Cd and As, adsorbents that can exhibit concurrent affinity to both contaminants, in a manner similar to RemB, are desirable.

With the intent of developing GBMs for mixed-mode remediation, a 1:1 GO+FeG combination was tested for sorption of Cd and As from co-contaminated solutions of varying concentrations. GO+FeG was effective in simultaneous removal of both contaminants from solution (Figure 6a). This can be attributed to the availability of multiple surface active sites (negative oxygenated functional groups on GO, and Fe-active sites on FeG) obtained on combining both adsorbents. For all concentrations tested, sorption by GO+FeG (Figure 6a) was significantly greater ($p < 0.05$) than by RemB (Figure 6b), and amounts adsorbed increased with increasing contaminant concentrations. Such an outcome, especially in intermediate pH conditions (pH 5.5), lends GO+FeG an added advantage of efficiency when compared to conventional adsorbents, which usually require contrasting pH conditions to target the contaminants individually.

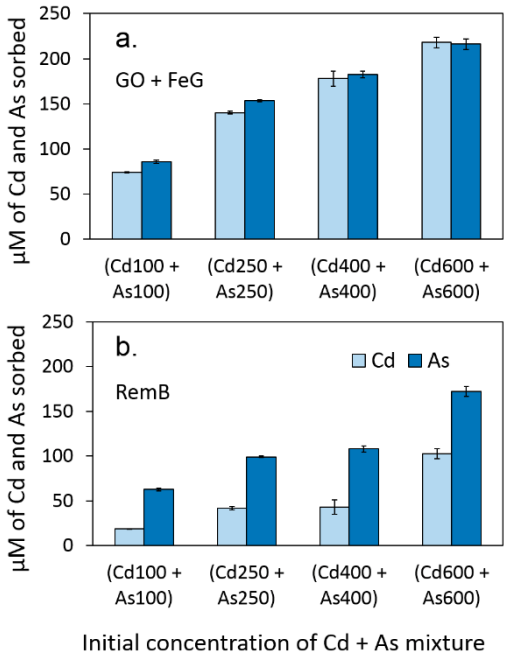

Figure 6. Mixed-mode sorption of co-contaminated solutions of Cd+As by combining graphene oxide and Fe-oxide-modified reduced-graphene oxide (GO+FeG; Figure 6a) was greater than that by RemBind™ (RemB; Figure 6b), at fixed solution pH (5.5 ± 0.1), and a range of contaminant concentrations (from 100 µM Cd + 100 µM As, to 600 µM Cd + 600 µM As).

Indeed, when tested using a natural dam water sample (complete elemental composition detailed in Table S6) as an environmental matrix, removal of 89% Cd and 76% As were achieved using GO+FeG (Figure 7). In comparison, removal of 72% Cd and 66% As were achieved using RemB. These results corroborate the prospect of using these adsorbents in a real environmental matrix.

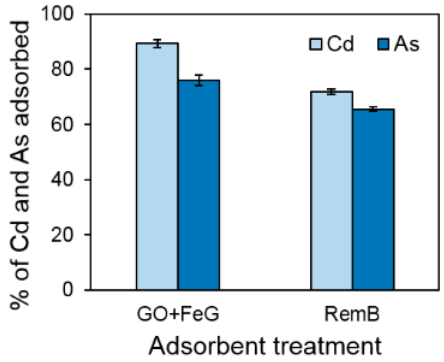

Figure 7. Sorption of Cd and As from a natural water sample (pH 7.9) by a mixture of graphene oxide and Fe-oxide-modified reduced-graphene oxide (GO+FeG) was greater than that by RemBind™. The initial concentrations of Cd and As were 5.9 µM and 5.1 µM, respectively.

4. Conclusions

The two adsorbents, GO and FeG, were capable of binding contaminants, Cd (cation) and As (anion) respectively. Their performance was either greater than, or comparable to that of a commercial mixed-mode adsorbent capable of binding both contaminants. Sorption was affected by the charge properties of the adsorbents, indicating the role of electrostatic interactions, with possible ligand-exchange important for As-sorption above the PZC. GO exhibited excellent Cd-sorption even in highly acidic conditions. Background ion (Ca, P) competition was only strong for Ca on Cd-sorption to GO, with no significant effect of P-competition on As-sorption. A mixture of GO and FeG was very effective in simultaneous removal of Cd and As from co-contaminated solutions, due to the availability of multiple surface-active sites from both adsorbents, illustrating their potential in mixed-mode remediation. Further studies on the performance of GBMs in other environmental matrices such as acid mine drainage and wastewater, and evaluation of their safety, long-term fate, transport, and stability (of contaminant-GBM complexes) in the environment are required to help consolidate their position as effective and competitive remediation solutions.

5. Acknowledgements

We would like to thank Bogumila Tomczak (University of Adelaide) for assistance with ICP-OES analyses, Dr. Mark Raven (CSIRO) for performing XRD analyses, Shervin Kabiri (University of Adelaide) for advice regarding material synthesis, as well as Adelaide and Waite Microscopy for access to SEM-EDX and TEM facilities. We would also like to thank Ziltek Pty. Ltd. for their support and provision of RemBind™. Financial support from Australian Research Council Discovery Grant DP150101760 is gratefully acknowledged.

6. Conflict of Interest

The authors have declared no conflicts of interest.

7. References

Andjelkovic I, Nesic J, Stankovic D, Manojlovic D, Pavlovic MB, Jovalekic C, Roglic G (2014). Investigation of sorbents synthesised by mechanical–chemical reaction for sorption of As(III) and As(V) from aqueous medium. *Clean Technologies and Environmental Policy,* **16,** 395-403.

Andjelkovic I, Tran DNH, Kabiri S, Azari S, Markovic M, Losic D (2015). Graphene aerogels decorated with α-FeOOH nanoparticles for efficient adsorption of arsenic from contaminated waters. *ACS Applied Materials & Interfaces,* **7,** 9758-9766.

Arai Y, Sparks DL, Davis JA (2005). Arsenate adsorption mechanisms at the allophane–water interface. *Environmental Science & Technology,* **39,** 2537-2544.

Arao T, Kawasaki A, Baba K, Mori S, Matsumoto S (2009). Effects of water management on cadmium and arsenic accumulation and dimethylarsinic acid concentrations in Japanese rice. *Environmental Science & Technology,* **43,** 9361-9367.

Basta NT, McGowen SL (2004). Evaluation of chemical immobilization treatments for reducing heavy metal transport in a smelter-contaminated soil. *Environmental Pollution,* **127,** 73-82.

Benaissa H, Benguella B (2004). Effect of anions and cations on cadmium sorption kinetics from aqueous solutions by chitin: experimental studies and modeling. *Environmental Pollution,* **130,** 157-163.

Bian Y, Bian Z-Y, Zhang J-X, Ding A-Z, Liu S-L, Wang H (2015). Effect of the oxygen-containing functional group of graphene oxide on the aqueous cadmium ions removal. *Applied Surface Science,* **329,** 269-275.

Buchauer MJ (1973). Contamination of soil and vegetation near a zinc smelter by zinc, cadmium, copper, and lead. *Environmental Science & Technology,* **7,** 131-135.

Chandra V, Park J, Chun Y, Lee JW, Hwang I-C, Kim KS (2010). Water-dispersible magnetite-reduced graphene oxide composites for arsenic removal. *ACS Nano,* **4,** 3979-3986.

Choong G, Liu Y, Templeton DM (2014). Interplay of calcium and cadmium in mediating cadmium toxicity. *Chemico-Biological Interactions,* **211,** 54-65.

Chowdhury S, Balasubramanian R (2014). Recent advances in the use of graphene-family nanoadsorbents for removal of toxic pollutants from wastewater. *Advances in Colloid and Interface Science,* **204,** 35-56.

Cong H-P, Ren X-C, Wang P, Yu S-H (2012). Macroscopic multifunctional graphene-based hydrogels and aerogels by a metal ion induced self-assembly process. *ACS Nano,* **6,** 2693-2703.

Deng X, Lü L, Li H, Luo F (2010). The adsorption properties of Pb(II) and Cd(II) on functionalized graphene prepared by electrolysis method. *Journal of Hazardous Materials,* **183,** 923-930.

Dreyer DR, Park S, Bielawski CW, Ruoff RS (2010). The chemistry of graphene oxide. *Chemical Society Reviews,* **39,** 228-240.

Guo X, Chen F (2005). Removal of arsenic by bead cellulose loaded with iron oxyhydroxide from groundwater. *Environmental Science & Technology,* **39,** 6808-6818.

Hameed BH, Din ATM, Ahmad AL (2007). Adsorption of methylene blue onto bamboo-based activated carbon: Kinetics and equilibrium studies. *Journal of Hazardous Materials,* **141,** 819-825.

Hartley W, Edwards R, Lepp NW (2004). Arsenic and heavy metal mobility in iron oxide-amended contaminated soils as evaluated by short-and long-term leaching tests. *Environmental Pollution,* **131,** 495-504.

Hughes MF (2002). Arsenic toxicity and potential mechanisms of action. *Toxicology Letters,* **133,** 1-16.

Jain A, Raven KP, Loeppert RH (1999). Arsenite and arsenate adsorption on ferrihydrite: surface charge reduction and net OH- release stoichiometry. *Environmental Science & Technology,* **33,** 1179-1184.

Jia Y, Yu XY, Luo T, Zhang MY, Liu JH, Huang XJ (2013). Two-step self-assembly of iron oxide into three-dimensional hollow magnetic porous microspheres and their toxic ion adsorption mechanism. *Dalton Transactions,* **42,** 1921-8.

Koptsik GN (2014). Modern approaches to remediation of heavy metal polluted soils: A review. *Eurasian Soil Science,* **47,** 707-722.

Lambert M, Pierzinski G, Erickson L, Schnoor J 1997. Remediation of lead-, zinc-and cadmium contaminated soils. *In:* Hester, RE & Harrison, RM (eds.) *Issues in Environmental Science and Technology.* Cambridge, United Kingdom: Royal Society of Chemistry.

Lim JE, Ahmad M, Lee SS, Shope CL, Hashimoto Y, Kim K-R, Usman ARA, Yang JE, Ok YS (2013). Effects of lime-based waste materials on immobilization and phytoavailability of cadmium and lead in contaminated soil. *CLEAN – Soil, Air, Water,* **41,** 1235-1241.

Luo C, Wei R, Guo D, Zhang S, Yan S (2013). Adsorption behavior of MnO_2 functionalized multi-walled carbon nanotubes for the removal of cadmium from aqueous solutions. *Chemical Engineering Journal,* **225,** 406-415.

Luo X, Wang C, Luo S, Dong R, Tu X, Zeng G (2012). Adsorption of As (III) and As (V) from water using magnetite Fe_3O_4-reduced graphite oxide–MnO_2 nanocomposites. *Chemical Engineering Journal,* **187,** 45-52.

Manceau A (1995). The mechanism of anion adsorption on iron oxides: Evidence for the bonding of arsenate tetrahedra on free $Fe(O, OH)_6$ edges. *Geochimica et Cosmochimica Acta,* **59,** 3647-3653.

Manning BA, Goldberg S (1996). Modeling competitive adsorption of arsenate with phosphate and molybdate on oxide minerals. *Soil Science Society of America Journal,* **60,** 121-131.

Marcano DC, Kosynkin DV, Berlin JM, Sinitskii A, Sun Z, Slesarev A, Alemany LB, Lu W, Tour JM (2010). Improved synthesis of graphene oxide. *ACS Nano,* **4,** 4806-4814.

Masel RI 1996. *Principles of adsorption and reaction on solid surfaces,* New York, John Wiley & Sons.

Niu Z, Liu L, Zhang L, Chen X (2014). Porous graphene materials for water remediation. *Small,* **10,** 3434-3441.

Novoselov KS, Falko VI, Colombo L, Gellert PR, Schwab MG, Kim K (2012). A roadmap for graphene. *Nature,* **490,** 192-200.

Nriagu JO, Bhattacharya P, Mukherjee AB, Bundschuh J, Zevenhoven R, Loeppert RH 2007. Arsenic in soil and groundwater: an overview. *In:* Bhattacharya, P, Mukherjee, AB, Bundschuh, J, Zevenhoven, R & Loeppert, RH (eds.) *Trace Metals and other Contaminants in the Environment.* Oxford, United Kingdom: Elsevier.

Pantuzzo FL, Santos LRG, Ciminelli VST (2014). Solubility-product constant of an amorphous aluminum-arsenate phase ($AlAsO_4 \cdot 3.5H_2O$) AT 25 °C. *Hydrometallurgy,* **144–145,** 63-68.

Schachtman DP, Reid RJ, Ayling SM (1998). Phosphorus uptake by plants: From soil to cell. *Plant Physiology,* **116,** 447-53.

Sitko R, Turek E, Zawisza B, Malicka E, Talik E, Heimann J, Gagor A, Feist B, Wrzalik R (2013). Adsorption of divalent metal ions from aqueous solutions using graphene oxide. *Dalton Transactions,* **42,** 5682-5689.

Smith SC, Rodrigues DF (2015). Carbon-based nanomaterials for removal of chemical and biological contaminants from water: A review of mechanisms and applications. *Carbon,* **91,** 122-143.

Stephenson M, Mackie GL (1988). Total cadmium concentrations in the water and littoral sediments of Central Ontario Lakes. *Water, Air, & Soil Pollution,* **38,** 121-136.

Temminghoff EJM, Van Der Zee SEATM, De Haan FAM (1995). Speciation and calcium competition effects on cadmium sorption by sandy soil at various pHs. *European Journal of Soil Science,* **46,** 649-655.

Tiller K, Nayyar V, Clayton P (1979). Specific and non-specific sorption of cadmium by soil clays as influenced by zinc and calcium. *Soil Research,* **17,** 17-28.

Uwamariya V, Petrusevski B, Lens PNL, Amy GL (2016). Effect of pH and calcium on the adsorptive removal of cadmium and copper by iron oxide–coated sand and granular ferric hydroxide. *Journal of Environmental Engineering,* **142,** 1-9.

Warren GP, Alloway BJ, Lepp NW, Singh B, Bochereau FJM, Penny C (2003). Field trials to assess the uptake of arsenic by vegetables from contaminated soils and soil remediation with iron oxides. *Science of the Total Environment,* **311,** 19-33.

Wenzel WW, Brandstetter A, Wutte H, Lombi E, Prohaska T, Stingeder G, Adriano DC (2002). Arsenic in field-collected soil solutions and extracts of contaminated soils and its implication to soil standards. *Journal of Plant Nutrition and Soil Science,* **165,** 221-228.

Woolson EA (1973). Arsenic phytotoxicity and uptake in six vegetable crops. *Weed Science,* **21,** 524-527.

Zhao G, Li J, Ren X, Chen C, Wang X (2011). Few-layered graphene oxide nanosheets as superior sorbents for heavy metal ion pollution management. *Environmental Science & Technology,* **45,** 10454-10462.

Zhu H, Jia Y, Wu X, Wang H (2009). Removal of arsenic from water by supported nano zero-valent iron on activated carbon. *Journal of Hazardous Materials,* **172,** 1591-1596.

8. Supporting Information

Mixed-mode remediation of cadmium and arsenate ions using graphene-based materials

Supriya Lath [*, 1], Divina Navarro [1, 2], Diana Tran [3], Anu Kumar [2], Dusan Losic [3], Michael J. McLaughlin [1, 2]

[1] School of Agriculture Food and Wine, The University of Adelaide, PMB 1 Glen Osmond, SA 5064, Australia.

[2] CSIRO Land and Water, PMB 2 Glen Osmond, SA 5064, Australia.

[3] School of Chemical Engineering, The University of Adelaide, Adelaide, SA 5005, Australia.

* Corresponding author (email: supriya.lath@adelaide.edu.au)
Ms. Supriya Lath, School of Agriculture Food and Wine, The University of Adelaide, PMB 1 Glen Osmond, SA 5064, Australia.

Text S1. Methods – Synthesis of graphene oxide (GO) and Fe-oxide-modified reduced-GO composite (FeG)

A top-down approach based on an improved Hummer's method (Marcano et al., 2010) which involves strong oxidative exfoliation of graphite using concentrated H_2SO_4, H_3PO_4 and $KMnO_4$ was used to synthesise GO. Unreacted $KMnO_4$ was reduced using 30% H_2O_2, and multiple wash cycles were performed with 30% HCl and distilled water to remove metal and acid residues. The material was dried (35 °C, 36 hours) to obtain the solid GO product, which was used as flakes. Based on a method reported by Cong et al. (Cong et al., 2012), GO was further modified by adding $FeSO_4.7H_2O$ to a stable suspension of well-exfoliated GO. After adjusting the pH to 3.5 using ammonia, the suspension was hydrothermally reduced at 90 °C for 6 hrs without stirring until a black 3D hydrogel monolith (FeG) was formed. The hydrogel was then separated, washed, freeze dried and crushed into the powdered FeG product.

Text S2. Methods – Sample preparation for characterisation of adsorbents

SEM-EDX samples were prepared by applying the dried adsorbents directly onto aluminium stubs covered with adhesive carbon tape. Images were obtained using a spot size of 3, and an accelerating voltage of 10 kV. For TEM, adsorbents were ultra-sonicated in ethanol (20 min), after which the suspensions were drop-casted onto a Lacey copper grid and dried for a few hours before imaging at an accelerating voltage of 100 kV.

FTIR and XRD analyses were performed using powdered adsorbent samples. FTIR spectra were recorded at wavelengths ranging from 400 - 4000 cm^{-1}. XRD spectra were recorded using Fe-filtered Co Kα radiation, automatic divergence slit, 2° anti-scatter slit and fast X'Celerator Si strip detector. The diffraction patterns were recorded from 3 to 80° in steps of 0.017° 2 theta with a 0.5 second counting time per step for an overall counting time of approximately 35 minutes.

Specific surface area (SSA) of adsorbents were measured using the Methylene Blue (MB) dye absorption method commonly used for carbonaceous materials. 15 mg of each adsorbent was added to 150 mL of 20 mg/L MB solutions and shaken for 60 hrs at 100 rpm to allow the solutions to attain equilibrium and maximum absorption. After centrifugation, supernatants were analysed using UV-visible spectrophotometry (at 664 nm) and compared to controls to determine the amount of MB absorbed. The SSA was then calculated using the following equation:

$$SSA = \frac{N_A . A_{MB} . (C_i - C_e) . V}{M_{MB} . m_s}$$

where, N_A represents Avogadro number (6.023 x 10^{23} molecules/mole), A_{MB} is the area covered per MB molecule (1.35 nm^2), C_i and C_e are the initial and equilibrium MB concentrations, respectively, V is the volume of MB solution, M_{MB} is the molecular mass of MB, and m_s is the mass of the adsorbent.

Surface charge and PZC of adsorbents were determined by using 0.1 % w/v suspensions in Milli Q water, that were adjusted to pHs ranging from around 2 – 10. The suspensions were placed on a shaker for 48 hours to equilibriate pH before measuring zeta potential across the pH gradient using dynamic light scattering (Malvern Zetasizer NanoZS).

Table S1. Elemental composition of adsorbents graphene oxide (GO), Fe-oxide-modified reduced-GO (FeG) and RemBind™ (RemB), as determined by energy dispersive X-ray (EDX) detector coupled to a scanning electron microscope. See Figure S1 for EDX spectra.

Adsorbent	**Element (series)**	**Weight %**	**Atomic %**
GO	C (K)	65.88	72.01
	O (K)	34.12	27.99
FeG	C (K)	37.19	56.39
	O (K)	28.48	32.42
	Fe (K)	34.34	11.20
RemB	C (K)	22.42	34.37
	O (K)	27.70	31.89
	Si (K)	38.63	26.36
	Al (K)	11.26	7.38

Figure S1. Energy dispersive X-ray (EDX) spectra collected for adsorbents graphene oxide (GO), Fe-oxide-modified reduced-GO (FeG) and RemBind™ (RemB) to elucidate elemental composition. All adsorbents exhibited signals for carbon and oxygen. FeG displayed an additional signal for iron, and RemB displayed additional signals for aluminium and silicon.

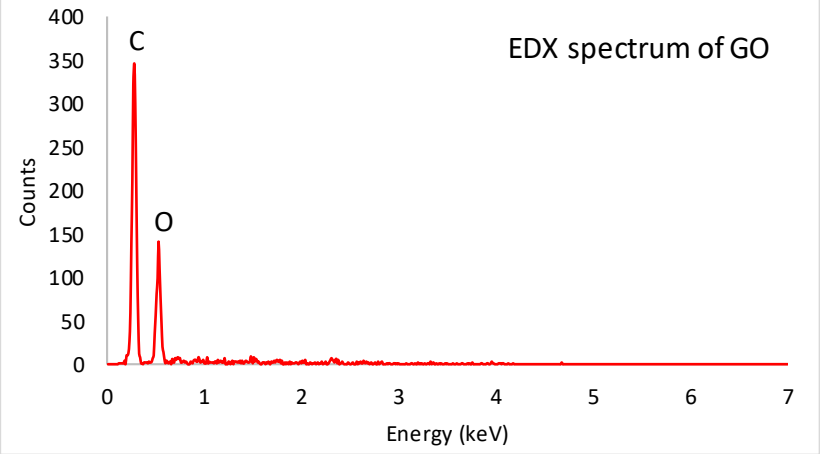

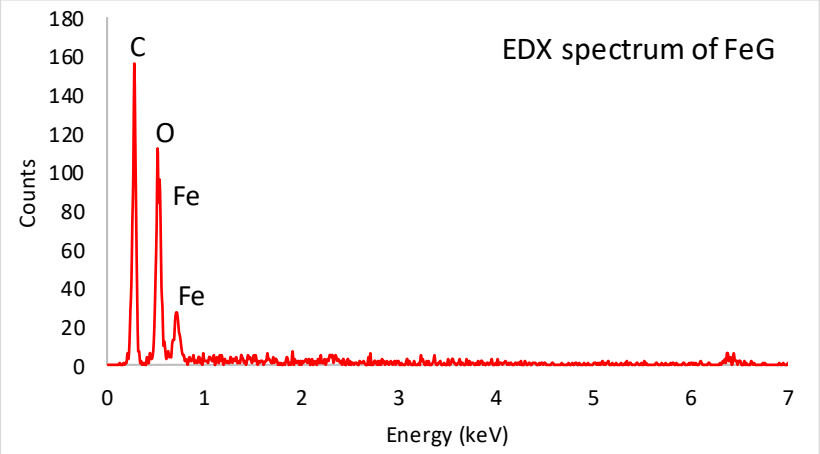

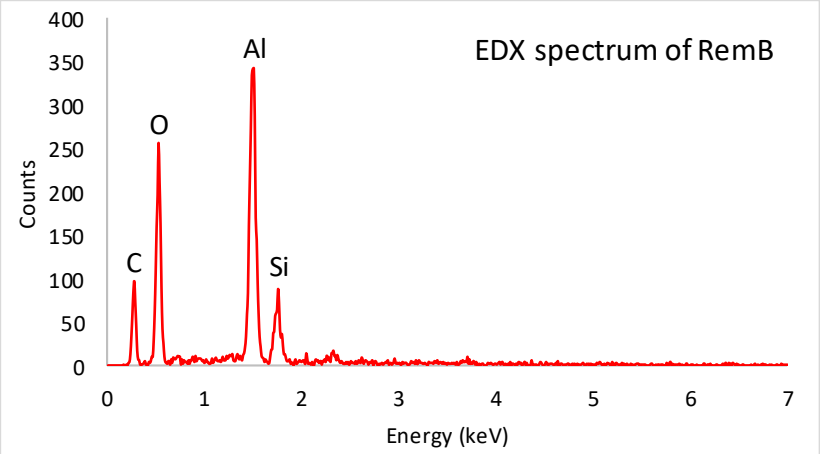

Figure S2. X-ray diffraction (XRD) spectra of adsorbents graphene oxide (GO), Fe-oxide-modified reduced-GO (FeG) and RemBind™ (RemB)

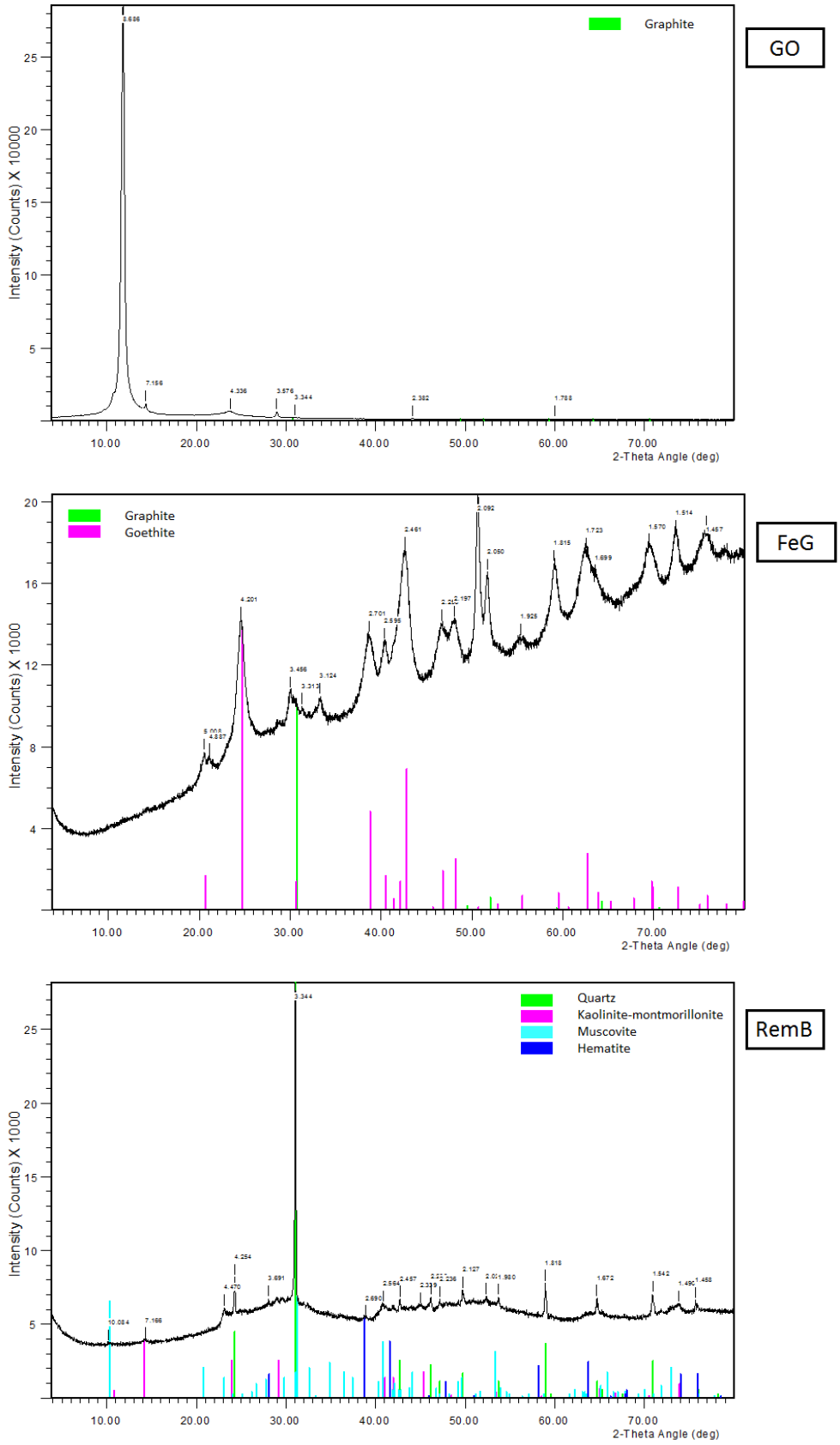

Figure S3. Fourier-transform infrared (FTIR) spectra of adsorbents graphene oxide (GO), Fe-oxide-modified reduced-GO (FeG) and RemBind™ (RemB)

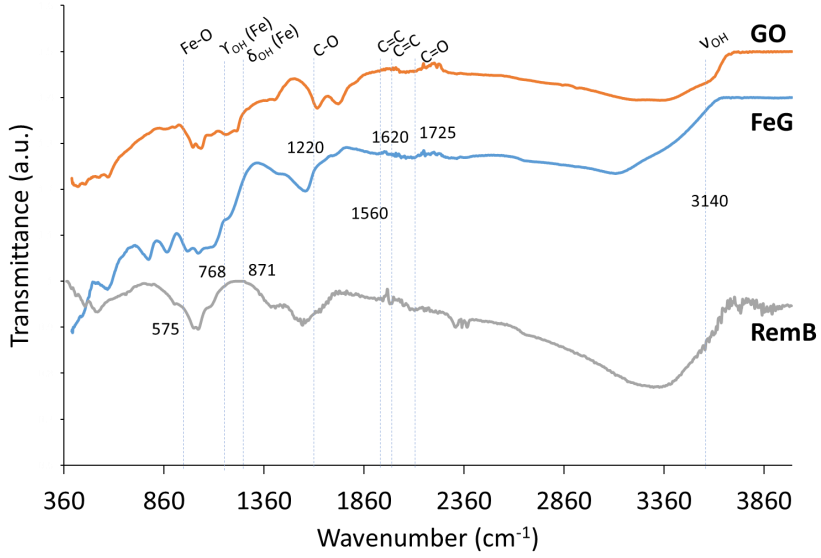

Figure S4. Methylene Blue standard calibration curve (664 nm) and sample analysis for measurement of surface areas of adsorbents graphene oxide (GO), Fe-oxide-modified reduced-GO (FeG) and RemBind™ (RemB).

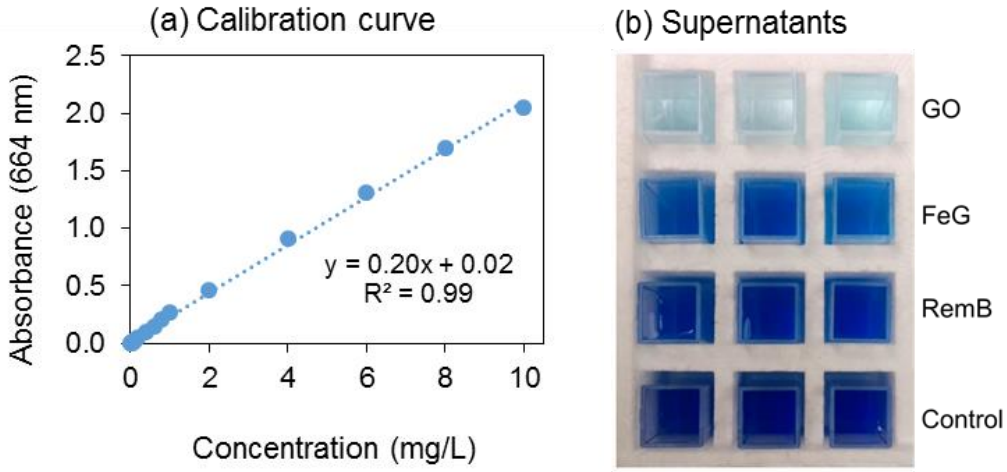

Table S2. Amounts of cadmium (Cd) adsorbed per gram of graphene oxide (GO) and RemBind™ (RemB) at pH 3 – 8. Initial concentration of Cd added was 0 - 1000 µM.

Adsorbent	Cadmium conc. C_i , µM	Sorption capacity at equilibrium, q_e, µmol/g					
		pH 3	pH 4	pH 5	pH 6	pH 7	pH 8
GO	100	151.6	190.7	229.9	269	308.2	347.3
	250	216.6	315.3	414	512.6	611.3	709.9
	500	320.9	430	539.1	648.1	757.2	866.2
	750	327.8	442.2	556.6	671.1	785.5	899.9
	1000	403.7	509.8	615.9	722.1	828.2	934.3
RemB	100	0	0	28.4	63.3	98.2	133.1
	250	0	0	34.4	73.2	112.1	150.9
	500	0	22.4	51.8	81.2	110.6	140.1
	750	0	14.9	51.6	88.3	125	161.8
	1000	0	32.3	69.3	106.2	143.1	180

Table S3. Amounts of arsenic (As) adsorbed per gram of Fe-oxide-modified reduced-graphene oxide (FeG) and RemBind™ (RemB) at pH 3 – 8. Initial concentration of As added was 0 - 1000 µM.

Adsorbent	Arsenic conc. C_i , µM	Sorption capacity at equilibrium, q_e, µmol/g					
		pH 3	pH 4	pH 5	pH 6	pH 7	pH 8
FeG	100	188.2	158.4	128.5	98.7	68.8	38.9
	250	305.9	253.7	201.5	149.2	97.0	44.8
	500	415.8	350.6	285.4	220.3	155.1	90.0
	750	455.6	391.3	327.0	262.7	198.4	134.1
	1000	505.9	441.4	376.9	312.4	247.9	183.3
RemB	100	94.3	85.3	76.3	67.4	58.4	49.4
	250	176.3	159.2	142.1	125.0	107.9	90.8
	500	462.4	401.5	340.6	279.7	218.8	157.9
	750	735.7	616.5	497.3	378.1	258.9	139.6
	1000	1003	833.0	663.1	493.1	323.2	153.2

Figure S5. Comparison of X-ray diffraction (XRD) spectra of Fe-oxide-modified reduced-graphene oxide (FeG) before and after As-sorption.

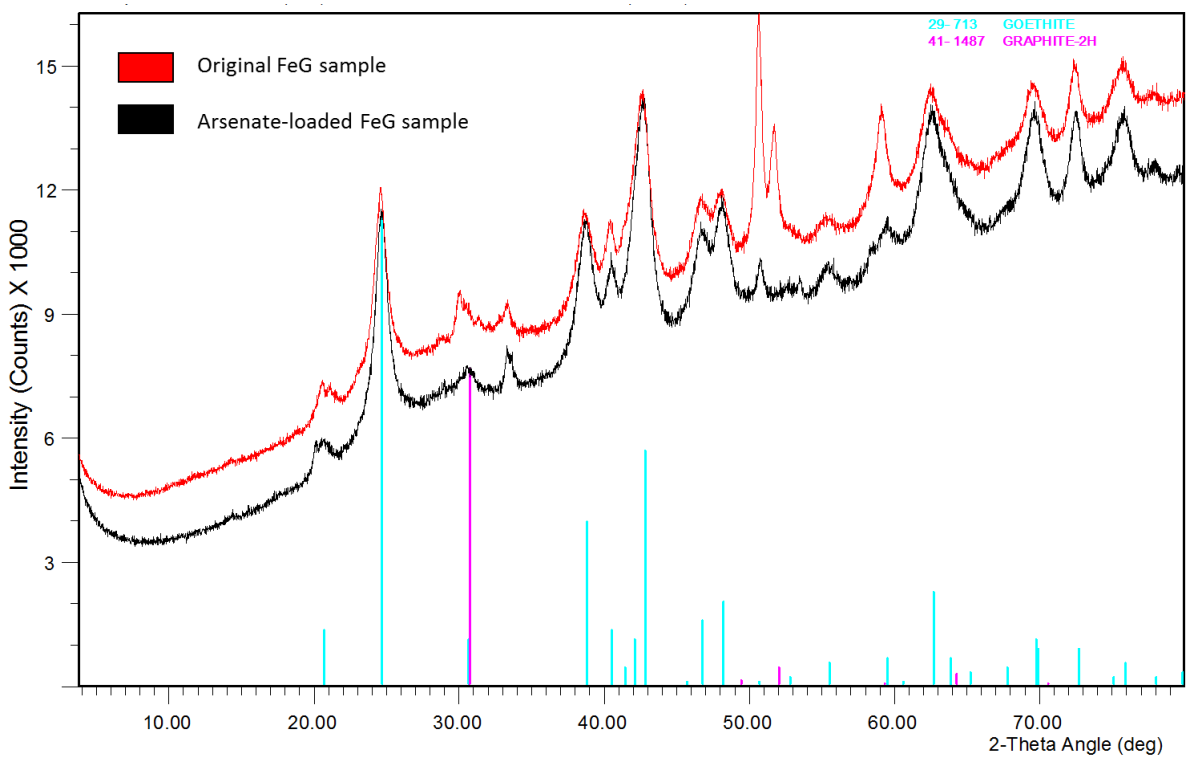

Figure S6. Dissolution of aluminium (Al) from adsorbent RemBind™ across a pH gradient (3 – 8) at initial As-concentrations of 0, 100 and 1000 µM.

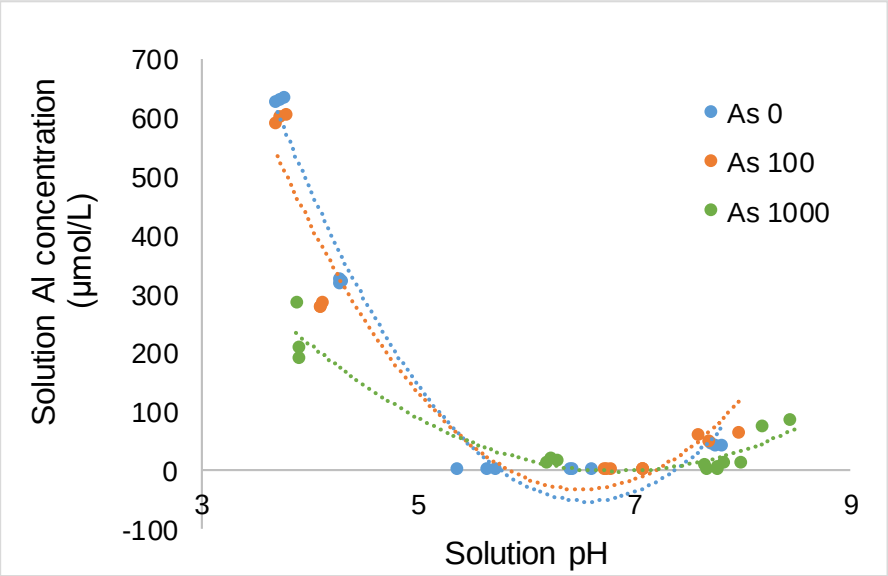

Table S4. Comparative performance of graphene oxide (GO) and Fe-oxide-modified reduced-GO (FeG) for cadmium (Cd) and arsenate (As) sorption with other reported novel adsorbents.

To compare sorption performance of GO and FeG with other reported novel adsorbents, we compared experimentally-observed amounts of Cd and As adsorbed in different studies. To enable valid assessment, we compared sorption observed around pH values 6, or as close to it as was possible to derive from available data (see table below). Any values reported in mg/L were converted to units of µmol/L for consistency. Initial contaminant concentrations in each case are also specified in the table for evaluation.

Cd / As	**Reference**	**Adsorbent material**	**Cd / As adsorbed (µmol/g)**	**Experimental pH and initial Cd / As concentration**
Cd	This study	GO	782 µmol/g	pH 6.1 1000 µmol/L Cd
Cd	Ref (Bian et al., 2015)	GO	213 µmol/g	pH 6.3 Cd conc. not specified
Cd	Ref (Deng et al., 2010)	Graphene-hexafluorophosphate composite	536 µmol/g	pH 6.1 1000 µmol/L Cd
Cd	Ref (Luo et al., 2013)	Oxidised MWCNTs coated with MnO_2	237 µmol/g	pH 7 267 µmol/L Cd
Cd	Ref (Gupta and Nayak, 2012)	magnetic Fe_3O_4 nanoparticles modified with orange peel powder	667 µmol/g	pH 6 142 µmol/L Cd
As	This study	FeG	408 µmol/g	pH 6.3 1000 µmol/L As
As	Ref (Andjelkovic et al., 2015)	graphene-αFeOOH hydrogel	427 µmol/g	pH 6 67 µmol/L As
As	Ref (Zhang et al., 2010)	GO-ferric hydroxide composite	83 µmol/g	pH 6.22 267 µmol/L As
As	Ref (Luo et al., 2012)	Fe_3O_4-reduced graphite oxide–MnO_2 nanocomposites	113 µmol/g	pH 6 133 µmol/L As
As	Ref (Kumar et al., 2014)	Magnetic GO- $MnFe_2O_4$ hybrid	1308 µmol/g	pH 6 1335 µmol/L

Figure S7. Sorption of cadmium (Cd) and arsenate (As) as a function of equilibrium solution concentration. Initial concentrations of Cd and As added were 0 - 1000 µM, at pH 3 - 8 (25 °C). Fitted lines for linearised isotherm models are shown in Figures S8a and S8b.

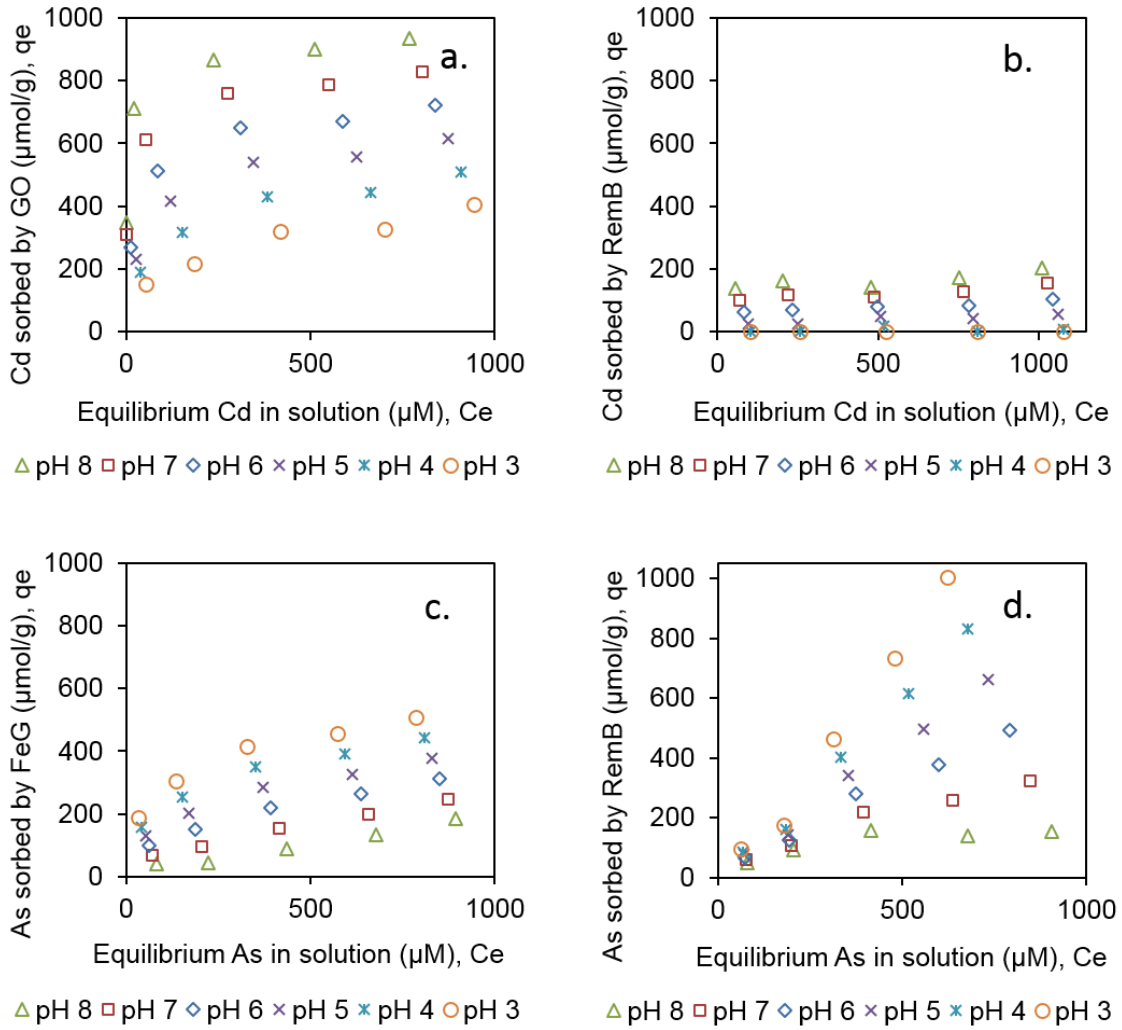

Figure S8a. Freundlich Isotherm models for Cd and As sorption by adsorbents graphene oxide (GO), Fe-oxide-modified reduced-GO (FeG) and RemBind™ (RemB).

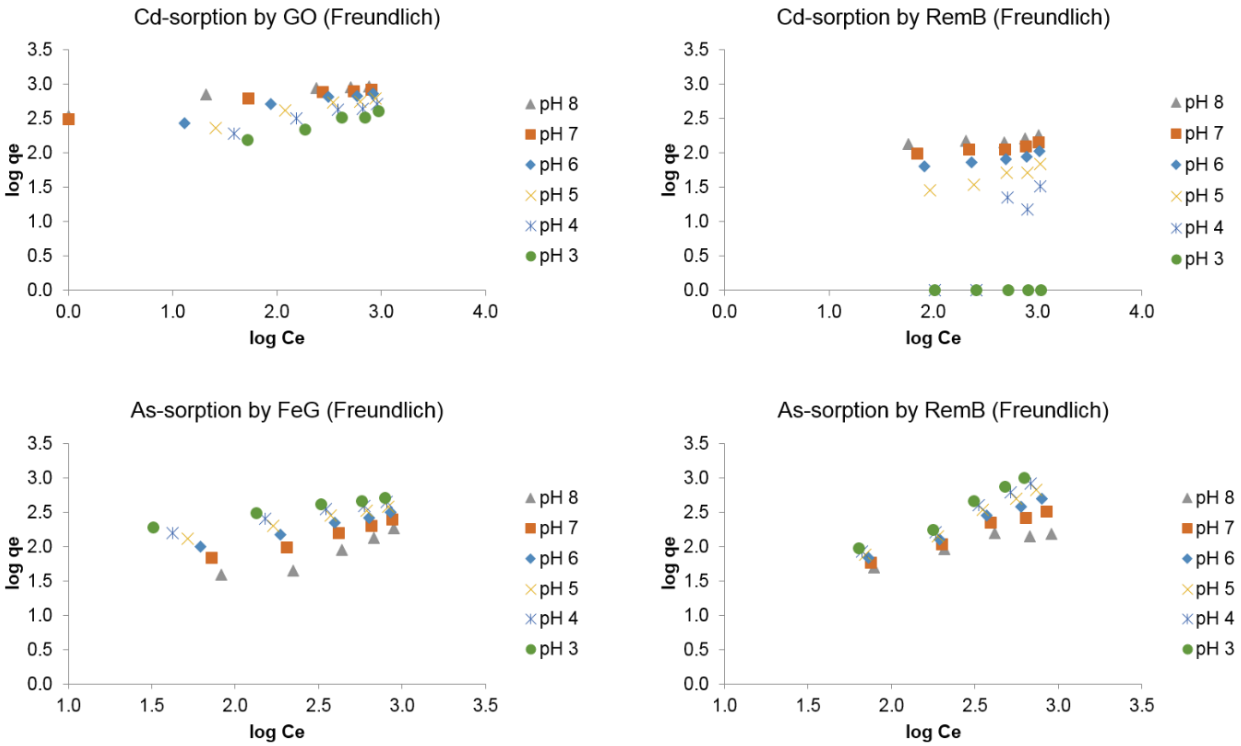

Figure S8b. Langmuir Isotherm models for Cd and As sorption by adsorbents graphene oxide (GO), Fe-oxide-modified reduced-GO (FeG) and RemBindTM (RemB).

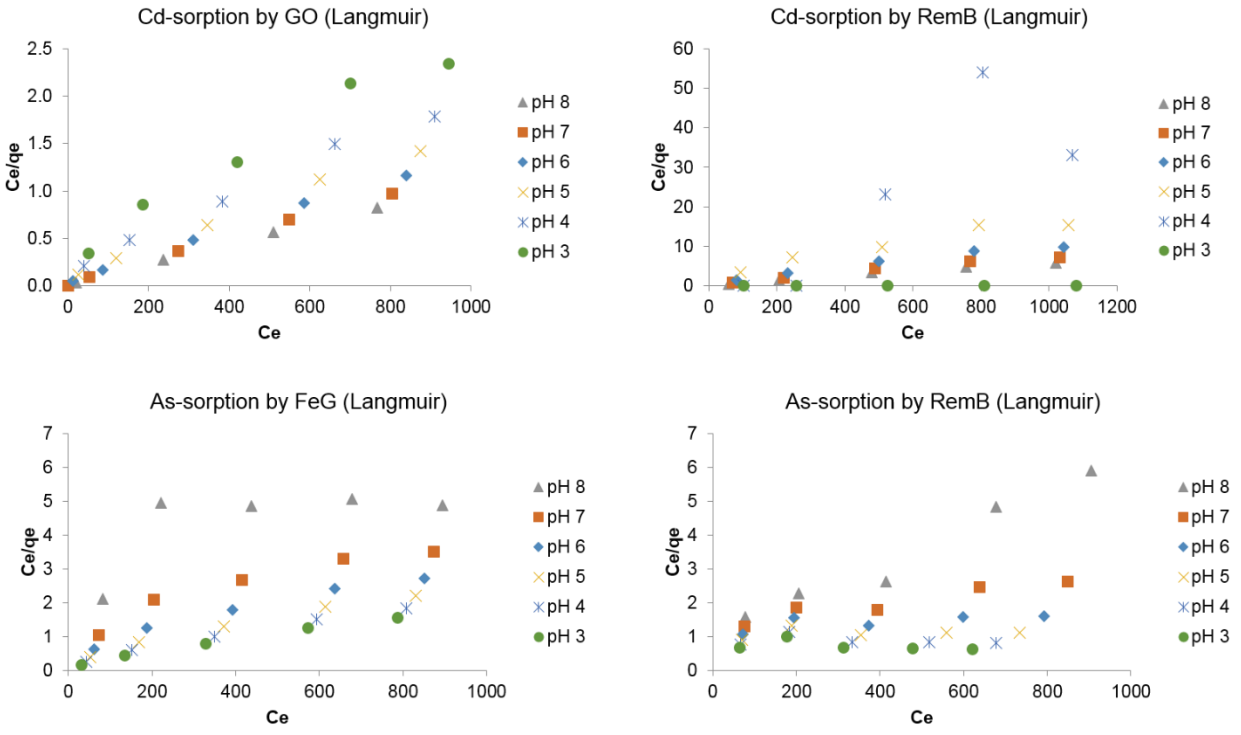

Table S5. Freundlich and Langmuir isotherm parameters obtained from the slopes and intercepts of the linear plots (Figure S8a and S8b) for sorption of Cd and As by graphene oxide (GO), Fe-oxide-modified reduced-GO (FeG) and RemBind™ (RemB).

Cd & As Sorption	Solution pH	Freundlich parameters			Langmuir parameters		
		r^2	n	K_F	r^2	q_m	K_L
Cd-sorption by GO	8	0.928	0.14	383.80	0.999	6.96	0.06
	7	0.988	0.15	317.32	0.998	6.72	0.06
	6	0.951	0.23	160.73	0.998	4.31	0.11
	5	0.959	0.27	101.23	0.996	3.66	0.14
	4	0.977	0.30	65.00	0.990	3.28	0.17
	3	0.976	0.33	40.43	0.970	3.02	0.21
Cd-sorption by RemB	8	0.655	0.08	93.52	0.981	11.95	0.04
	7	0.808	0.12	58.48	0.978	8.50	0.07
	6	0.915	0.18	27.67	0.971	5.51	0.13
	5	0.933	0.35	5.45	0.926	2.84	0.48
	4	0.815	1.64	0.00	0.691	0.61	-0.47
	3	N/A*	N/A*	N/A*	N/A*	N/A*	N/A*
As-sorption by FeG	8	0.904	0.67	1.67	0.415	1.50	3.00
	7	0.977	0.52	7.00	0.905	1.94	0.61
	6	0.995	0.44	15.67	0.968	2.27	0.37
	5	0.998	0.39	27.82	0.985	2.58	0.27
	4	0.995	0.35	44.09	0.991	2.89	0.21
	3	0.992	0.31	65.83	0.993	3.24	0.17
As-sorption by RemB	8	0.887	0.47	6.98	0.966	2.12	0.56
	7	0.986	0.72	2.55	0.906	1.39	1.78
	6	0.986	0.85	1.62	0.518	1.17	4.09
	5	0.980	0.94	1.25	0.020	1.06	9.78
	4	0.973	1.01	1.06	0.087	0.99	42.98
	3	0.965	1.07	0.94	0.242	0.93	-36.87

* Since no Cd-sorption was displayed by RemB at pH 3 in the concentration ranges tested (0-1000 µM Cd), sorption parameters could not be calculated.

Table S6. Detailed elemental composition of a natural dam water sample, as determined using ICPOES analysis, before spiking with Cd and As solutions.

Major elements			**Minor elements**		
Ca	29.3	mg/L	Si	2.8	mg/L
K	5.1	mg/L	Sr	0.1	mg/L
Mg	9.3	mg/L	P	< 0.2	mg/L
Na	16.9	mg/L	Fe, Sb	<0.1	mg/L
S	1.1	mg/L	Al, As, B, Cd, Co, Cr, Cu, Mn, Mo, Ni, Pb, Se, Zn	<0.05	mg/L

REFERENCES

Andjelkovic I, Tran DNH, Kabiri S, Azari S, Markovic M, Losic D (2015). Graphene aerogels decorated with α-FeOOH nanoparticles for efficient adsorption of arsenic from contaminated waters. *ACS Applied Materials & Interfaces,* **7,** 9758-9766.

Bian Y, Bian Z-Y, Zhang J-X, Ding A-Z, Liu S-L, Wang H (2015). Effect of the oxygen-containing functional group of graphene oxide on the aqueous cadmium ions removal. *Applied Surface Science,* **329,** 269-275.

Cong H-P, Ren X-C, Wang P, Yu S-H (2012). Macroscopic multifunctional graphene-based hydrogels and aerogels by a metal ion induced self-assembly process. *ACS Nano,* **6,** 2693-2703.

Deng X, Lü L, Li H, Luo F (2010). The adsorption properties of Pb(II) and Cd(II) on functionalized graphene prepared by electrolysis method. *Journal of Hazardous Materials,* **183,** 923-930.

Gupta VK, Nayak A (2012). Cadmium removal and recovery from aqueous solutions by novel adsorbents prepared from orange peel and Fe_2O_3 nanoparticles. *Chemical Engineering Journal,* **180,** 81-90.

Kumar S, Nair RR, Pillai PB, Gupta SN, Iyengar MAR, Sood AK (2014). Graphene Oxide–$MnFe_2O_4$ Magnetic Nanohybrids for Efficient Removal of Lead and Arsenic from Water. *ACS Applied Materials & Interfaces,* **6,** 17426-17436.

Luo C, Wei R, Guo D, Zhang S, Yan S (2013). Adsorption behavior of MnO_2 functionalized multi-walled carbon nanotubes for the removal of cadmium from aqueous solutions. *Chemical Engineering Journal,* **225,** 406-415.

Luo X, Wang C, Luo S, Dong R, Tu X, Zeng G (2012). Adsorption of As (III) and As (V) from water using magnetite Fe_3O_4-reduced graphite oxide–MnO_2 nanocomposites. *Chemical Engineering Journal,* **187,** 45-52.

Marcano DC, Kosynkin DV, Berlin JM, Sinitskii A, Sun Z, Slesarev A, Alemany LB, Lu W, Tour JM (2010). Improved synthesis of graphene oxide. *ACS Nano,* **4,** 4806-4814.

Zhang K, Dwivedi V, Chi C, Wu J (2010). Graphene oxide/ferric hydroxide composites for efficient arsenate removal from drinking water. *Journal of Hazardous Materials,* **182,** 162-168.

CHAPTER 4. Sorptive Remediation of Perfluorooctanoic Acid (PFOA) Using Mixed Mineral and Carbon-Based Materials

The work contained in this chapter has been submitted for publication to *Environmental Chemistry*, and has subsequently been recommended for publication pending minor changes.

Statement of Authorship

Title of Paper	Sorptive remediation of perfluorooctanoic acid (PFOA) using mixed mineral and carbon-based materials
Publication Status	☐ Published; ☐ Accepted for publication; ☐ Submitted for publication; ☐ Unpublished and unsubmitted work prepared in manuscript style for publication
Publication Details	

Principal Author

Name (Candidate)	Supriya Lath		
Contribution to the Paper	Experimental development; set-up and performed experiments; data analysis and critical interpretation; wrote the manuscript; acted as corresponding author.		
Overall percentage (%)	85%		
Certification:	This paper reports on original research I conducted during the period of my PhD candidature and is not subject to any obligations or contractual agreements with a third party that would constrain its inclusion in this thesis. I am the primary author of this paper.		
Signature		Date	3 Sept 2018

Co-Author Contributions

By signing the Statement of Authorship, each author certifies that: the candidate's stated contribution to the publication is accurate (as detailed above); permission is granted for the candidate in include the publication in the thesis; and the sum of all co-author contributions is equal to 100% less the candidate's stated contribution.

Divina A. Navarro	Assisted with project development; experimental design; data interpretation; manuscript evaluation.		
Signature		Date	28 Aug 2018

Dusan Losic	Assisted in project planning; advised on graphene-materials; manuscript evaluation.		
Signature		Date	30/08/2018

Anu Kumar	Assisted in project planning; manuscript evaluation.		
Signature		Date	28 August 2018

Michael J. McLaughlin	Supervised project development; experimental design; data interpretation; manuscript evaluation.		
Signature		Date	3rd Sept 2018

Sorptive Remediation of Perfluorooctanoic Acid (PFOA) Using Mixed Mineral and Carbon-Based Materials

Supriya Lath [*, 1], Divina A. Navarro [1, 2], Dusan Losic [3], Anupama Kumar [2], Michael J. McLaughlin [1, 2]

[1] School of Agriculture Food and Wine, The University of Adelaide, PMB 1 Glen Osmond, SA 5064, Australia.

[2] CSIRO Land and Water, PMB 2 Glen Osmond, SA 5064, Australia.

[3] School of Chemical Engineering, The University of Adelaide, Adelaide, SA 5005, Australia.

* Corresponding author email: supriya.lath@adelaide.edu.au

Abstract

As degradation of perfluorooctanoic acid (PFOA) and related per- and polyfluoroalkyl substances (PFASs) is energy-intensive, there is a need to develop *in situ* remediation strategies to manage PFAS-contamination. The sorption of PFOA by two types of graphene-based materials, graphene oxide (GO) and an iron-oxide-modified reduced-GO composite (FeG), as well as an activated-carbon(C)/clay/alumina-based adsorbent, RemBind™ (RemB), were evaluated. Sorption by FeG and RemB (>90%) was much greater than GO (60%). While increases in pH hindered PFOA-sorption by GO due to increased repulsion of anionic PFOA, variations in pH and ionic strength did not significantly influence PFOA-sorption by FeG and RemB, indicating that binding was predominantly controlled by non-electrostatic forces. Hydrophobic interactions are assumed at the graphene or C-surface for all adsorbents, with added ligand-exchange mechanisms involving the associated Fe and Al-minerals in FeG and RemB, respectively. Desorption of adsorbed PFOA was greatest in polar organic solvents like methanol, rather than water, toluene or hexane, providing estimates of binding strength and reversibility from an environmental-partitioning perspective; i.e. risk of remobilisation of bound PFOA due to rainfall events is low, but presence of polar organic solvents may increase leaching risk. Iron-mineral-functionalisation of GO enhanced the amount of PFOA adsorbed (by 30%) as well as binding strength, highlighting the advantage of combining mineral and C-phases. Successful sorption of a range of PFASs from a contaminated-site water sample highlight the potential of using 'mixed' adsorbents like FeG and RemB *in situ* for PFAS-remediation, as they provide avenues for enhanced sorption through multiple mechanisms.

Keywords: Sorption; PFOA; PFASs; remediation; graphene; mixed mineral and C-based adsorbents.

1. Introduction

Perfluorooctanioc acid (PFOA) is an anthropogenic fluoro-chemical belonging to the broader class of chemicals known as per- and polyfluoroalkyl substances (PFASs). Owing to their unique physico-chemical properties, they have found use in a wide range of consumer and industrial applications including food packaging, stain and water-repellent fabrics and coatings, as well as fire-fighting foams (Renner, 2001). However, due to their bioaccumulation potential and persistence in the environment, PFOA and related PFASs have raised environmental and human health concerns over the last decade (Higgins et al., 2007, Moody and Field, 2000, Sundström et al., 2011), with several cases of contamination reported worldwide (Lein et al., 2008, Washington et al., 2010). Concentrations of up to 4 µg/L have been detected in drinking water supplies and surface environmental waters around the world (Rumsby et al., 2009), and up to 50 µg/kg have been found in soils (Zareitalabad et al., 2013). Point source concentrations (e.g. at a PFAS-waste storage pond) can reach up to the low mg/L levels (Arias et al., 2014). Despite production largely being phased out, PFASs are ubiquitous in the environment due to their persistence and mobility (Moody and Field, 2000).

The strong carbon-fluorine (C–F) bonds of the structure make PFOA extremely resistant to chemical and biological degradation (O'Hagan, 2008). While thermal decomposition of PFOA has been demonstrated at high temperatures of up to 1000 °C (Kucharzyk et al., 2017), this is very energy-intensive and often cannot be achieved *in situ*. Various physico-chemical techniques like sonochemical degradation (Cheng et al., 2009) and advanced oxidation (Bruton and Sedlak, 2017, Lee et al., 2013) have also been used to breakdown PFASs, however complete mineralisation and de-fluorination are not always achieved, and sometimes, toxic by-products may be formed (Kucharzyk et al., 2017).

As degradation of these chemicals is an energy-intensive process and presents challenges especially for use *in situ*, adsorption is a cost-effective strategy to manage PFOA contamination *in situ* by reducing contaminant mobility. Sorption of PFOA onto surfaces of carbonaceous materials (like chars, activated-C and nanotubes) (Deng et al., 2012, Wang et al., 2015) have been demonstrated, with granular activated-C used most commonly for treatment of PFASs in *ex situ* filtration systems. These rely on hydrophobic interactions at the non-polar C-phase (Kucharzyk et al., 2017). Aluminium (Al) and iron (Fe)-based minerals (Feng et al., 2017, Gao and Chorover, 2012, Hellsing et al., 2016, Wang et al., 2012) like alumina, hematite and goethite have also been shown to bind PFASs through electrostatic or ligand-exchange mechanisms (Du et al., 2014). Graphene, composed of closely packed sp^2 hybridised carbon atoms (Novoselov et al., 2012), the latest addition to the nanocarbon

family, is an excellent candidate for use as an adsorbent due to its high surface area and versatile surface chemistry. Sorption of various organic contaminants (e.g. polycyclic aromatic hydrocarbons, dyes and pharmaceuticals) *via* hydrophobic interactions and pi-pi interactions with conjugated regions on the graphitic basal surface of graphene-based materials (GBMs) have been demonstrated (Fan et al., 2013, Ji et al., 2013). However, there is a lack of studies investigating the use of GBMs for PFAS-sorption. One study has reported the use of graphene oxide (GO), the most common graphene-derivative, for sorption of perfluorooctanesulfonate (PFOS) in the presence of magnesium ions (Mg^{2+}), due to the ability of Mg^{2+} to form a bridge between PFOS and GO (Zhao et al., 2016). Similar demonstrations for PFOA and other PFASs are not available.

Graphene oxide is known to have a highly negative surface charge due to the presence of oxygen-functional groups including epoxides, carboxyls and hydroxyls on its surface (Dreyer et al., 2010, Marcano et al., 2010). The most common PFASs of concern, including PFOA and PFOS, exist as anions, which can be repelled by negatively charged adsorbents. It is thus reasonable to assume that despite avenues for hydrophobic or bridging interactions (Zhao et al., 2016), GO is not the best candidate for PFAS-sorption, and other GBMs may provide opportunities for superior binding. Graphene oxide is remarkably amenable to surface modifications, owing to its oxygen functionalities, and can be strategically functionalised for enhanced contaminant sorption. For instance, GO has been used widely for adsorption of organic dyes and heavy metals (Yusuf et al., 2015). However, functionalisation of GO with polydopamine further improved dye and metal adsorption, compared to pure GO, due to additional surface active sites (Dong et al., 2014). We propose that the suitable functionalisation of GO could lead to improved sorption of PFOA and other PFASs compared to GO. Given that Fe-based minerals have been shown to adsorb PFASs (Feng et al., 2017, Gao and Chorover, 2012), an Fe-functionalisation was performed to prepare an Fe-oxide-modified reduced-GO composite (FeG) for testing. Given the separate successes of carbonaceous materials and minerals in PFAS-sorption, we hypothesise that designing adsorbents composed of both carbon and mineral phases together may improve opportunities to explore a new generation of advanced 'mixed' adsorbents that provide multiple binding sites with high affinity for PFOA and other PFASs. To our knowledge, this has not been explored before, particularly in the case of GBMs. To further support this, we also tested a non-graphene-based 'mixed' commercial adsorbent, RemBind™ (RemB; Ziltek Pty. Ltd.), which is composed of activated C, kaolin, alumina, and other proprietary additives.

In this study, we evaluated three adsorbents – GO, FeG and RemB – for PFOA-sorption, with potential for *in situ* remediation application. The carbonaceous nature of GO is in contrast to the 'mixed' mineral and C-based nature of the FeG composite (prepared from

GO) and RemB. The influence of different pH conditions, ionic strength, and PFOA concentrations were investigated using model PFOA solutions to evaluate sorption efficiency under different environmental conditions. Subsequent desorption experiments were conducted to test the strength of PFOA-binding by the adsorbents, as well as to gain insight into the possible binding mechanisms involved. Finally, successful sorption of a variety of PFASs from a contaminated field water was demonstrated, showing the practical application of the 'mixed' adsorbents for remediation of PFOA and related PFASs.

2. Materials and Methods

2.1. Materials and chemicals

Natural graphite flakes were obtained from the Uley graphite mine (South Australia). All chemicals including potassium permanganate, sulfuric acid, phosphoric acid, 30% hydrogen peroxide, ferrous sulfate heptahydrate, hydrochloric acid (HCl), sodium hydroxide (NaOH), methanol, toluene and hexane were of analytical grade. Radiolabelled ^{14}C- PFOA (specific activity 2035 Bq/nmol) was purchased from American Radiolabelled Chemicals Inc. (USA). RemBind™ was sourced from an environmental remediation company in South Australia (Ziltek Pty. Ltd.).

2.2. Synthesis and characterisation of adsorbents

Two adsorbents were synthesised using the same base material, graphite. Briefly, strong oxidative exfoliation based on an improved Hummer's method (Marcano et al., 2010) was used to synthesise GO, which was then hydrothermally reduced in the presence of ferrous sulfate (Cong et al., 2012) to form synthesise FeG. The morphology of the adsorbents was examined by transmission electron microscopy (TEM Philips-CM100). An energy dispersive X-ray (EDX) detector coupled to a scanning electron microscope elucidated elemental composition. X-ray diffraction (XRD, PANalytical X'Pert Pro MPD) and Fourier-transform infrared (FTIR, Nicolet 6700, Thermo Fisher) spectra were recorded for structural and functional characterisation. Surface area was determined by the methylene blue dye adsorption method using ultraviolet-visible spectroscopy (664nm). Surface charge properties and point of zero charge (PZC) were determined by measuring zeta potential across a pH gradient using dynamic light scattering (Malvern Zetasizer NanoZS). The complete synthesis and characterisation of these adsorbents have been published previously (Lath et al., 2018), and details are provided in the Supporting Information.

2.3. Batch sorption studies

Radiolabelled ^{14}C-PFOA was used to prepare contaminated test solutions. A 10 mM $CaCl_2$ background electrolyte was used to minimise effects of ionic strength variability, and pH was

maintained at pH 5.5. Batch sorption tests were carried out by mixing 5 mg adsorbent with 10 mL of the test solutions, under constant agitation on an orbital shaker (100 rpm, 25 °C) to attain equilibrium. The equilibrium time for each adsorbent was determined by testing sorption for durations from 0 – 96 hours. Sorption was also investigated as a function of concentration, by using initial PFOA concentrations ranging from 0 – 650 µg/L. The influence of pH was studied across a pH range from 3 to 9; minimal volumes (< 100 µL) of 1M HCl or 1M NaOH were used to adjust pH. By using background electrolyte solutions of different concentrations (0 – 100 mM $CaCl_2$), effects of ionic strength (salt effects) (0 – 17 dS/m) on sorption were also investigated. At the end of each sorption step, solutions were centrifuged (5500 g, 1 hour) and 0.5 mL aliquots of the supernatants were analysed (see below).

Desorption of adsorbed PFOA from the adsorbents was also investigated. We used a 30 µg/L PFOA solution, and mixed it with the adsorbents. The equilibrium solutions were then discarded and the remaining PFOA-loaded adsorbents were mixed with different solvents having increasing hydrophobicity and decreasing polarity (water, methanol, toluene and hexane). Amounts of PFOA desorbed from the adsorbents into the solvents were calculated as a percentage of initial amounts adsorbed.

To assess efficiency and potential of using GO, FeG and RemB in a field sample, sorption was also tested in a PFAS-contaminated water sample (pH 7.9) collected near a commercial airport in Australia.

2.4. Quantitative analyses

All samples with ^{14}C-PFOA were subjected to radiochemical analysis. Aliquots of supernatants (0.5 mL) were collected and transferred into scintillation vials and topped up with 4 mL of scintillation cocktail. The activity of ^{14}C in the samples was measured *via* β-liquid scintillation counting (Tri-Carb 3110 RT, Perkin Elmer). Concentrations of PFOA were calculated from the measured ^{14}C activity, and the specific activity.

Analysis of a suite of PFASs from the contaminated field water samples (before and after remediation) were completed by a NATA-accredited facility, National Measurement Institute (Australia), based on the USEPA 537 methodology utilising liquid chromatography-tandem mass spectrometry (LC-MS/MS) detection. Samples were extracted using solid-phase extraction (weak anion exchange) and retained analytes were eluted with ammonia solution. High concentration samples were diluted prior to extraction. Quantitation was based on recoveries of isotopically labelled standards used as internal standards. Recoveries from laboratory control samples ranged from 90% to 103%. Reporting limits ranged from 0.01 – 0.05 µg/L. Full names and abbreviations for PFASs measured in the field water sample are listed in Supporting Information Table S1.

2.5. Data analyses

The amount of PFOA adsorbed was calculated as the difference between PFOA concentrations in solution before and after equilibration. The performance of each adsorbent was expressed either as a percentage, or as amount of PFOA adsorbed per gram of adsorbent (µg/g). All experiments were performed in triplicate. Losses of PFOA due to sorption onto the polypropylene sorption tubes were observed; any such losses were corrected for in the calculations.

3. Results and Discussion

3.1. Characterisation of prepared graphene-based adsorbents

The morphology of GO and FeG were examined using TEM imaging (Figure 1). Oxidative exfoliation of graphite resulted in the formation of thin GO sheets (Figure 1a). Hydrothermal reduction of GO with Fe^{2+} led to the formation of an Fe-oxide-modified, reduced-GO composite, FeG (Figure 1b); the attached Fe-oxide-based nanoparticles were seen as dense spots (50 - 100 nm) distributed on the surface. EDX spectra (Table S2 and Figure S1) confirmed the elemental composition of the adsorbents, all of which exhibited the presence of carbon and oxygen. FeG displayed an additional signal for Fe, and RemB displayed additional signals for Al and silicon (Si).

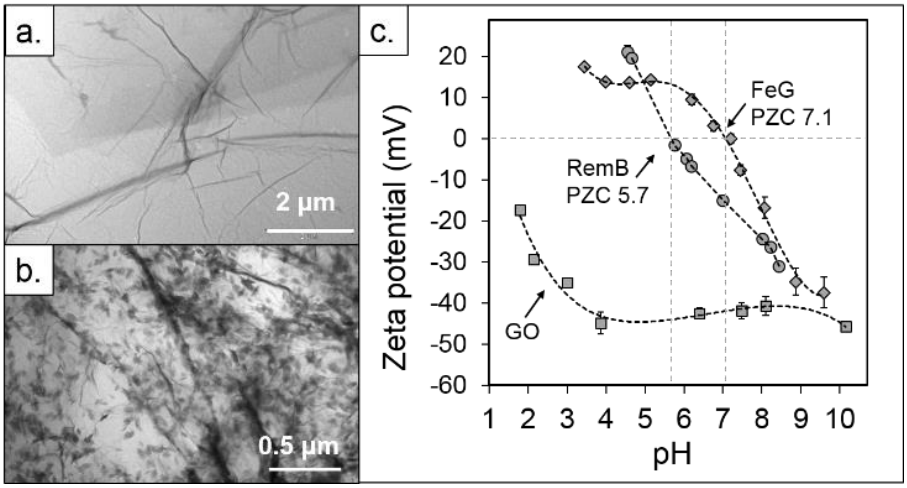

Figure 1. Surface characterisation of adsorbents: (a) TEM image of graphene oxide (GO), (b) TEM image of an Fe-oxide-modified reduced-GO (FeG) where dark spots confirm the attachment of Fe-based nanoparticles (50 - 100 nm), and (c) surface zeta potential measurements of GO, FeG and a commercial adsorbent, RemBind™ (RemB) as a function of pH (25 °C).

The mineralogical phase and crystal structure of the adsorbents were confirmed by XRD (Figure S2). GO displayed an oriented 'platy' phase with a unit cell of 7.16Å, consistent with monolayer spacings typically observed for GO (Marcano et al., 2010). Goethite mineral (α-FeOOH) was detected as the crystalline phase in FeG, confirming the identity of the Fe-oxide nanoparticles. A dominant amorphous activated-carbon phase was detected in RemB, along with aluminosilicate clays, kaolinite and muscovite. FTIR spectra (Figure S3) revealed characteristic peaks of GO including the CO_2H stretching (1725 cm^{-1}) and COH bending vibrations (1220 cm^{-1}) (Marcano et al., 2010), indicating the presence of carboxylic and alcohol groups. Appearance of additional peaks associated with Fe-OH bending (768 cm^{-1} and 871 cm^{-1}), and Fe-O stretching vibrations (575 cm^{-1}) (Cong et al., 2012) on FeG confirmed the attachment of goethite.

The surface area and charge properties of a material play an important role in adsorbent-adsorbate interactions. Surface areas of GO, FeG and RemB as determined by the methylene blue adsorption method (Figure S4) were 434.6, 242.4 and 123.4 m^2/g respectively. Surface charge for FeG and RemB varied notably with pH (Figure 1c). Their PZC (pH at which zeta potential is zero) were determined to be 7.1 and 5.7, respectively. Conversely, GO maintained a highly negative charge across the pH range investigated.

3.2. Batch sorption studies

Sorption by FeG and RemB took 3 – 4 hours to attain equilibrium, whereas GO required at least 48 hours to attain equilibrium (Figure 2a). Using an initial PFOA concentration of 30 µg/L, FeG and RemB showed > 90% sorption, while only up to 60% of the PFOA was adsorbed by GO; the incorporation of the goethite mineral phase onto the modified GO surface enhanced PFOA-sorption by 30%, highlighting the advantage of combining mineral and C-phases. Considerable sorption despite the highly negatively charged surface of GO suggests the role of non-electrostatic interactions with PFOA. Interestingly, the performance of the adsorbents in terms of amounts adsorbed (RemB = FeG > GO) was inverse to what would be expected from the measured surface areas of the adsorbents (GO > FeG > RemB).

By testing a range of initial PFOA concentrations (0 – 650 µg/L), amounts of PFOA adsorbed per gram of adsorbent were plotted as a function of equilibrium solution concentration (Figure 2b). In the range tested, sorption followed a linear trend, indicating that the surface sorption sites were not fully saturated, with more active sites available for sorption. At higher concentrations, the so-called sorption plateau may be reached; a state in which the adsorbed amounts become independent of the concentration in solution. However, at the environmentally relevant concentrations used in our studies, sorption was not saturable.

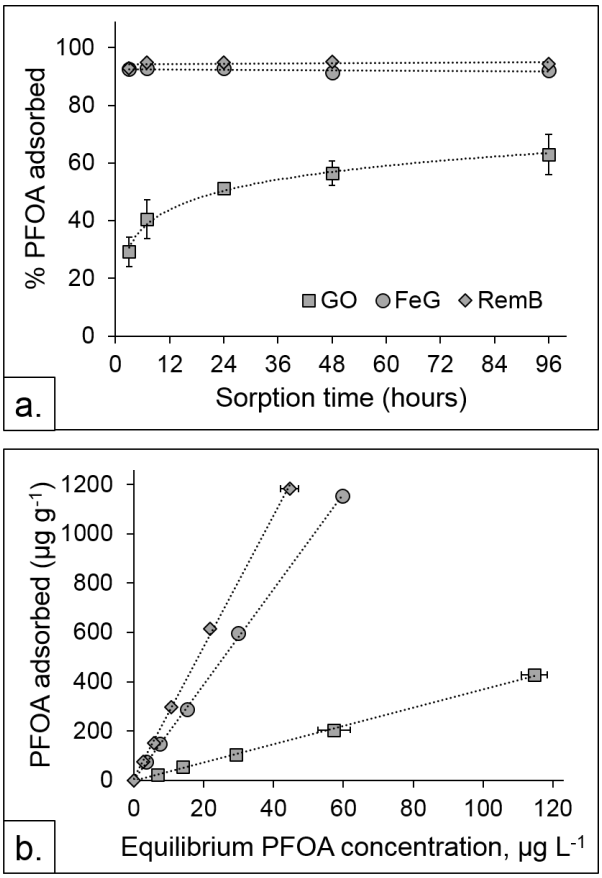

Figure 2. Sorption curves showing (a) PFOA sorption equilibrium was attained in 48 hrs by graphene oxide (GO), and in 3 – 4 hrs by Fe-oxide-modified reduced-GO (FeG) and a commercial adsorbent, RemBind™ (RemB), at initial PFOA concentration of 30 µg/L in 10 mM $CaCl_2$ background at 25°C, and (b) effect of increasing initial PFOA concentration ranging from 0 – 650 µg/L, in 10 mM $CaCl_2$ background (pH 5.6, 25°C, 48 hrs). Error bars represent standard deviation (n = 3). Error bars for FeG and RemB are small and hence not visible in the graphs.

The effect of solution chemistry, specifically pH and ionic strength, are illustrated in Figure 3a and 3b, respectively. The acid dissociation constant, pK_a, of PFOA has been reported to be 2.8 (Moody and Field, 2000). Hence, at the pH range investigated in this study (pH 3 – 9), PFOA is expected to exist in its deprotonated anionic form. Despite GO having a high (net) negative charge (Figure 1c), a considerable amount of sorption of the PFOA anion was observed, overcoming the anticipated repulsion between the adsorbate and adsorbent. This indicates the role of non-electrostatic sorptive mechanisms in binding. Given the carbonaceous nature of GBMs, these could be hydrophobic interactions between the graphene surface and the hydrophobic tails of the PFOA molecules (Zhi and Liu, 2015). On

increasing the pH from 3 to 9, a 20% reduction in the sorption of PFOA by GO was observed (Figure 3a), likely due to increased repulsion between GO and anionic PFOA, with GO acquiring greater negative charge at higher pH (zeta potential of GO was -35 mV at pH 3, and -43 mV at pH 9; Figure 1c). This increased repulsion can reduce the likelihood of contact between GO and PFOA molecules, thus deterring the hydrophobic sorption interactions. Interestingly, variations in pH did not influence the sorption behaviour of FeG and RemB (Figure 3a). Even above the PZC, where FeG and RemB have net negatively charged surfaces, there was no significant reduction in PFOA-sorption, again suggesting the involvement of non-electrostatic forces in binding PFOA. A variety of results have been reported for effect of pH on PFOA-sorption depending on the type of adsorbent. Sorption onto activated carbon fibre and single-walled carbon nanotubes (CNTs) decreased by 12% and 32%, respectively (Deng et al., 2012, Wang et al., 2015), when pH increased from 3 to 9 (attributed to increased repulsion), whereas sorption onto powdered activated carbon was relatively unaffected (Deng et al., 2012) due to a stable zeta potential in that pH range. A study comparing PFAS-sorption onto different types of CNTs found that pristine CNTs showed greater sorption compared to hydroxyl and carboxyl-functionalised CNTs (Deng et al., 2012), demonstrating the role of hydrophobic interactions in PFAS-sorption by carbonaceous adsorbents.

Changes in ionic strength will usually affect the electrostatic nature of the adsorbents' surface, and as a result, the interactions that occur at the surface. Ionic strength can also alter the activity or solubility of ionic species, and soil surface charge, hence influencing sorption. While a slight negative effect (20 – 25%) of increasing ionic strength on the sorption by GO was observed, it did not alter PFOA-sorption by FeG and RemB (Figure 3b), giving further support to the hypothesis that binding may be non-electrostatic. It is important to note that in a sense, both FeG and RemB are 'mixed' adsorbents as they are comprised not only of a dominant carbonaceous phase, but also encompass mineral phases. Structural analysis *via* XRD revealed the presence of goethite mineral particles in FeG, and confirmed the presence of aluminosilicate clay minerals in RemB. It is thus possible that in addition to hydrophobic interactions with the carbonaceous phases of the adsorbents, the Fe, Al and Si mineral phases are involved in strong ligand-exchange or inner-sphere complexation mechanisms with PFOA. Gao and Chorover (Gao and Chorover, 2012) suggested PFOA-sorption onto Fe-oxide surfaces was possible due to ligand-exchange of the carboxylate functional group at surface hydroxy groups of the minerals. Similar mechanisms have also been observed at the surface hydroxy groups of an Al-based mineral, boehmite (AlOOH) (Du et al., 2014, Wang et al., 2012). In fact, some of these studies investigating PFOA-sorption by Fe- and Al- based minerals indicated that sorption decreased considerably with increase

in ionic strength, due to charge screening and diminished electrostatic interactions (Gao and Chorover, 2012, Wang et al., 2012, Wang and Shih, 2011). In these cases, the portion of sorption that was attributed to electrostatic interactions and outer-sphere complexation was thought to be influenced by variations in ionic strength, whereas sorption controlled by inner-sphere complexation was not considered to be affected (Gao and Chorover, 2012).

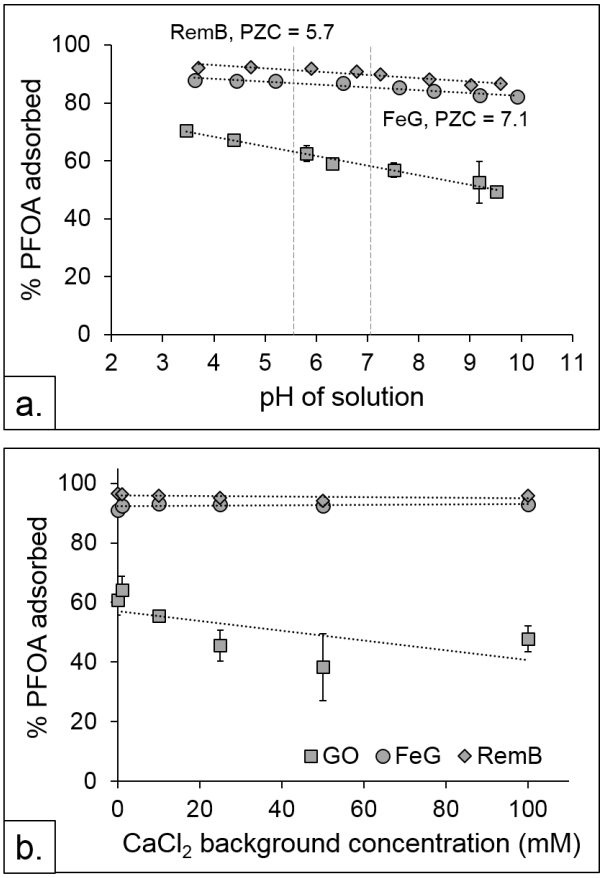

Figure 3. (a) Effect of pH on PFOA-sorption by graphene oxide (GO), Fe-oxide-modified reduced-GO (FeG) and a commercial adsorbent, RemBind™ (RemB) at initial PFOA concentration of 100 µg/L in 10 mM CaCl2 background at 25°C, and (b) effect of ionic strength variability on sorption at initial PFOA concentration of 20 µg/L (pH 5.6, 25°C). Error bars represent standard deviation (n = 3). Error bars for FeG and RemB are small and hence not visible in the graphs.

By varying the background electrolyte concentrations in this study (0, 1, 10, 25, 50 and 100 mM $CaCl_2$), the corresponding electrical conductivity conditions that the test solutions were exposed to were 0, 0.24, 2.11, 4.93, 9.24 and 17.11 dS/m, respectively. This covers a broad range of environmental conditions, and is particularly interesting from a practical perspective. For instance, soils with extracts of conductivities > 4 dS/m are usually considered saline. In

landfills, leachates could be expected to have a conductivity of 5 – 17 dS/m (Marttinen et al., 2002). In addition to accepting PFAS-contaminated soils, landfills receive several other PFAS-containing commercial products which are discarded at the end of their functional life (Benskin et al., 2012). As a result, unlined landfills can act as a source of PFAS-release to groundwater (Lang et al., 2017). The resistance of FeG- and RemB-sorbed PFOA to desorption in such conditions suggests that the risk of diffusive transport of PFOA from landfills through leachates into the groundwater will be minimised, making these adsorbents highly favourable. Consequently, FeG and RemB could also potentially be laid down in landfill sites as a barrier-lining in multi-liner systems to mitigate the leakage or migration of landfill leachates into the water table. Previous research has demonstrated the applicability of GO for PFOS-sorption (Zhao et al., 2016). In this study, we prove that the performance of GO can be improved through strategic mineral-functionalisation, making FeG a better adsorbent (for a variety of PFASs, as shown in section 3.4). It is possible that with further optimisation, the performance of the FeG may be further improved to surpass RemB. By increasing the Fe-loading during the synthesis procedure, the number of goethite nanoparticles on the FeG surface may be increased, providing additional active sites for greater PFOA-binding.

3.3. Desorption experiments

Like adsorption, desorption from a solid phase is another fundamental process controlling the fate and transport of soluble contaminants in the environment. To further test the strength of PFOA-binding, and to gain insight into the possible binding mechanisms involved, we investigated desorption of adsorbed PFOA into 4 solvents with different polarities - Milli-Q water, methanol, toluene and hexane. In the initial sorption step (before desorption) GO, FeG and RemB adsorbed 16.3, 26.7 and 25.8 µg PFOA/g adsorbent, respectively. The proportion of this adsorbed PFOA that was desorbed by the solvents is illustrated in Figure 4. Overall, these results show methanol was the strongest desorbing solvent. This is not surprising given that methanol is known to impart PFOA with improved solubility (Kutsuna et al., 2012), and is the solvent of choice for extracting PFOA from various biological and environmental media (Du et al., 2014). The proportions of sorbed PFOA desorbed by methanol were 80%, 37% and 27% for GO, FeG and RemB, respectively. In the case of FeG and RemB, where the binding appears to be stronger than GO (as observed in Figures 3a and 3b), toluene was able to desorb a small fraction of the adsorbed PFOA (13% and 17%, respectively). Only a small amount (8%) of PFOA was desorbed by water from GO, whereas no desorption from FeG and RemB were observed in water. No PFOA was desorbed from either of the adsorbents by hexane.

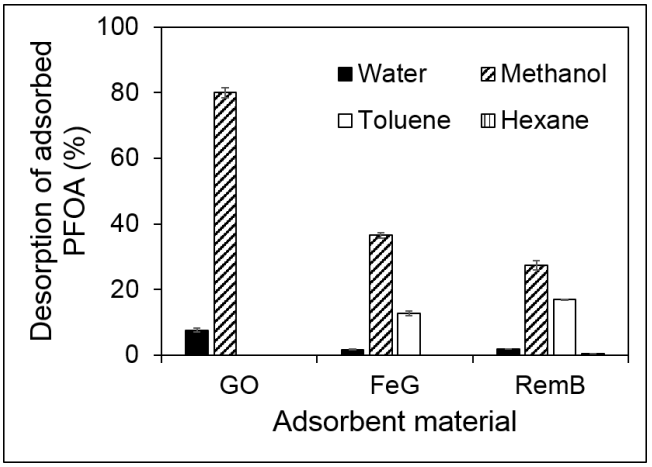

Figure 4. Desorption of PFOA (expressed as a percentage of adsorbed amount) into Milli-Q water, methanol, toluene and hexane. Using an initial PFOA concentration of 30 µg/L, amounts adsorbed by graphene oxide (GO), Fe-oxide-modified reduced-GO (FeG) and a commercial adsorbent, RemBind™ (RemB) were 16.3, 26.7 and 25.8 µg PFOA/g adsorbent, respectively.

PFOA is an anionic polar molecule, with a long hydrophobic tail. Our results suggest that ionic PFOA molecules require polar to moderately polar organic solvents (i.e. methanol and toluene) to solubilise or desorb PFOA, rather than non-polar solvents like hexane. The polarity of the solvents tested are in the order of water > methanol > toluene > hexane. Measures of desorption by these solvents can be considered as estimates of strength of binding (Navarro et al., 2017), in the order opposite to that of polarity (toluene > methanol > water). Consequently, PFOA fractions desorbed by water are weakly bound, whereas fractions desorbed by methanol and toluene are bound much more strongly on the adsorbent surface. The PFOA molecules that were not desorbed could be regarded as bound irreversibly to the adsorbents (in the case of GO, FeG and RemB, these were 12%, 49% and 53% of adsorbed PFOA, respectively). These desorption data are important from an environmental partitioning perspective, and can help us estimate the risks of remobilisation of adsorbent-bound PFOA, especially when used for *in situ* remediation of contaminated soils. For instance, it is reasonable to assume that precipitation from rainfall events is unlikely to desorb PFOA bound by FeG and RemB, hence disregarding any concerns for subsequent leaching into subsurface soils or groundwater. Consequently, this would also suggest reduced bioavailability to plants and organisms exposed to the treated soil. However, at a waste disposal or landfill site, where PFASs may co-occur with organic solvent waste from accidental spills, increased PFOA mobility is likely. Considering the

desorption behaviour of the two different GBMs tested here, FeG is expected to be a better adsorbent than GO for *in situ* remediation, given the potential for reduced leachability and reduced bioavailability of PFOA.

3.4. Remediation of a contaminated-site water sample

To demonstrate the efficiency of the adsorbents in a real environmental matrix, in a final experiment, we tested sorption of PFOA and other PFASs from a contaminated field water sample collected from a commercial airport site in Australia. The PFAS-composition of the water sample is detailed in Table 1 (PFASs that were present at concentrations below detection limits have been excluded); treatment efficiency is expressed as a percentage of removal of each PFAS.

Of the 30 µg/L of PFOA present in the sample, the 'mixed' adsorbents, FeG and RemB adsorbed 94% and 95.7% PFOA, respectively. However, GO only adsorbed 3.3% of the PFOA. This could be due to the presence of several other competing ions as well as other PFAS species in the water sample. As already observed in the batch experiments, PFOA sorption onto GO could be compromised by high pH and also affected by ionic strength (Figures 3a and 3b). The main component of the contaminated water sample was PFOS at 600 µg/L, of which > 99% was removed by FeG and RemB. It has been observed in previous studies that for the same perfluorocarbon chain lengths, PFASs with sulfonate head groups exhibit greater sorption than those with carboxylate groups (Hellsing et al., 2016, Higgins and Luthy, 2006, Wang and Shih, 2011). Hence the extraordinary sorption of PFOS over PFOA can be attributed to differences in functional groups. For the fluorotelomer sulfonates (6:2 FTS and 8:2 FTS), > 96% sorption was observed in the case of all adsorbents, including GO. Fluorotelomers are only partially fluorinated, and comprise of a $–CH_2–CH_2–$ spacer group occurring in between the fluorinated tail and the polar sulfonate head. The lower degree of fluorination may be the reason why GO was able to display enhanced sorption of these compounds over the fully fluorinated compounds. The presence of the $–CH_2–CH_2–$ group potentially allows interactions with the aliphatic regions (sp^3 hybridised carbon atoms) in the oxygenated GO structure (Dreyer et al., 2010).

Another important observation in the data is the apparent effect of chain length of the PFASs on sorption performance, specifically for FeG and RemB. For both, perfluoroalkyl carboxylates as well as perfluoroalkyl sulfonates, greater sorption was detected as chain length increased, further substantiating the dominant role of hydrophobic interactions. This is consistent with what has been previously reported in the literature for sorption to other carbon-based remediation materials (Deng et al., 2012, Xiao et al., 2017). When keeping the functional group the same, increase in the C–F chain length decreases the solubility

(Hellsing et al., 2016) and increases hydrophobicity of PFASs, allowing stronger hydrophobic interactions with the adsorbents (Du et al., 2014).

Table 1. Treatment of PFAS-contaminated water by GO, FeG and RemB.

PFASs detected in contaminated water sample	PFAS-concentrations in contaminated water (µg/L)	% Removal of PFASs		
		GO	FeG	RemB
Perfluoroalkyl carboxylates (increasing order of chain length)				
PFBuA	9.7	10.3	8.2	26.8
PFPeA	12	0	8.3	8.3
PFHxA	60	3.3	28.3	36.7
PFHpA	13	15.4	73.1	78.5
PFOA	30	3.3	94	95.7
PFNA	2.8	10.7	98.9	99.1
PFDA	1	5	98.0 (bdl)[A]	98.0 (bdl)
Perfluoroalkyl sulfonates (increasing order of chain length)				
PFBS	13	7.7	15.4	46.9
PFHxS	100	5	90.5	96
PFOS	600	-15	99.3	99.7
Fluorotelomers and perfluoroalkylsulfonamides				
6:2 FTS	2.6	98.1 (bdl)	96.3	98.1 (bdl)
8:2 FTS	6.1	99.2 (bdl)	99.2 (bdl)	99.2 (bdl)
PFOSA	2.3	43.5	99.1 (bdl)	99.1 (bdl)

[A] Where treated PFAS-concentrations were below detection limits (bdl), the detection limit value (0.02 or 0.05 µg/L, depending on the type of PFAS) was used to calculate percentage adsorbed.

4. Conclusions

Overall, the mixed' mineral and C-based adsorbents, FeG and RemB, showed excellent potential for PFOA-sorption, when compared to GO. While variations in pH and ionic strength conditions hindered PFOA-sorption by GO, they did not compromise the performance of FeG. Results from our desorption study demonstrate that the binding of PFOA by FeG is strong in aqueous as well as ionic media ($CaCl_2$) and risk of contaminant remobilisation through rainfall events, solubilisation, desorption or leachability is minimal,

unless polar organic solvents like methanol and toluene co-occur at the contaminated sites. Such resistance to changes in environmental solution chemistry and strength of binding make FeG and RemB favourable *in situ* adsorbents for PFASs, with added potential for use as barriers to line landfills that accept PFAS-waste, to mitigate migration of leachate. Finally, successful sorption of a range of PFASs from a contaminated field water sample by FeG and RemB demonstrates the potential application of these 'mixed' adsorbents for PFAS-remediation. Due to the versatile surface functionality of GBMs, further modifications and optimisation of the FeG surface (e.g. increased loading of Fe-minerals during synthesis) could be performed to achieve a greater amount of sorption. To our knowledge, this is the first study highlighting the advantage of using mixed mineral and C-based materials for enhanced PFAS-sorption, and demonstrating the potential of novel graphene technology for this purpose.

5. Acknowledgements

We would like to thank Dr. Mark Raven (CSIRO) for performing XRD analyses, as well as Adelaide and Waite Microscopy for access to TEM and SEM-EDX facilities. Financial support from Australian Research Council Discovery Grant DP150101760 is gratefully acknowledged. We would also like to thank Ziltek Pty. Ltd. for their financial support and provision of RemBind™.

6. Conflicts of Interest

The authors declare no conflicts of interest.

7. References

Arias EVA, Mallavarapu M, Naidu R (2014). Identification of the source of PFOS and PFOA contamination at a military air base site. *Environmental Monitoring and Assessment,* **187,** 4111.

Benskin JP, Li B, Ikonomou MG, Grace JR, Li LY (2012). Per- and polyfluoroalkyl substances in landfill leachate: patterns, time trends, and sources. *Environmental Science & Technology,* **46,** 11532-11540.

Bruton TA, Sedlak DL (2017). Treatment of aqueous film-forming foam by heat-activated persulfate under conditions representative of in situ chemical oxidation. *Environmental Science & Technology,* **51,** 13878-13885.

Cheng J, Vecitis CD, Park H, Mader BT, Hoffmann MR (2009). Sonochemical degradation of perfluorooctane sulfonate (PFOS) and perfluorooctanoate (PFOA) in groundwater: kinetic effects of matrix inorganics. *Environmental Science & Technology,* **44,** 445-450.

Cong H-P, Ren X-C, Wang P, Yu S-H (2012). Macroscopic multifunctional graphene-based hydrogels and aerogels by a metal ion induced self-assembly process. *ACS Nano,* **6,** 2693-2703.

Deng S, Zhang Q, Nie Y, Wei H, Wang B, Huang J, Yu G, Xing B (2012). Sorption mechanisms of perfluorinated compounds on carbon nanotubes. *Environmental Pollution,* **168,** 138-144.

Dong Z, Wang D, Liu X, Pei X, Chen L, Jin J (2014). Bio-inspired surface-functionalization of graphene oxide for the adsorption of organic dyes and heavy metal ions with a superhigh capacity. *Journal of Materials Chemistry A,* **2,** 5034-5040.

Dreyer DR, Park S, Bielawski CW, Ruoff RS (2010). The chemistry of graphene oxide. *Chemical Society Reviews,* **39,** 228-240.

Du Z, Deng S, Bei Y, Huang Q, Wang B, Huang J, Yu G (2014). Adsorption behavior and mechanism of perfluorinated compounds on various adsorbents—A review. *Journal of Hazardous Materials,* **274,** 443-454.

Fan L, Luo C, Sun M, Qiu H, Li X (2013). Synthesis of magnetic β-cyclodextrin–chitosan/graphene oxide as nanoadsorbent and its application in dye adsorption and removal. *Colloids and Surfaces B: Biointerfaces,* **103,** 601-607.

Feng H, Lin Y, Sun Y, Cao H, Fu J, Gao K, Zhang A (2017). In silico approach to investigating the adsorption mechanisms of short chain perfluorinated sulfonic acids and perfluorooctane sulfonic acid on hydrated hematite surface. *Water Research,* **114,** 144-150.

Gao X, Chorover J (2012). Adsorption of perfluorooctanoic acid and perfluorooctanesulfonic acid to iron oxide surfaces as studied by flow-through ATR-FTIR spectroscopy. *Environmental Chemistry,* **9,** 148-157.

Hellsing MS, Josefsson S, Hughes AV, Ahrens L (2016). Sorption of perfluoroalkyl substances to two types of minerals. *Chemosphere,* **159,** 385-391.

Higgins CP, Luthy RG (2006). Sorption of perfluorinated surfactants on sediments. *Environmental Science & Technology,* **40,** 7251-7256.

Higgins CP, McLeod PB, MacManus-Spencer LA, Luthy RG (2007). Bioaccumulation of perfluorochemicals in sediments by the aquatic oligochaete Lumbriculus variegatus. *Environmental Science & Technology,* **41,** 4600-4606.

Ji L, Chen W, Xu Z, Zheng S, Zhu D (2013). Graphene nanosheets and graphite oxide as promising adsorbents for removal of organic contaminants from aqueous solution. *Journal of Environmental Quality,* **42,** 191-198.

Kucharzyk KH, Darlington R, Benotti M, Deeb R, Hawley E (2017). Novel treatment technologies for PFAS compounds: A critical review. *Journal of Environmental Management,* **204,** 757-764.

Kutsuna S, Hori H, Sonoda T, Iwakami T, Wakisaka A (2012). Preferential solvation of perfluorooctanoic acid (PFOA) by methanol in methanol–water mixtures: A potential overestimation of the dissociation constant of PFOA using a Yasuda–Shedlovsky plot. *Atmospheric Environment,* **49,** 411-414.

Lang JR, Allred BM, Field JA, Levis JW, Barlaz MA (2017). National estimate of per- and polyfluoroalkyl substance (PFAS) release to U.S. municipal landfill leachate. *Environmental Science & Technology,* **51,** 2197-2205.

Lath S, Navarro D, Tran D, Kumar A, Losic D, McLaughlin MJ (2018). Mixed-mode remediation of cadmium and arsenate ions using graphene-based materials. *CLEAN – Soil, Air, Water,* **46,** 1800073.

Lee YC, Lo SL, Kuo J, Huang CP (2013). Promoted degradation of perfluorooctanic acid by persulfate when adding activated carbon. *Journal of Hazardous Materials,* **261,** 463-469.

Lein NPH, Fujii S, Tanaka S, Nozoe M, Tanaka H (2008). Contamination of perfluorooctane sulfonate (PFOS) and perfluorooctanoate (PFOA) in surface water of the Yodo River basin (Japan). *Desalination,* **226,** 338-347.

Marcano DC, Kosynkin DV, Berlin JM, Sinitskii A, Sun Z, Slesarev A, Alemany LB, Lu W, Tour JM (2010). Improved synthesis of graphene oxide. *ACS Nano,* **4,** 4806-4814.

Marttinen SK, Kettunen RH, Sormunen KM, Soimasuo RM, Rintala JA (2002). Screening of physical–chemical methods for removal of organic material, nitrogen and toxicity from low strength landfill leachates. *Chemosphere,* **46,** 851-858.

Moody CA, Field JA (2000). Perfluorinated surfactants and the environmental implications of their use in fire-fighting foams. *Environmental Science & Technology,* **34,** 3864-3870.

Navarro DA, Kookana RS, McLaughlin MJ, Kirby JK (2017). Fate of radiolabeled C60 fullerenes in aged soils. *Environmental Pollution,* **221,** 293-300.

Novoselov KS, Falko VI, Colombo L, Gellert PR, Schwab MG, Kim K (2012). A roadmap for graphene. *Nature,* **490,** 192-200.

O'Hagan D (2008). Understanding organofluorine chemistry. An introduction to the C–F bond. *Chemical Society Reviews,* **37,** 308-319.

Renner R (2001). Growing concern over perfluorinated chemicals. *Environmental Science & Technology,* **35,** 154A-160A.

Rumsby PC, McLaughlin CL, Hall T (2009). Perfluorooctane sulphonate and perfluorooctanoic acid in drinking and environmental waters. *Philosophical Transactions of the Royal Society A: Mathematical, Physical and Engineering Sciences,* **367,** 4119-4136.

Sundström M, Ehresman DJ, Bignert A, Butenhoff JL, Olsen GW, Chang S-C, Bergman A (2011). A temporal trend study (1972–2008) of perfluorooctanesulfonate,

perfluorohexanesulfonate, and perfluorooctanoate in pooled human milk samples from Stockholm, Sweden. *Environment International,* **37,** 178-183.

Wang F, Liu C, Shih K (2012). Adsorption behavior of perfluorooctanesulfonate (PFOS) and perfluorooctanoate (PFOA) on boehmite. *Chemosphere,* **89,** 1009-1014.

Wang F, Shih K (2011). Adsorption of perfluorooctanesulfonate (PFOS) and perfluorooctanoate (PFOA) on alumina: Influence of solution pH and cations. *Water Research,* **45,** 2925-2930.

Wang Y, Niu J, Li Y, Zheng T, Xu Y, Liu Y (2015). Performance and mechanisms for removal of perfluorooctanoate (PFOA) from aqueous solution by activated carbon fiber. *RSC Advances,* **5,** 86927-86933.

Washington JW, Yoo H, Ellington JJ, Jenkins TM, Libelo EL (2010). Concentrations, distribution, and persistence of perfluoroalkylates in sludge-applied soils near Decatur, Alabama, USA. *Environmental Science & Technology,* **44,** 8390-8396.

Xiao X, Ulrich BA, Chen B, Higgins CP (2017). Sorption of poly- and perfluoroalkyl substances (PFASs) relevant to aqueous film-forming foam (AFFF)-impacted groundwater by biochars and activated carbon. *Environmental Science & Technology,* **51,** 6342-6351.

Yusuf M, Elfghi FM, Zaidi SA, Abdullah EC, Khan MA (2015). Applications of graphene and its derivatives as an adsorbent for heavy metal and dye removal: a systematic and comprehensive overview. *RSC Advances,* **5,** 50392-50420.

Zareitalabad P, Siemens J, Hamer M, Amelung W (2013). Perfluorooctanoic acid (PFOA) and perfluorooctanesulfonic acid (PFOS) in surface waters, sediments, soils and wastewater–A review on concentrations and distribution coefficients. *Chemosphere,* **91,** 725-732.

Zhao C, Fan J, Chen D, Xu Y, Wang T (2016). Microfluidics-generated graphene oxide microspheres and their application to removal of perfluorooctane sulfonate from polluted water. *Nano Research,* **9,** 866-875.

Zhi Y, Liu J (2015). Adsorption of perfluoroalkyl acids by carbonaceous adsorbents: Effect of carbon surface chemistry. *Environmental Pollution,* **202,** 168-176.

8. Supporting Information

Sorptive Remediation of Perfluorooctanoic Acid (PFOA) Using Mixed Mineral and Carbon-Based Materials

Supriya Lath [*, 1], Divina A. Navarro [1, 2], Dusan Losic [3], Anupama Kumar [2], Michael J. McLaughlin [1, 2]

[1] School of Agriculture Food and Wine, The University of Adelaide, PMB 1 Glen Osmond, SA 5064, Australia.

[2] CSIRO Land and Water, PMB 2 Glen Osmond, SA 5064, Australia.

[3] School of Chemical Engineering, The University of Adelaide, Adelaide, SA 5005, Australia.

* Corresponding author email: supriya.lath@adelaide.edu.au

Text S1. Synthesis of graphene oxide (GO) and Fe-oxide-modified reduced GO composite (FeG).

A top-down approach based on an improved Hummer's method (Marcano et al., 2010) which involves strong oxidative exfoliation of graphite using concentrated H_2SO_4, H_3PO_4 and $KMnO_4$ was used to synthesise GO. Unreacted $KMnO_4$ was reduced using 30% H_2O_2, and multiple wash cycles were performed with 30% HCl and distilled water to remove metal and acid residues. The material was dried (35 °C, 36 hours) to obtain the solid GO product, which was used as flakes. Based on a method reported by Cong et al. (Cong et al., 2012), GO was further modified by adding $FeSO_4.7H_2O$ to a stable suspension of well-exfoliated GO. After adjusting the pH to 3.5 using ammonia, the suspension was hydrothermally reduced at 90 °C for 6 hrs without stirring until a black 3D hydrogel monolith (FeG) was formed. The hydrogel was then separated, washed, freeze dried and crushed into the powdered FeG product.

Text S2. Sample preparation for characterisation of adsorbents.

SEM-EDX samples were prepared by applying the dried adsorbents directly onto aluminium stubs covered with adhesive carbon tape. Images were obtained using a spot size of 3, and an accelerating voltage of 10 kV. For TEM, adsorbents were ultra-sonicated in ethanol (20 min), after which the suspensions were drop-casted onto a Lacey copper grid and dried for a few hours before imaging at an accelerating voltage of 100 kV.

FTIR and XRD analyses were performed using powdered adsorbent samples. FTIR spectra were recorded at wavelengths ranging from 400 - 4000 cm^{-1}. XRD spectra were recorded using Fe-filtered Co Kα radiation, automatic divergence slit, 2° anti-scatter slit and fast X'Celerator Si strip detector. The diffraction patterns were recorded from 3 - 80° in steps of 0.017° 2 theta with a 0.5 second counting time per step for an overall counting time of approximately 35 minutes.

Specific surface area (SSA) of adsorbents were measured using the Methylene Blue (MB) dye absorption method commonly used for carbonaceous materials. 15 mg of each adsorbent was added to 150 mL of 20 mg/L MB solutions and shaken for 60 hrs at 100 rpm to allow the solutions to attain equilibrium and maximum absorption. After centrifugation, supernatants were analysed using UV-visible spectrophotometry (at 664 nm) and compared to controls to determine the amount of MB absorbed.

The SSA was then calculated using the following equation:

$$SSA = \frac{N_A . A_{MB} . (C_i - C_e) . V}{M_{MB} . m_s}$$

where, N_A represents Avogadro number (6.023×10^{23} molecules/mole), A_{MB} is the area covered per MB molecule (1.35 nm^2), C_i and C_e are the initial and equilibrium MB concentrations, respectively, V is the volume of MB solution, M_{MB} is the molecular mass of MB, and m_s is the mass of the adsorbent.

Surface charge and PZC of adsorbents were determined by using 0.1 % w/v suspensions in Milli Q water, that were adjusted to pHs ranging from around 2 – 10. The suspensions were placed on a shaker for 48 hours to equilibriate pH before measuring zeta potential across the pH gradient using dynamic light scattering (Malvern Zetasizer NanoZS).

Table S1. Full names and abbreviations for the suite of PFAS measured in the field water sample.

PFAS name	Abbreviation and CAS No.
Perfluoroalkyl carboxylates (increasing order of chain length)	
Perfluoro-n-butyrate	PFBuA (375-22-4)
Perfluoro-n-pentanoate	PFPeA (2706-90-3)
Perfluoro-n-hexanoate	PFHxA (307-24-4)
Perfluoro-n-heptanoate	PFHpA (375-85-9)
Perfluoro-n-octanoate	PFOA (335-67-1)
Perfluoro-n-nonanoate	PFNA (375-95-1)
Perfluoro-n-decanoate	PFDA (335-76-2)
Perfluoroalkyl sulphonates (increasing order of chain length)	
Perfluoro-n-butanesulfonate	PFBS (375-73-5)
Perfluoro-n-hexanesulfonate	PFHxS (432-50-7)
Perfluoro-n-octanesulfonate	PFOS (1763-23-1)
Fluorotelomers and perfluoroalkylsulphonamides	
1H,1H,2H,2H-perfluoro-n-octane sulfonate	6:2 FTS (27619-97-2)
1H,1H,2H,2H-perfluoro-n-decane sulfonate	8:2 FTS (39108-34-4)
Perfluorooctanesulfonamide	PFOSA (754-91-6)

Table S2. Elemental composition of adsorbents graphene oxide (GO), iron-modified graphene (FeG) and RemBind™ (RemB), as determined by energy dispersive X-ray (EDX) detector coupled to a scanning electron microscope. See Figure S1 for EDX spectra.

Adsorbent	Element (series)	Weight %	Atomic %
GO	C (K)	65.88	72.01
	O (K)	34.12	27.99
FeG	C (K)	37.19	56.39
	O (K)	28.48	32.42
	Fe (K)	34.34	11.20
RemB	C (K)	22.42	34.37
	O (K)	27.70	31.89
	Si (K)	38.63	26.36
	Al (K)	11.26	7.38

Figure S1. Energy dispersive X-ray (EDX) spectra collected for adsorbents graphene oxide (GO), iron-modified graphene (FeG) and RemBind™ (RemB) to elucidate elemental composition. All adsorbents exhibited signals for carbon and oxygen. FeG displayed an additional signal for iron, and RemB displayed additional signals for aluminium and silicon.

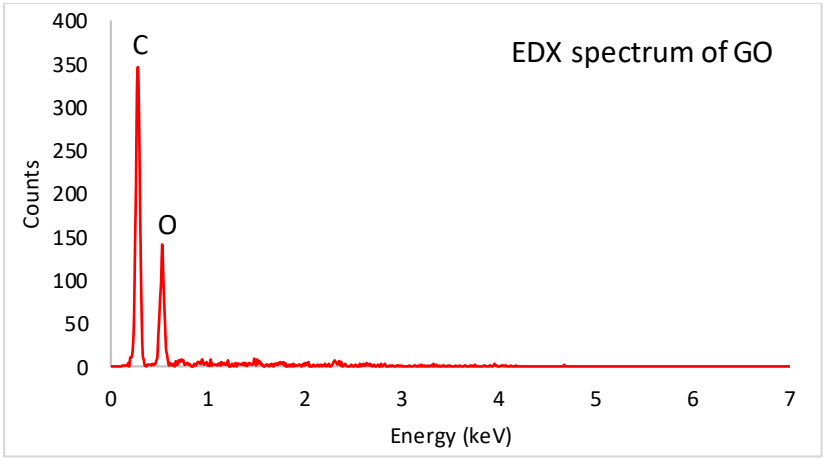

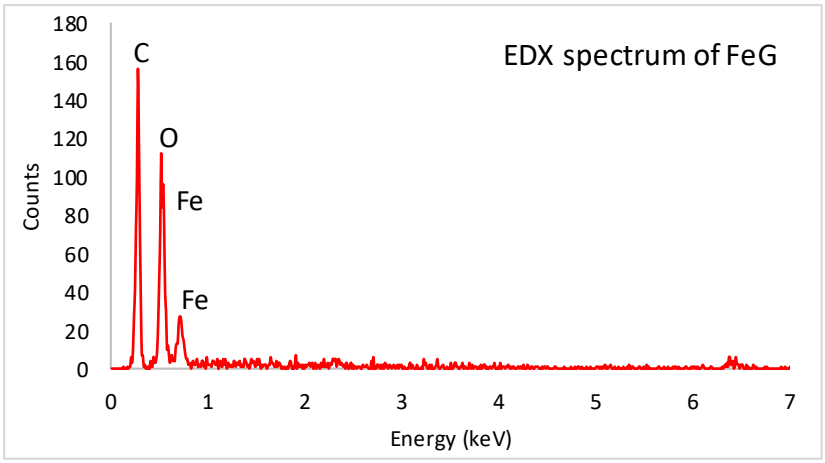

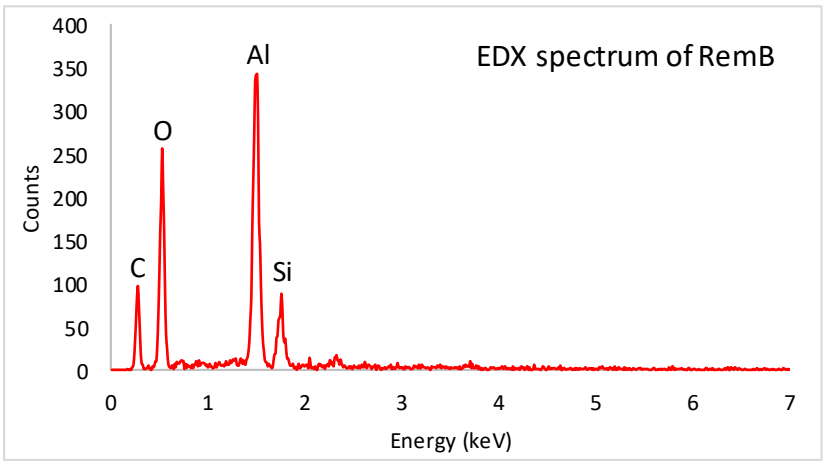

Figure S2. X-ray diffraction (XRD) spectra of adsorbents graphene oxide (GO), iron-modified graphene (FeG) and RemBind™ (RemB)

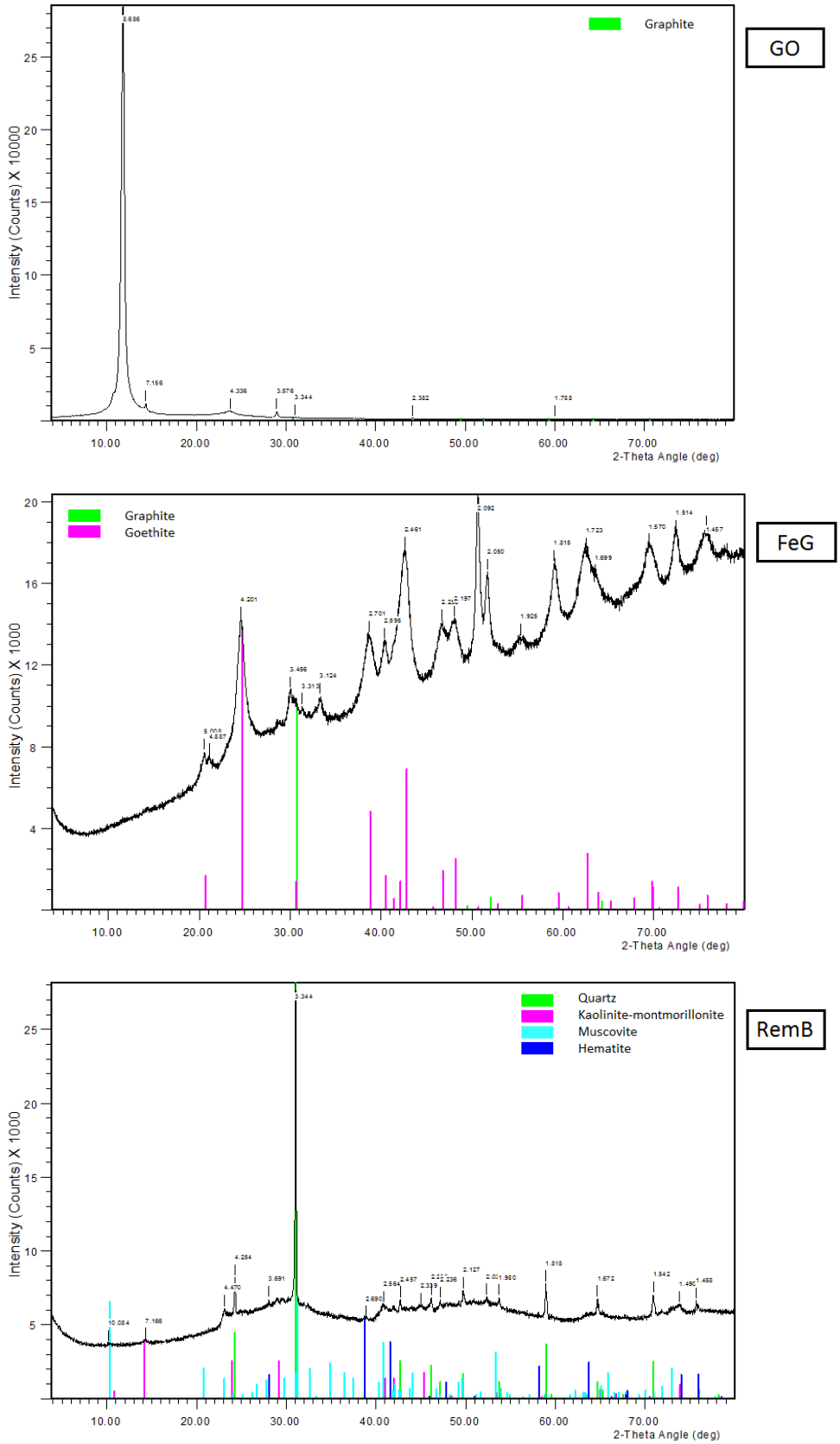

Figure S3. Fourier-transform infrared (FTIR) spectra of adsorbents graphene oxide (GO), iron-modified graphene (FeG) and RemBind™ (RemB)

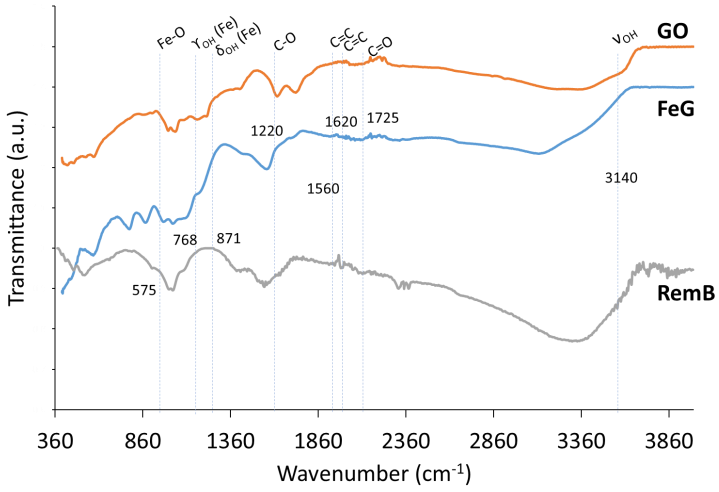

Figure S4. Methylene Blue standard calibration curve (664 nm) and sample analysis for measurement of surface areas of adsorbents graphene oxide (GO), iron-modified graphene (FeG) and RemBind™ (RemB).

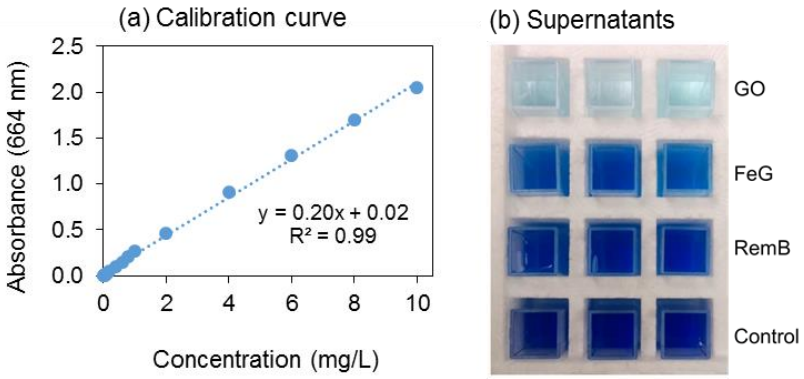

REFERENCES

Cong H-P, Ren X-C, Wang P, Yu S-H (2012). Macroscopic multifunctional graphene-based hydrogels and aerogels by a metal ion induced self-assembly process. *ACS Nano,* **6,** 2693-2703.

Marcano DC, Kosynkin DV, Berlin JM, Sinitskii A, Sun Z, Slesarev A, Alemany LB, Lu W, Tour JM (2010). Improved synthesis of graphene oxide. *ACS Nano,* **4,** 4806-4814.

CHAPTER 5. Sorption of PFOA onto Different Laboratory Materials: Filter Membranes and Centrifuge Tubes

A condensed version of the work contained in this chapter is being prepared for submission to *Environmental Research Letters* for publication.

Statement of Authorship

Title of Paper	Sorption losses of PFOA onto different materials: filter membranes and centrifuge tubes
Publication Status	☐ Published; ☐ Accepted for publication; ☐ Submitted for publication; ☐ Unpublished and unsubmitted work prepared in manuscript style for publication
Publication Details	

Principal Author

Name (Candidate)	Supriya Lath		
Contribution to the Paper	Experimental development; set-up and performed experiments; data analysis and critical interpretation; manuscript writing.		
Overall percentage (%)	75%		
Certification:	This paper reports on original research I conducted during the period of my PhD candidature and is not subject to any obligations or contractual agreements with a third party that would constrain its inclusion in this thesis. I am the primary author of this paper.		
Signature		Date	3 Sept 2018

Co-Author Contributions

By signing the Statement of Authorship, each author certifies that: the candidate's stated contribution to the publication is accurate (as detailed above); permission is granted for the candidate in include the publication in the thesis; and the sum of all co-author contributions is equal to 100% less the candidate's stated contribution.

Emma R. Knight	Assisted in experimental development; conducting experiments; data analysis; manuscript writing.		
Signature		Date	29 Aug 2018

Divina A. Navarro	Assisted with project development; data interpretation; manuscript evaluation.		
Signature		Date	28 Aug 2018

Rai Kookana	Assisted in project planning; data interpretation; manuscript evaluation.		
Signature		Date	29 Aug 2018

Michael J. McLaughlin	Supervised project development; data interpretation; manuscript evaluation.		
Signature		Date	3rd Sept 2018

Sorption of PFOA onto different laboratory materials: filter membranes and centrifuge tubes

Supriya Lath [1], Emma R. Knight [1, 2], Michael J. McLaughlin [1], Divina Navarro [1, 2], Rai Kookana [2]

[a] School of Agriculture, Food and Wine, Faculty of Sciences, The University of Adelaide, Waite Campus, Adelaide, South Australia, 5064, Australia.

[b] CSIRO Land and Water, Waite Campus, Adelaide, South Australia, 5064, Australia.

Abstract

The measuring and reporting of concentrations of contaminants of emerging concern such as per- and polyfluoroalkyl substances (PFASs), including perfluorooctanoic acid (PFOA), is an integral part of most investigations. Sorption losses of PFAS analytes onto particular laboratory-ware (e.g. glass containers) have been suggested in the published literature but they have not been investigated in detail. We examined sorption losses from aqueous PFOA solutions in contact with different commonly-used materials in disposable filter units and centrifuge tubes (glass and plastics). Sorption of PFOA onto different filter membrane types ranged from 21 to 79 % indicating that filtration can introduce a major source of error in PFOA analysis in laboratory and environmental samples. The pre-rinsing of filter membranes with phosphate or methanol solutions did not significantly affect the recovery of PFOA. Substantial adsorption of PFOA was also observed on tubes made from polypropylene (PP), polystyrene (PS), polycarbonate (PC), and glass where losses observed were between 32 to 45%, 27 to 35%, 16 to 31% and 14 to 24%, respectively. Contrary to the suggestions in the literature, our results indicated the greatest sorption losses for PFOA were observed on PP whereas the sorption losses on glass tubes were much lower. Variations in ionic strength and pH did not greatly influence the recovery of PFOA. When PFOA concentrations were increased the percent recovery of PFOA increased, irrespective of tube type, indicating that binding sites on tube-walls were saturable. This study draws attention towards potential analytical bias that can occur due to sorption losses during routine procedures, and highlights the importance of testing the suitability of chosen laboratory ware for specific PFAS analytes of interest prior to experimental use.

Keywords: PFOA, PFAS, filters, centrifuge tubes, polystyrene, polycarbonate, polypropylene, glass

1. Introduction

Perfluorooctanoic acid (PFOA) and other related per- and polyfluoroalkyl substances (PFASs) have been recognised as contaminants of emerging concern due to their ubiquitous and persistent nature in the environment, as well as their bioaccumulative properties. As a result, these chemicals are being studied extensively with respect to their human and ecological toxicity (Hekster et al., 2003, Sundström et al., 2011), their occurrence, fate and transport in different environmental compartments (Ahrens et al., 2015, Hansen et al., 2002) as well as management and remediation strategies (Ochoa-Herrera and Sierra-Alvarez, 2008, Ross et al., 2018). At various stages of such laboratory and field studies, the PFAS analytes being researched come in contact with a variety of apparatus that are usually made from glass, steel or plastics. The most common apparatus in any study are sampling and storage containers, including a range of tubes, vials and bottles. Others examples include disposable polystyrene (PS) well-plates used as exposure-vessels for toxicity assays, glass aquariums for fish toxicity tests, as well as disposable filtration membranes used for the separation of aqueous phases from solid or particulate matrices prior to analysis.

Regardless of the types of experiments conducted, one aspect that is commonly cited in the methods' section of several published studies relates to the use of sample containers made of particular materials. Specifically, several studies exclude the use of equipment made from glass in experimental or analytical protocols involving PFASs (Ahrens et al., 2015, Hansen et al., 2002). The justification regularly provided for this is that glass adsorbs PFAS analytes. The USEPA and ISO methods, which are the most widely accepted test methods for PFAS analytes, also stipulate that PFAS standards, extracts and samples should not come in contact with any glass containers or pipettes (ISO, 2009, Shoemaker et al., 2009). They recommend that polypropylene (PP) containers be used for all sample, standard and extraction preparation and storage, and suggest that other plastics may be used if they meet quality control requirements (Shoemaker et al., 2009). As a result, PP has been adopted as the material of choice in several studies (Ahrens et al., 2010, Ahrens et al., 2011, Hellsing et al., 2016, Higgins et al., 2007). However, a number of studies have used materials other than PP for PFAS-related studies. For example, Higgins and Luthy (2006) chose PS tubes over PP or glass because their preliminary, unpublished data provided higher recoveries when using PS tubes for a range of PFASs. Other studies have used polyethylene (PE), polycarbonate (PC) and high-density PE containers (Johnson et al., 2007, Washington et al., 2010), often without any indication as to the suitability of these materials.

One consensus in the published literature is the avoidance of equipment containing fluoropolymer materials like polytetrafluoroethylene (PTFE) in PFAS studies, as their manufacture has historically involved the use of some PFASs as a 'polymerisation aid' (Prevedouros et al., 2006). Leaching of remnant PFASs from such products can cause contamination of the dissolved phase (Martin et al., 2004). However, in the case of glass and plastics, there is considerable contradiction and inconsistency in the published literature regarding which materials may be best suited. Losses to laboratory ware could lead to considerable bias in analytical data. Despite the severe implications of such routine losses due to adsorption onto glass and plastics, it has not been investigated in its own right.

Apart from choice of containers, filtration is another routine consideration in sample handling and preparation. Filtration is often employed as a major clean-up stage for most environmental and laboratory samples, during which additional losses can occur (Ahmad et al., 2001, Carlson and Thompson, 2000). A study investigating active air-sampling of gaseous PFOA using glass fibre (GF) filters observed that gas-phase PFOA was underestimated due to its sorption onto the GF filters (Johansson et al., 2017). However, an investigation using a variety of PFASs from the aqueous phase, testing four different filter membranes, determined GF filters to be suitable for several PFASs, but recommended specific testing to account for unpredictable effects (Chandramouli et al., 2015).

The aim of this study was to examine the sorption losses of PFOA on common glass and plastic materials – specifically, centrifuge tubes and disposable syringe filter membranes – during routine laboratory procedures. Sorption of PFOA from aqueous solutions onto a variety of filter-membranes was tested; the influence of varying concentrations, and two pre-rinsing treatments were investigated. Additionally, sorption onto a variety of glass and plastic (PP, PC, PS) tubes was tested. The influence of contact time, pH, ionic strength and PFOA-concentrations were examined to gain insights into the nature of PFOA-binding interactions.

2. Materials and Methods

2.1. Materials

Radiolabelled ^{14}C-PFOA with a specific activity of 2.04 GBq/mmol was purchased from American Radiolabelled Chemicals Incorporation. Optiphase HiSafe 3 scintillation fluid for radiochemical analysis was purchased from PerkinElmer, Australia. All other chemicals used including calcium chloride dihydrate ($CaCl_2.2H_20$), dipotassium hydrogen phosphate (K_2HPO_4), methanol, hydrochloric acid (HCl) and sodium hydroxide (NaOH) were of analytical grade. The specifications of filter-types and tube-types used in this study are listed in Table 1 and Table 2 respectively.

Table 1. Specifications of different filter-types tested for sorption of PFOA.

No.	Filter code	Membrane type	Housing material	Pore size (µm)	Diameter (mm)	Source (product number)
1	PP	Polypropylene	Polypropylene	0.45	30	MicroAnalytix (30AP045AN)
2	GF	Glass fibre	Polyvinyl chloride	20	25	Millipore (SLAP02550)
3	PVDF	Polyvinylidene fluoride	Polypropylene	0.45	33	Millipore Millex (SLHV033NK)
4	PES	Polyethersulphone	Polypropylene	0.45	35	MicroAnalytix (MS SF35PS045)
6	PES+GF*	PES with GF pre-filter	Polypropylene	GF 1, PES 0.45	35	MicroAnalytix (MS SF35GPS045)
7	PTFE	Polytetrafluoroethylene (hydrophobic)	Polypropylene	0.45	25	Sartorius (17576-K)
8	RC	Regenerated cellulose	Polypropylene	0.45	25	Sartorius (17765-K)
9	CA	Cellulose acetate	Acrylic resin methacrylate butadiene styrene (MBS)	0.45	28	Sartorius (16555-K)
11	CA+GF*	CA with GF pre-filter	Acrylic resin MBS	GF 0.7µm^2, CA 0.45	28	Sartorius (17829-K)
12	NY	Nylon	Polypropylene	0.45	25	ProSciTech (WS1-04525N)

* These filter units have two filter membranes in one housing unit, where the GF pre-filter membrane preceded the PES or CA membranes.

Table 2. Specifications of different tubes tested for sorption of PFOA.

No.	Tube code	Material	Capacity (mL)	Source (product number)
1	PP1	Polypropylene	10	LabServ (LBSCT1202)
2	PP2	Polypropylene	10	LabServ (LBSSP1201)
3	PS	Polystyrene	10	Rowe Scientific (S10316UU)
5	PC	Polycarbonate	10	ThermoFisher (NAL 3118-0010)
6	G1	Glass	10	Kimble Kimax (45066A-16100)
7	G2	Glass	10	BD Vacutainer (366430)
8	PS2	Polystyrene	11	ThermoFisher (LBSCT1002)

2.2. Filter sorption studies

The sorptive losses through retention of dissolved PFOA onto different filter membrane-types was investigated in triplicate using syringe-filtration through disposable filter units. By means of single-use 10 mL PP syringes, 4 mL of a 14 µg/L PFOA solution was drawn into the syringes, following which filter units were attached to the end of the syringe before plunging the solution through the filter membrane. The initial 2 mL volume of the filtrate was discarded and the subsequent 2 mL was collected, of which 0.5 mL aliquots were used for quantitative analysis. Losses of PFOA through adsorption onto the filters were calculated using the difference between the amounts of PFOA in the unfiltered and the filtered solutions; results are reported as a percentage recovery of PFOA compared to the unfiltered controls. To determine if recovery of PFOA from the filters could be improved, two pre-rinsing treatments, using phosphate solution (100 mM K_2HPO_4) and methanol, were applied to the filters. For the phosphate pre-rinse treatment, 10 mL of a 100 mM K_2HPO_4 solution was plunged through the filter units, followed by 10 mL of Milli-Q water, prior to PFOA filtration. Similarly, for the methanol treatment, 10 mL of methanol was plunged through the

filters; membrane-types that were incompatible with methanol were excluded. Finally, the influence of increasing concentrations of PFOA on sorptive losses on three filter membranes (PP, RC and GF) was also tested using an environmentally relevant range of concentrations (0 to 415 µg/L). The critical micelle concentration (CMC) of PFOA has been reported to be in the range of 1 to 1.6 x 10^7 µg/L (i.e., 25 to 38 mM), at which PFOA molecules can agglomerate to form micelles and hemi-micelles; such phase separation can affect interfacial activity like sorption (Harada et al., 2005, Rattanaoudom et al., 2012). The concentrations used in our studies were around 10^4 to 10^6 times lower than the CMC, so the impact of micelle-formation on sorption losses is expected to be negligible.

2.3. Tube sorption studies

To measure sorption of PFOA onto different centrifuge tube-types (PP, PS, PC, G1 and G2, Table 2), tests were performed in triplicate under different conditions by varying the contact times, solution pH, ionic strength as well as PFOA concentrations. When not being varied, the standard test parameters included the use of 8 mL volumes of PFOA solutions of concentrations of 20.5 ± 1 µg/L, prepared in a 10 mM $CaCl_2$ background electrolyte solution or Milli-Q water, and a contact time of 24 to 48 hrs. To investigate the influence of contact time, tubes were subjected to shaking times of 1, 2 and 7 days. The influence of pH was examined across a pH range from 4 to 9 where 0.1M HCl or 0.1M NaOH was used to adjust solution pH. Background electrolyte solutions of varying concentrations (0 to 100 mM $CaCl_2$) were used to determine the effect of ionic strength on retention of PFOA. Sorptive losses as a function of concentration were also examined by testing initial PFOA concentrations ranging from 0 to 420 µg/L. All tubes with test PFOA solutions were placed on an end-over-end shaker for the duration of the test, after which subsamples (0.5 mL) were taken for quantitative analysis. Instrumental analysis

Aliquots (0.5 mL) of all samples, blanks (Milli-Q water) and stock solutions were combined with 4 mL of scintillation fluid in a scintillation vial and analysed radio-chemically using a β-liquid scintillation counter (Perkin Elmer Tri-Carb 3110 RT). The activity of ^{14}C in the samples was measured as disintegrations per minute, thrice for 2 min each. Concentrations of PFOA were then calculated using the specific activity and the measured ^{14}C activity.

2.4. Data and statistical analysis

Statistical software, IBM SPSS (v. 24), was used to determine if there were significant differences ($p < 0.05$) between treatments. After using analysis of variance test (ANOVA), a Tukey's honestly significant difference test was used to compare treatment means.

3. Results and Discussion

3.1. Filter sorption studies

3.1.1. Sorption losses observed on different filter membrane-types

Irrespective of the type of membrane tested, recovery of PFOA was < 100% in all cases (Figure 1). This implies that at least a certain proportion of PFOA was retained onto the filter membrane or housing material due to adsorption, leading to underestimation of dissolved PFOA concentrations. As it was not possible to make a distinction between the amount of PFOA retained on the membrane and the housing material separately, sorption was considered for the filter unit as a whole. Specifically, recovery ranged from 76% at best to 21.2% at worst, depending on the type of membrane used (Figure 1). The highest recoveries were achieved when using PVDF (76%), glass-fibre (74.2%), RC (74%) and PP (72.3%) membranes. The lowest recovery due to adsorption was displayed by the NY membrane filter (21.2%). Overall, the percentage recoveries after filtration were in the order PVDF ≈ GF ≈ RC > PP > PES > CA > PES > PTFE > NY.

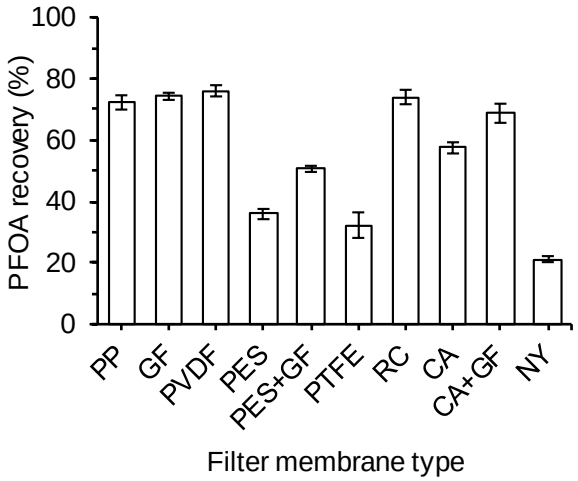

Figure 1. The percentage recovery of ^{14}C-PFOA filtrate solution (13.6 µg/L) from different syringe filter membranes. Error bars represent the standard deviation (n = 4).

While PVDF showed a high recovery, it is a fluoropolymer, and like PTFE, may cause contamination of analytical blanks, or over-estimation of dissolved PFAS concentrations (Martin et al., 2004), so it should generally be avoided in PFAS-based analysis. We did not test for PFAS contamination issues during filtration as a radiolabelled PFOA solution was

used. Interestingly, despite both PVDF and PTFE being fluoropolymers, PFOA-sorption on PTFE was more than 2 times greater than on PVDF; this may be attributed to the differences in their chemical properties. The carbon-backbone of the polymeric structure in PVDF (chemical formula $[–CH_2–CF_2–]_n$) is partially fluorinated, whereas that in PTFE (chemical formula $[–CF_2–CF_2–]_n$) is fully fluorinated, making PTFE more hydrophobic than PVDF. It is likely that the PFOA tail, being hydrophobic, is able to undergo greater hydrophobic interactions with PTFE, leading to greater PFOA sorption.

When testing a range of filter media with PFAS-spiked water, Chandramouli et al. (2015) reported that the poorest recoveries were observed with PTFE (2 to 24%), followed by NY (62 to 80%) filters, while GF filters displayed the best recovery (> 85%) overall. For a range of perfluorinated carboxylate and sulphonate compounds, Labadie and Chevreuil (2011) also reported better recoveries using GF (70 to 98%), as opposed to NY (40 to 98%); however, specifically in the case of PFOA, GF and NY were reported to perform equally. Like in the case of GF membrane, the recoveries obtained from RC as well as PP membranes in our study were greater compared to other filters, however accounts of the use of these membranes in the published literature are rare. Chain-length of the PFASs were an important factor controlling sorption losses reported in these studies (Chandramouli et al., 2015, Labadie and Chevreuil, 2011), where greater sorption occurred as chain-length increased. This has been reported in studies related to sorption in environmental media such as soil and sediments, as well as adsorbents such as activated carbon (Du et al., 2014).

While the literature focussing on PFAS-investigations in water, soil and sediments commonly use GF filters (Ahrens et al., 2015, Kwadijk et al., 2010, Lein et al., 2008), the literature dealing with air-sampling of PFAS is exploring ways to reduce the sorption of PFAS onto GF-filters (Arp and Goss, 2008, Johansson et al., 2017). This contrast may be attributed to the differences in sampling and filtration equipment set-up for different environmental media. Moreover, it appears that membrane-types, apart from GF and quartz-fibre filters, have not been tested for PFAS sorption.

While GF filters have been reported to show the best recoveries for aqueous phases (Chandramouli et al., 2015, Labadie and Chevreuil, 2011), it is important to note that glass fibres used in membranes usually have variable structural integrity. As a result, they are often ascribed with a particle retention rating, covering a range of sizes, and in our case it was 0.8 to 8 µm rather than a specific pore-size. The GF membranes used in this study were stated to be of 20 µm pore size, but the manufacturer cannot guarantee an actual pore size. An interesting observation was that the inclusion of a GF membrane as a pre-filter in the

case of PES and CA membranes, caused recovery to improve by up to 18% and 11%, respectively, when compared to the PES and CA membranes where no pre-filter was included. Usually, pre-filters are effective at improving recovery in samples with high particulate load. The solutions used in this study were devoid of any particulate matter, thus it is unclear why an improvement was observed.

On pre-rinsing the membranes with either a phosphate solution (100 mM), or methanol (99% purity), no significant improvements in PFOA-recovery were observed (Figure S1 and Figure S2; supplementary material). In the case of the methanol pre-rinse, in fact, a decrease in recovery of 7 to 28%, was observed for some membranes (RC, PP and PES; Figure S2). The exact mechanisms controlling the binding of PFOA to the different filter membranes are not known. In the study on active air-sampling of PFOA using GF filters, pre-treatment with a siliconizing reagent led to an appreciable reduction in sorption of gaseous PFOA onto the GF filters (Johansson et al., 2017), particularly when atmospheric concentrations of PFOA were high. While no specific mechanism was identified, it was attributed to deactivation of surface active sites on the GF filter. Given that no benefits in terms of reduction in sorption losses were observed in our study, combined with the added inconvenience, time and expense associated with the process, pre-treatment of disposable filter-units is not recommended for improving recovery from solution. However, pre-rinsing remains a suitable strategy to reduce contamination of the dissolved phase from certain filters (e.g. PTFE) (Labadie and Chevreuil, 2011).

3.1.2. Effect of PFOA concentration on PFOA recovery

To test the influence of increasing PFOA concentrations on recovery, three of the filters exhibiting the lowest sorptive losses – PP, RC and GF – were used; PVDF was excluded on account of being a fluoropolymer. In terms of percentage of PFOA recovered (Figure 2), there was no evidence for consistent effect of PFOA concentration on recovery. A similar outcome was reported for PFOA by Chandramouli et al. (2015) when tested on NY filters; PFOA concentrations used ranged from 0.02 to 1 µg/L, which were 2 to 3 orders of magnitude lower than the concentrations tested in our study. We used higher concentrations with the expectation that sorption might be saturable, but this was not observed.

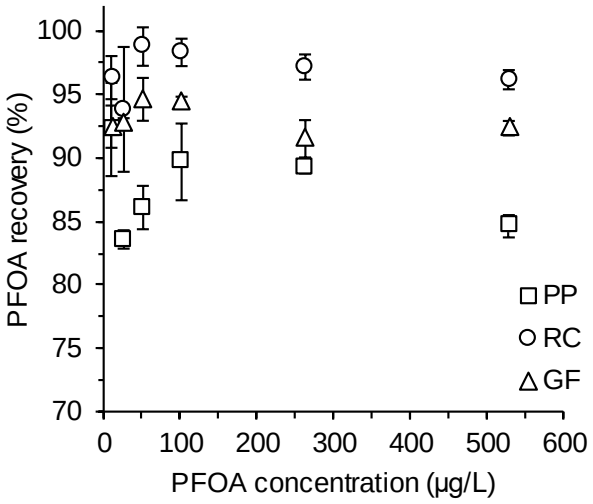

Figure 2. Percentage recovery of dissolved PFOA after filtering through three different filters types (PP, RC, GF) when using a range of ^{14}C-PFOA concentrations (12 – 415 µg/L). Error bars represent standard deviation (n = 3).

As all filter-membranes displayed some losses of PFOA through adsorption, we recommend that it is better to avoid filtration, wherever possible. Other studies have also advised against the use of filtration in sample-preparation steps for the same reasons (Schultz et al., 2006, Voogt and Sáez, 2006). For instance, Schultz et al. (2006) elected centrifugation as their only viable sample clean-up step when analysing PFAS-contaminated municipal wastewater samples due to such losses. If, however, filtration is considered necessary in any procedures, we advise that specific testing of analyte-sorption onto filter media is undertaken to account for potential underestimation of dissolved PFAS concentrations due to such losses.

3.2. Tube sorption studies

3.2.1. Effect of contact time on recovery of PFOA

Recovery of PFOA decreased in the order G1 ≈ G2 > PC > PS > PP (Figure 3). Greater sorption losses occurred in plastic tubes, compared to glass tubes. Specifically, PFOA-recovery observed from glass (G1 and G2) tubes ranged from 77 to 86%, whereas that in PP tubes ranged from 55 to 68%, which is contrary to what is widely implicit in the published literature. Amongst the plastics tested, the recoveries from PC (69 to 78%) and PS tubes (65 to 73%) were greater than from PP tubes. No significant changes were observed over time (1, 2 and 7 days) in the case of G1, G2 and PC tubes (Figure 3).

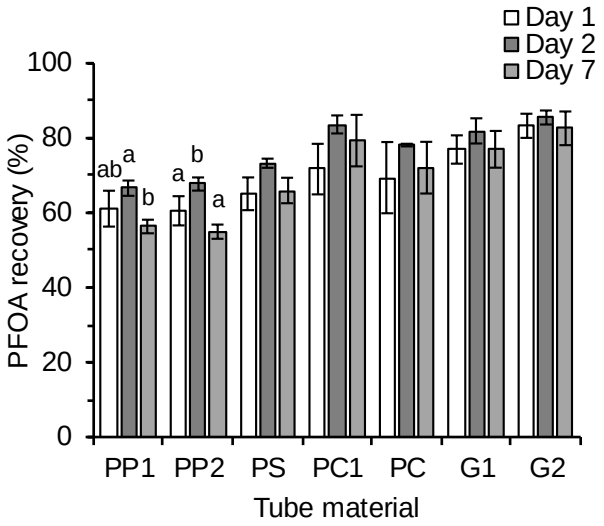

Figure 3. The average concentration of ^{14}C-PFOA remaining in solution after 1, 2 and 7 days when in contact with different centrifuge-tube materials. Error bars represent the standard deviation (n = 3). Concentration of ^{14}C-PFOA used was 21.3 µg/L. Different letters denote significant differences between days on individual centrifuge tube types.

In the case of PP and PS tubes, however, some small time effects were observed. Losses at day 7 were similar to losses observed at day 1. In the case of PP1, PP2 and PS tubes, in fact, losses at day 2 were greater (by 8 to 13%) than those at days 1 and 7 (Figure 3). Theoretically, at a fixed analyte concentration, recovery was expected to decrease with time and reach equilibrium at a stage where no more PFOA was being sorbed onto the tube walls. As this trend was not observed in our data, it is possible that PFOA sorption onto the glass and plastic surfaces occurred in a much shorter time frame (within hours) than was investigated in this study. Further studies would be required to corroborate this.

3.2.2. Effect of solution chemistry on recovery of PFOA

The influence of solution chemistry on sorption of PFOA in different tubes was determined by measuring PFOA-recovery under varying pH (Figure 4a) and ionic strength (Figure 4b) conditions. Both tests corroborated our previous observations that greater sorption losses occurred in the plastic tubes, compared to the glass tubes (G1 ≈ G2 > PC > PS > PP). Specifically, PFOA-recovery observed from glass (G1 and G2) tubes ranged from 93 to 103%, whereas that in PP tubes ranged from 74 to 81%. Recoveries from PC and PS tubes were 85 to 89% and 81 to 86%, respectively.

On increasing the pH from 4 to 8, the PFOA-recovery from the glass tubes (G1 and G2) remained largely unaffected. In the PC, PS and PP, a slight increase in recovery, by 4.1%, 4.7% and 6.5%, respectively, was apparent. Glass tubes, G1 and G2 displayed the least fluctuations and PP the most. Despite some of these pH effects being statistically significant ($p < 0.05$), on the whole, the sorption losses due to variations in pH (i.e., 1.4 to 6.5%) were minor when compared to the underlying losses due to the inherent nature of the different materials being tested (i.e., 5 to 25%).

By using PFOA solutions prepared in background $CaCl_2$ electrolyte solutions of varying concentrations, effects of ionic strength on PFOA recovery were examined. No significant effects of increasing $CaCl_2$ concentrations were observed on recovery of PFOA in PP, PS and PC tubes ($p > 0.05$). Recovery of PFOA from G1 tubes decreased by 5.3% and 6.2%, respectively, in the presence of 25 mM and 100 mM $CaCl_2$ treatments ($p = 0.043$ and 0.015), but no effects were observed for other treatments. In the case of G2 tubes, recovery decreased by 3.5 to 6.4% ($p < 0.025$) for all treatments except for in the presence of 50 mM $CaCl_2$ ($p = 0.132$).

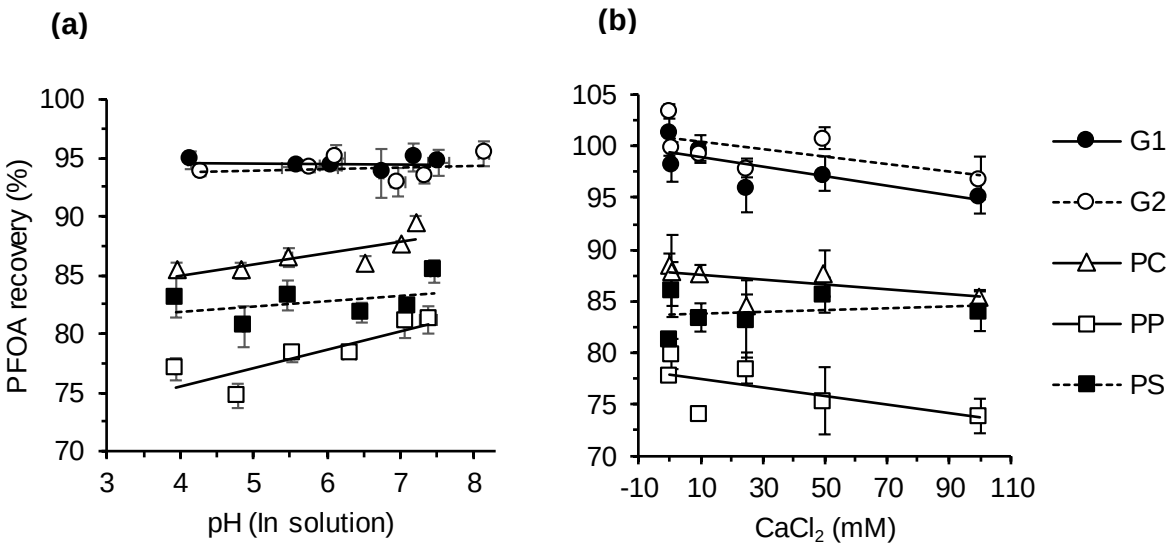

Figure 4. Effect of solution chemistry, pH (a) and ionic strength (b), on the average percentage recovery of PFOA when in contact with different centrifuge tubes. Test conditions ranged from pH 3 to pH 9 and ionic strength ranged from 0 to 100 mM $CaCl_2$. Concentration of ^{14}C-PFOA used was 20.8 and 19.1 µg/L for pH and ionic strength respectively. Error bars represent the standard deviation (n = 3).

Ionic strength usually affects the electrostatic nature of a surface as well the solubility of the compound, thus controlling interactions occurring at that surface. Glass is known to have a negative zeta potential above pH 2.6 (Gu and Li, 2000), whereas a variety of plastics (including PP) have been reported to carry a negative zeta potential above pH 3.5 to 4 (Lameiras et al., 2008, Leininger et al., 1964). In the experimental conditions used in this study (pH 5.6 ± 0.2), all tubes may be expected to carry a slight negative charge. Divalent cations like Ca^{2+} have been found to act as a bridge between the negatively charged functional head groups of PFASs and the negatively charged surfaces of a variety of adsorbents (Higgins and Luthy, 2006). It is thus possible that as ionic strength increased, the Ca^{2+}-induced bridging effect caused more PFOA to be retained on the negative surfaces of the glass tubes, thereby slightly decreasing recovery. However, as in the case of solution pH, these variations were relatively minor compared to the considerably greater underlying losses resulting due to the physiochemical nature of the materials themselves.

3.2.3. Effect of PFOA concentration on recovery of PFOA

On increasing the concentrations of PFOA in the test solutions, the percentage of PFOA recovered from the solutions within each tube-type increased (Figure 5). For instance, as the spiked concentration of PFOA increased from 12 to 415 µg/L, the recovery of PFOA from PP, PC and G1 tubes improved from 53.7% to 85.5%, 66.7 to 95.1% and 75.3 to 106.3%, respectively. Essentially, the higher the concentration of PFOA in the test solutions, the lower the proportional loss of PFOA onto the container walls, irrespective of the tube-type. This suggests that all plastic and glass tubes tested herein contained a limited number of binding sites on their surface, and can only interact with a finite amount of PFOA. Therefore, as the concentration of PFOA increases, the binding sites on the container walls become increasingly saturated. Similar concentration-dependent results for sorption losses have been reported in the case of other organic chemicals such as pesticides (Sharom and Solomon, 1981) and polycyclic aromatic hydrocarbons (Chlebowski et al., 2016), as well as inorganic substances such as silver nanoparticles (Malysheva et al., 2016).

Poor recovery, particularly at low concentrations, can present serious implications. One current topic of interest in PFAS-research is the determination of the toxicity profiles of these chemicals. When conducting ecotoxicological testing, if significant sorption losses occur, the test organisms will be exposed to reduced concentrations of the analytes, resulting in inaccurate toxicity thresholds (Sekine et al., 2015). Similarly, when testing drinking water quality, and comparing to guideline values to determine safety, erroneous risk assessments may be made due to such losses. The lowest PFOA concentration tested in this study (12

µg/L) was around 170 times greater than the current USEPA drinking water health advisory limit for PFOA (0.07 µg/L) (USEPA, 2016).

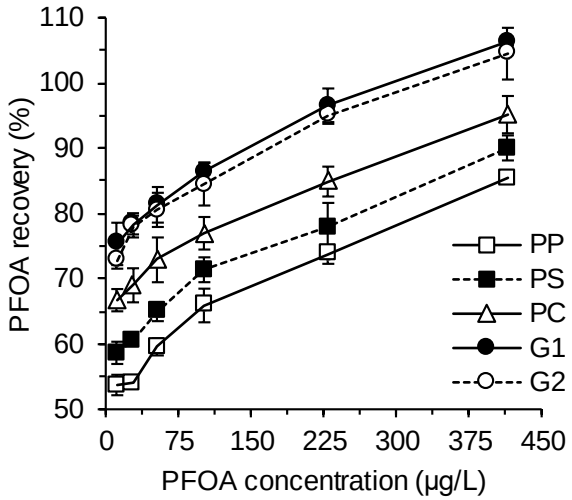

Figure 5. The average (n = 3) percentage recovery of ^{14}C-PFOA in different centrifuge-tube types when in contact with increasing concentrations of ^{14}C-PFOA (0 to 415 µg/L) in solution.

4. Conclusions and Implications

To our knowledge, this is the first study to systematically quantify and report on sorptive losses of dissolved PFOA observed on tubes made from different materials (PP, PC, PS and glass), despite the serious implications of this issue. References to such losses have been made in the published literature, but remain largely unsubstantiated. Moreover, contrary to what is implicit in standard protocols (e.g. USEPA and ISO methods) and the published literature, our data emphasise that greater sorption losses of PFOA occurred on PP containers than on glass containers. Irrespective of solution chemistry (pH and ionic strength) or concentration of PFOA tested, sorption of PFOA onto the tube-walls increased in the order glass < PC < PS < PP. Proportional losses decreased when PFOA concentrations of test solutions increased. Due to this concentration-effect, losses can be especially exaggerated when dealing with PFAS solutions of low concentrations, for instance, when reporting on the quality of drinking water samples.

Our results also confirm that filtration of aqueous PFOA solutions can introduce a major source of error, leading to an underestimation of dissolved concentrations. Our

recommendation is therefore to avoid filtration of PFAS solutions where possible. However, if use of filtration is inevitable, the sorptive losses associated with the chosen filter-membranes must be measured for each specific analyte.

Although it is not possible to extrapolate from the current dataset for PFOA to apply to other types of PFASs, it is reasonable to suggest that the specific trends may differ depending on the type of PFAS. This could be due to differences in their chain lengths and functional properties, as well as the matrix (e.g. environmental, biological) being tested. Consequently, our study highlights the need to account for losses associated with common laboratory ware for each analyte separately. It is conceivable that losses associated with stronger-sorbing PFASs (e.g. PFOS) may be higher than those observed here and *vice versa*. Clearly, the choice of suitable tubes and filter materials for use in PFAS-work should be considered carefully as part of sampling and experimental protocols.

5. Acknowledgements

Financial support from Australian Research Council Discovery Grant DP150101760 is gratefully acknowledged. The authors would like to thank Ziltek Pty. Ltd. for their financial support and provision of RemBind™. The authors also thank Gavin Stevenson from National Measurement Institute (NMI, Australia) for technical insights on the analytical procedures used by NMI, including laboratory ware and filters.

6. References

Ahmad R, Kookana SR, Alston MA (2001). Syringe filtration as a source of error in pesticide residue analysis in environmental samples. *Bulletin of Environmental Contamination and Toxicology,* **66,** 313-318.

Ahrens L, Norström K, Viktor T, Cousins AP, Josefsson S (2015). Stockholm Arlanda Airport as a source of per- and polyfluoroalkyl substances to water, sediment and fish. *Chemosphere,* **129,** 33-38.

Ahrens L, Taniyasu S, Yeung LWY, Yamashita N, Lam PKS, Ebinghaus R (2010). Distribution of polyfluoroalkyl compounds in water, suspended particulate matter and sediment from Tokyo Bay, Japan. *Chemosphere,* **79,** 266-272.

Ahrens L, Yeung LWY, Taniyasu S, Lam PKS, Yamashita N (2011). Partitioning of perfluorooctanoate (PFOA), perfluorooctane sulfonate (PFOS) and perfluorooctane sulfonamide (PFOSA) between water and sediment. *Chemosphere,* **85,** 731-737.

Arp HPH, Goss K-U (2008). Irreversible sorption of trace concentrations of perfluorocarboxylic acids to fiber filters used for air sampling. *Atmospheric Environment,* **42,** 6869-6872.

Carlson M, Thompson RD (2000). Analyte loss due to membrane filter adsorption as determined by high-performance liquid chromatography. *Journal of Chromatographic Science,* **38,** 77-83.

Chandramouli B, Benskin JP, Hamilton MC, Cosgrove JR (2015). Sorption of per- and polyfluoroalkyl substances (PFASs) on filter media: implications for phase partitioning studies. *Environmental Toxicology and Chemistry,* **34,** 30-6.

Chlebowski AC, Tanguay RL, Simonich SLM (2016). Quantitation and prediction of sorptive losses during toxicity testing of polycyclic aromatic hydrocarbon (PAH) and nitrated PAH (NPAH) using polystyrene 96-well plates. *Neurotoxicology and Teratology,* **57,** 30-38.

Du Z, Deng S, Bei Y, Huang Q, Wang B, Huang J, Yu G (2014). Adsorption behavior and mechanism of perfluorinated compounds on various adsorbents—A review. *Journal of Hazardous Materials,* **274,** 443-454.

Gu Y, Li D (2000). The ζ-potential of glass surface in contact with aqueous solutions. *Journal of Colloid and Interface Science,* **226,** 328-339.

Hansen KJ, Johnson HO, Eldridge JS, Butenhoff JL, Dick LA (2002). Quantitative characterization of trace levels of PFOS and PFOA in the Tennessee River. *Environmental Science & Technology,* **36,** 1681-1685.

Harada K, Xu F, Ono K, Iijima T, Koizumi A (2005). Effects of PFOS and PFOA on L-type Ca^{2+} currents in guinea-pig ventricular myocytes. *Biochemical and Biophysical Research Communications,* **329,** 487-94.

Hekster F, Laane RPM, de Voogt P 2003. Environmental and toxicity effects of perfluoroalkylated substances. *Reviews of Environmental Contamination and Toxicology.* Springer New York.

Hellsing MS, Josefsson S, Hughes AV, Ahrens L (2016). Sorption of perfluoroalkyl substances to two types of minerals. *Chemosphere,* **159,** 385-391.

Higgins CP, Luthy RG (2006). Sorption of perfluorinated surfactants on sediments. *Environmental Science & Technology,* **40,** 7251-7256.

Higgins CP, McLeod PB, MacManus-Spencer LA, Luthy RG (2007). Bioaccumulation of perfluorochemicals in sediments by the aquatic oligochaete Lumbriculus variegatus. *Environmental Science & Technology,* **41,** 4600-4606.

ISO (2009). Water quality - Determination of perfluorooctanesulfonate (PFOS) and perfluorooctanoate (PFOA) - Method for unfiltered samples using solid phase extraction and liquid chromatography/mass spectroscopy. Geneva, Switzerland.

Johansson JH, Berger U, Cousins IT (2017). Can the use of deactivated glass fibre filters eliminate sorption artefacts associated with active air sampling of perfluorooctanoic acid? *Environmental Pollution,* **224,** 779-786.

Johnson RL, Anschutz AJ, Smolen JM, Simcik MF, Penn RL (2007). The adsorption of perfluorooctane sulfonate onto sand, clay, and iron oxide surfaces. *Journal of Chemical & Engineering Data,* **52,** 1165-1170.

Kwadijk CJAF, Korytár P, Koelmans AA (2010). Distribution of perfluorinated compounds in aquatic systems in the Netherlands. *Environmental Science & Technology,* **44,** 3746-3751.

Labadie P, Chevreuil M (2011). Biogeochemical dynamics of perfluorinated alkyl acids and sulfonates in the River Seine (Paris, France) under contrasting hydrological conditions. *Environmental Pollution,* **159,** 3634-3639.

Lameiras FS, Souza ALd, Melo VARd, Nunes EHM, Braga ID (2008). Measurement of the zeta potential of planar surfaces with a rotating disk. *Materials Research,* **11,** 217-219.

Lein NPH, Fujii S, Tanaka S, Nozoe M, Tanaka H (2008). Contamination of perfluorooctane sulfonate (PFOS) and perfluorooctanoate (PFOA) in surface water of the Yodo River basin (Japan). *Desalination,* **226,** 338-347.

Leininger RI, Mirkovitch V, Beck RE, Andrus PG, Kolff WJ (1964). The zeta potentials of some selected solids in respect to plasma and plasma fractions. *ASAIO Journal,* **10,** 237-243.

Malysheva A, Ivask A, Hager C, Brunetti G, Marzouk ER, Lombi E, Voelcker NH (2016). Sorption of silver nanoparticles to laboratory plastic during (eco)toxicological testing. *Nanotoxicology,* **10,** 385-390.

Martin JW, Kannan K, Berger U, Voogt PD, Field J, Franklin J, Giesy JP, Harner T, Muir DCG, Scott B, Kaiser M, Järnberg U, Jones KC, Mabury SA, Schroeder H, Simcik M, Sottani C, Bavel BV, Kärrman A, Lindström G, Leeuwen SV (2004). Analytical challenges hamper perfluoroalkyl research. *Environmental Science & Technology,* **38,** 248A-255A.

Ochoa-Herrera V, Sierra-Alvarez R (2008). Removal of perfluorinated surfactants by sorption onto granular activated carbon, zeolite and sludge. *Chemosphere,* **72,** 1588-1593.

Prevedouros K, Cousins IT, Buck RC, Korzeniowski SH (2006). Sources, fate and transport of perfluorocarboxylates. *Environmental Science & Technology,* **40,** 32-44.

Rattanaoudom R, Visvanathan C, Boontanon SK (2012). Removal of concentrated PFOS and PFOA in synthetic industrial wastewater by powder activated carbon and hydrotalcite. *Journal of Water Sustainability,* **2,** 245-258.

Ross I, McDonough J, Miles J, Storch P, Thelakkat Kochunarayanan P, Kalve E, Hurst J, S. Dasgupta S, Burdick J (2018). A review of emerging technologies for remediation of PFASs. *Remediation Journal,* **28,** 101-126.

Schultz MM, Barofsky DF, Field JA (2006). Quantitative determination of fluorinated alkyl substances by large-volume-injection liquid chromatography tandem mass spectrometry - Characterization of municipal wastewaters. *Environmental Science & Technology,* **40,** 289-295.

Sekine R, Khurana K, Vasilev K, Lombi E, Donner E (2015). Quantifying the adsorption of ionic silver and functionalized nanoparticles during ecotoxicity testing: Test container effects and recommendations. *Nanotoxicology,* **9,** 1005-1012.

Sharom MS, Solomon KR (1981). Adsorption and desorption of permethrin and other pesticides on glass and plastic materials used in bioassay procedures. *Canadian Journal of Fisheries and Aquatic Sciences,* **38,** 199-204.

Shoemaker JA, Grimmett PE, Boutin BK (2009). Determination of selected perfluorinated alkyl acids in drinking water by solid-phase extraction and liquid chromatography/tandem mass spectrometry (LC/MS/MS). *Tandem Mass Spectrometry (LC/MS/MS), in, US Environmental Protection Agency, Washington, DC*.

Sundström M, Ehresman DJ, Bignert A, Butenhoff JL, Olsen GW, Chang S-C, Bergman A (2011). A temporal trend study (1972–2008) of perfluorooctanesulfonate, perfluorohexanesulfonate, and perfluorooctanoate in pooled human milk samples from Stockholm, Sweden. *Environment International,* **37,** 178-183.

USEPA (2016). Drinking water health advisory for perfluorooctanoic acid (PFOA). EPA Document Number: 822-R-16-005. Washington, D C.

Voogt Pd, Sáez M (2006). Analytical chemistry of perfluoroalkylated substances. *TrAC Trends in Analytical Chemistry,* **25,** 326-342.

Washington JW, Yoo H, Ellington JJ, Jenkins TM, Libelo EL (2010). Concentrations, distribution, and persistence of perfluoroalkylates in sludge-applied soils near Decatur, Alabama, USA. *Environmental Science & Technology,* **44,** 8390-8396.

7. Supporting Information

Sorption of PFOA onto different laboratory materials: filter membranes and centrifuge tubes

Supriya Lath [1], Emma R. Knight [1, 2], Michael J. McLaughlin [1], Divina Navarro [1, 2], Rai Kookana [2]

[1] School of Agriculture, Food and Wine, Faculty of Sciences, The University of Adelaide, Waite Campus, Adelaide, South Australia, 5064, Australia.

[2] CSIRO Land and Water, Waite Campus, Adelaide, South Australia, 5064, Australia.

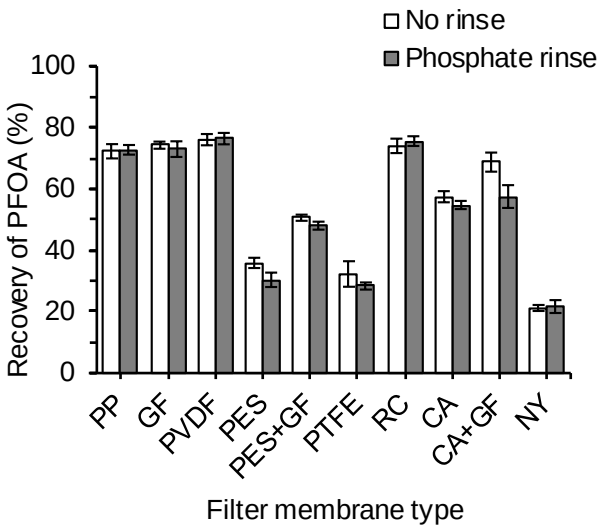

Figure S1. The percentage recovery of PFOA from different syringe filter membranes where the filters were pre-rinsed using a phosphate solution prior to filtering ^{14}C-PFOA solution (13.6 ng/mL). Asterisks denote significant differences between control (no-rinse) and pre-rinsed filters for individual filter types. Error bars represent the standard deviation (n = 4).

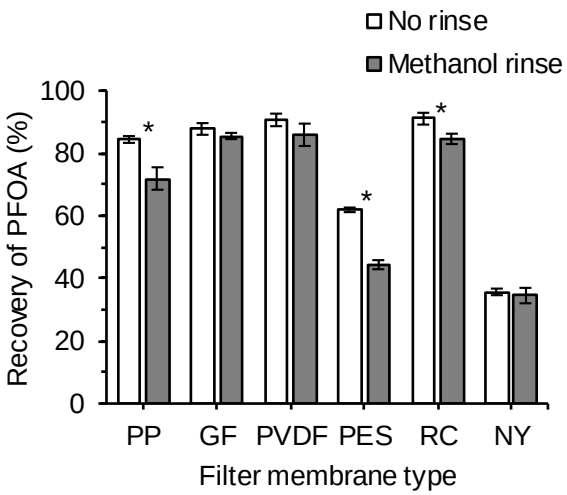

Figure S2. The percentage recovery of PFOA from different syringe filter membranes where the filters were pre-rinsed using a methanol solution prior to filtering ^{14}C-PFOA solution (15.7 ng/mL). Asterisks denote significant differences between control (no-rinse) and pre-rinsed filters for individual filter types. Error bars represent the standard deviation (n = 3).

CHAPTER 6. Mixed-Mode Mineral, Carbon and Graphene-Based Materials for Simultaneous Remediation of Arsenic, Cadmium, PFOA and PFOS in Soils

The work contained in this chapter has been prepared for submission to *Environmental Chemistry* for publication.

Statement of Authorship

Title of Paper	Mixed-mode mineral, carbon and graphene-based materials for simultaneous remediation of arsenic, cadmium, PFOA and PFOS in soils
Publication Status	☐ Published; ☐ Accepted for publication; ☐ Submitted for publication; ☐ Unpublished and unsubmitted work prepared in manuscript style for publication
Publication Details	

Principal Author

Name (Candidate)	Supriya Lath		
Contribution to the Paper	Experimental development; set-up and performed experiments; data analysis and critical interpretation; wrote the manuscript; acted as corresponding author.		
Overall percentage (%)	85%		
Certification:	This paper reports on original research I conducted during the period of my PhD candidature and is not subject to any obligations or contractual agreements with a third party that would constrain its inclusion in this thesis. I am the primary author of this paper.		
Signature		Date	3 Sept 2018

Co-Author Contributions

By signing the Statement of Authorship, each author certifies that: the candidate's stated contribution to the publication is accurate (as detailed above); permission is granted for the candidate in include the publication in the thesis; and the sum of all co-author contributions is equal to 100% less the candidate's stated contribution.

Divina A. Navarro	Assisted with project development; experimental design; data interpretation; manuscript evaluation.		
Signature		Date	28 Aug 2018

Dusan Losic	Assisted in project planning; advised on graphene-materials; manuscript evaluation.		
Signature		Date	30/08/2018

Michael J. McLaughlin	Supervised project development; experimental design; data interpretation; manuscript evaluation.		
Signature		Date	3rd Sept 2018

Mixed-mode mineral, carbon and graphene-based materials for simultaneous remediation of arsenic, cadmium, PFOA and PFOS in soils

Supriya Lath [*, 1], Divina A. Navarro [1, 2], Dusan Losic [3], Michael J. McLaughlin [1, 2]

[1] School of Agriculture Food and Wine, The University of Adelaide, PMB 1 Glen Osmond, SA 5064, Australia.

[2] CSIRO Land and Water, PMB 2 Glen Osmond, SA 5064, Australia.

[3] School of Chemical Engineering, The University of Adelaide, Adelaide, SA 5005, Australia.

* Corresponding author email: supriya.lath@adelaide.edu.au

Abstract

In situ remediation of soils contaminated with different contaminant-types is a challenge. For the first time, we report on simultaneous *in situ* remediation of arsenate (As), cadmium (Cd), perfluorooctanoic acid (PFOA) and perfluorooctane sulfonate (PFOS), using two graphene-based materials (GBMs) – graphene oxide (GO), and an iron-oxide-modified reduced-GO composite (FeG) – and a mineral and carbon-based adsorbent, RemBind™ (RemB). In particular, FeG and RemB greatly reduced bioaccessibility of As, PFOA and PFOS (but not Cd) by 89 – 100%, compared to GO (36 – 86%), from both singly-contaminated and co-contaminated soils. The mixed-mineral and carbonaceous nature of FeG and RemB offered multiple binding pathways – i.e. hydrophobic interactions at the graphitic plane (for PFOA and PFOS), and ligand-exchange with the goethite and alumina phase (for As, PFOA and PFOS) for FeG and RemB, respectively. Despite the widely-demonstrated success of GO for Cd-removal from water, GO did not bind Cd in the soils. In fact, GO increased Cd-bioaccessibility by 2 fold compared to the unremediated control due to lowered pH (3.5) and concurrent release of calcium ions (Ca^{2+}), which competed with Cd^{2+} for GO's binding sites. Addition of GBMs severely impaired microbial-driven soil nitrification processes (55 – 99% inhibition) due to soil acidification. As healthy soils need physiochemical and biological processes to operate in unison, the inherent acidity of GBMs presents challenges when considered for *in situ* soil application. While GBMs (particularly FeG) show great promise for reducing bioaccessibility of contaminant-mixtures, their potential to be used for effective *in situ* soil remediation requires that the acidity generated by the materials is neutralised.

Keywords: Adsorption; contaminant mixtures; graphene; nitrification; bioaccessibility; remediation.

1. Introduction

Rapid urbanisation and industrialisation has caused a plethora of contaminants to enter our environment (soil, sediments, groundwater and surface water), which can have long-term adverse effects on ecological and human health. Maintaining and restoring the quality of the environment has thus become one of the greatest challenges of our time. Most contaminated sites contain a mix of contaminants (i.e. metals, metalloids and polar or non-polar organic chemicals). Technologies that can target multiple contaminants simultaneously are favourable for remediation.

Adsorption or *in situ* immobilisation onto solid surfaces is a commonly adopted remediation strategy, which relies on binding contaminants to minimise their solubility and bioavailability, hence alleviating toxicity and risk. Adsorbents like zeolites, clay (Abollino et al., 2003) as well as aluminium (Al)/iron (Fe)/manganese (Mn)-based minerals (O'Day and Vlassopoulos, 2010) have been employed for immobilisation of inorganic contaminants. Carbon (C)-based materials such as biochar and activated-C have commonly been used to bind organic contaminants like pesticides, drugs and dyes (Rakowska et al., 2012). It is thus possible that combined mineral and C-phases in adsorbents may prove advantageous in simultaneous remediation of multiple contaminant types (inorganic and organic).

Recently, novel C-based materials like C-nanotubes and graphene have been tested extensively for adsorptive remediation of contaminants in water and wastewater (Bei et al., 2014, Tofighy and Mohammadi, 2011, Upadhyay et al., 2014). Graphene, the latest addition to the nanocarbon family, is composed of closely packed sp^2 hybridised C-atoms (Novoselov et al., 2012). The high surface area and versatile surface chemistry of graphene-based materials (GBMs) make them excellent candidates for development as adsorbents. Pristine graphene has been used for adsorption of organic contaminants such as polycyclic aromatic hydrocarbons (PAHs, e.g. naphthalene), antibiotics (e.g. tetracycline) and dyes (e.g. methylene blue) (Ersan et al., 2017); these interactions were attributed to either hydrogen bonding, or π–π electron donor–acceptor interactions at the graphitic basal plane. The surface of GBMs can be functionalised to allow for interactions with different types of contaminants. Graphene oxide (GO) is a negatively-charged GBM with several oxygen (O) functional groups, i.e. epoxy, hydroxyl, and carboxyl (Dreyer et al., 2010). Consequently, it has been used to bind divalent heavy metal cations such as cadmium (Cd), copper (Cu), lead (Pb) and zinc (Zn) through complexation and electrostatic interactions (Sitko et al., 2013). Several graphene/metal oxide composites, mainly iron (Fe) or manganese (Mn)-based, have also been developed as adsorbents. For instance, magnetite-graphene/GO composites have been successful in adsorbing a variety of PAHs, dyes, and metals *via*

previously mentioned mechanisms, as well as metalloids like arsenate (As^{V}) and chromate (Cr^{VI}) *via* ligand-exchange and inner-sphere complexation mechanisms (Upadhyay et al., 2014).

While GBMs have been investigated extensively for water and wastewater treatment, their *in situ* application in soil remediation is underexplored, with only a handful of accounts in the published literature. In one study, two PAHs, phenanthrene (hydrophobic) and 1-naphthol (polar) were adsorbed using colloidal GO, *via* hydrophobic interactions and hydrogen-bonding, respectively, though significant mobility of the GO-bound PAHs was observed in saturated soil conditions (Qi et al., 2014). In a study with Cd-spiked soil, GO was reported to reduce Cd-bioavailability, however changes in soil microbial parameters were reported (Xiong et al., 2018) – e.g. dehydrogenase enzyme activity was enhanced, but urease activity was inhibited. Moreover, the relative abundance of some sensitive functional bacteria which are related to nitrogen (N)-cycling (*Nitrospira*) and C-cycling (*Actinobateria*) processes decreased, whereas other dominant phyla increased (Xiong et al., 2018). Such changes in soil function can have a bearing on overall soil health, which is a consideration during *in situ* remediation. In natural As-enriched soils, As is usually linked to Fe-(hydr)oxides within the soil, through adsorption or co-precipitation to form Fe^{III}/As^{V} minerals (e.g. scorodite) (Paktunc and Bruggeman, 2010). In an investigation using such a soil, in flooding (anaerobic) conditions, the addition of reduced GO enhanced the microbial reduction of Fe^{III}/As^{V} precipitates, mobilising Fe^{II} and As^{III} from the soil (Chen et al., 2018), leading to an increase in bioavailable-As. Overall, the outcomes with respect to the application of GBMs in soil are varied, and studies are scarce.

When assessing efficacy of *in situ* remediation, reduced 'bioavailability' and 'bioaccessibility' are essential indicators. Bioavailability refers to the amount of contaminant absorbed by a receptor, while bioaccessibility refers to the 'soluble' or 'extractable' fraction of the total contaminant mass in soils that is mobile and available for potential interaction with receptor organisms (Adriano et al., 2004, Semple et al. 2007). The presence or absence of contaminants can also affect soil microbial communities, which are known to play a vital role in maintaining soil health and function (Ramakrishnan et al., 2011). For example, nitrification (conversion of ammonium to nitrite, and then into a plant-available form, nitrate), which is a key process in N-cycling in soil, is controlled by a limited number of specialist soil microorganisms – *Archaea*, *Nitrosomonas* (ammonia-oxidising bacteria), *Nitrobacter* and *Nitrospira* (nitrite-oxidising bacteria) (Leininger et al., 2006, Robertson and Groffman, 2015). As these processes are extremely sensitive to soil contamination, monitoring of nitrification can also be used to evaluate efficacy of remediation processes.

The graphene-based adsorbents chosen for remediation in this study were GO, and an Fe-oxide-modified reduced-GO composite (FeG). The latter is a composite mineral and graphene-based adsorbent that could potentially bind multiple contaminants. Similarly, a non-graphene adsorbent, RemBind™ (RemB), which is a powdered mixture of activated-C, amorphous alumina and kaolin clay, was also tested from the same perspective. The model contaminants chosen were As, Cd, and two perfluorinated alkyl substances of current interest, perfluorooctanoic acid (PFOA) and perfluorooctane sulphonate (PFOS). Arsenic and Cd, released into the environment *via* the application of fertilisers and sewage sludge, and mining operations, are notorious for posing human health risks through intake of contaminated food and water (Hughes, 2002, Lim et al., 2013). On the other hand, PFOA and PFOS are anthropogenic contaminants, belonging to the broader class of chemicals known as per- and polyfluoroalkyl substances (PFASs). They have recently been the focus of regulatory attention due to their persistence, mobility, bioaccumulative properties and potential toxicity (USEPA, 2016). These contaminants were selected based on their environmental significance, and to cover a range of contaminant types (i.e., organic, inorganic, cationic, anionic). Each of these contaminants is either not amenable or is resistant to destructive remediation technologies, making adsorption a preferred management strategy for them.

Specifically, this work investigated the remediation efficacy of GO, FeG and RemB in soils singly-contaminated, as well as co-contaminated with As, Cd, PFOA, and PFOS, using an integrated approach: (1) using a chemical measure, the extractable/bioaccessible concentrations of As, Cd, PFOA and PFOS from contaminated soils before and after treatment with GO, FeG and RemB were determined, and (2) using a biological measure, the microbially-mediated soil nitrification function in treated soils was compared with unremediated contaminated soil. To our knowledge, this is the first study investigating the use of graphene-based adsorbents for simultaneous *in situ* remediation of multiple contaminant-types (anionic *vs* cationic; organic *vs* inorganic) in soil.

2. Materials and Methods

2.1. Materials and chemicals

2.1.1. *Contaminants*

Contaminant solutions were prepared in water using cadmium sulphate, sodium arsenate, PFOA (96% purity) and PFOS (potassium salt, ≥98% purity) salts purchased from Sigma-Aldrich.

2.1.2. *Other chemicals and materials*

Calcium chloride, calcium hydroxide (lime) and other chemicals used in the

synthesis of GO and FeG (details in supporting information, SI), were of analytical grade. Graphite raw material used in the synthesis (described below) was obtained from the Uley graphite mines (South Australia). A commercial adsorbent RemBind™, supplied by Ziltek Pty. Ltd. (South Australia), was used as an additional (non-graphene) mixed mineral and C-based adsorbent.

2.2. Synthesis and characterisation of GO and FeG

The complete synthesis and characterisation of these adsorbents have been published previously (Lath et al., 2018a) (details provided in SI). Briefly, strong oxidative exfoliation of graphite based on an improved Hummer's method was used to synthesise GO, which was then hydrothermally reduced in the presence of ferrous sulphate to form an Fe-oxide-modified reduced-GO powder (FeG). The morphology of GO and FeG was examined by scanning and transmission electron microscopy (SEM and TEM); elemental composition was elucidated by an energy dispersive X-ray (EDX) detector coupled to the SEM. Fourier-transform infrared (FTIR) and X-ray diffraction (XRD) spectra were recorded for functional and structural characterisation. Surface charge properties (point of zero charge, PZC) were determined by measuring zeta potential across a pH gradient using dynamic light scattering. Surface area was determined by the methylene blue dye-adsorption method.

2.3. Soil

An uncontaminated sandy soil (pH 6.4, 96% sand) collected from a site in Karoonda (South Australia) was used for this study. Sandy soils usually possess low cation exchange capacity as well as low mineral and organic matter content, which create conditions for low contaminant sorption and increased bioaccessibility. Employing such a 'worse-case' scenario allows for the toxic effects of the contaminants to be more apparent for investigative purposes. The soil was air-dried and sieved (< 2 mm); selected physio-chemical characteristics of the soil are detailed in Table S1.

2.4. Soil spiking

Soils used for the remediation trial were to be spiked to achieve concentrations equivalent to the effective concentration of the contaminant that could cause 50% decrease in nitrification compared to the uncontaminated control soil (EC50). In that way, addition of adsorbents would be expected to bind the contaminants, alleviating contaminant-induced inhibition of nitrification, essentially restoring the levels of nitrification. To determine EC50, soils were spiked at concentrations ranging from 0.1 - 2500 mg/kg for As, 0.1 - 1000 mg/kg for Cd, 0.1 - 40 mg/kg for PFOA and 0.08 - 225 mg/kg for PFOS, using aqueous contaminant solutions. To improve solubility, PFOA and PFOS solutions were prepared in 5% methanol. The

spiking volume for each treatment was kept the same, and soils were thoroughly mixed to ensure homogenous distribution of the test contaminants. Soils amended with only Milli-Q water and 5% methanol served as uncontaminated controls. For the main remediation trial, in addition to singly-contaminated soils, a 'cocktail'-contaminant treatment was prepared, where a mixture of all 4 contaminants were spiked to co-occur at their EC50 concentrations.

2.5. Soil nitrification tests

2.5.1. *Experimental setup*

The effect of different contaminants on nitrification was investigated using OECD Method No. 216 for soil N-transformation (OECD, 2000). Contaminant-spiked soils (20 g) were first pre-incubated in 50 mL polypropylene tubes under constant temperature (25°C) at 60% maximum water holding capacity (MWHC), with daily aeration. After 5 days, powdered lucerne meal (C:N molar ratio of 13.6:1) was added as a source of N to the soils at a rate of 5 mg/g soil (dry weight). Moisture levels for each treatment were maintained during the 28-day nitrification incubation test period (60% MWHC). Subsamples (2 g) were collected from each treatment after 28 days, and extracted with 2M KCl (1:5 soil:solution ratio) by mixing in an end-over-end shaker (2 hrs). The samples were then centrifuged (3000g, 10 min) and supernatants were collected and analysed immediately for nitrate content.

2.5.2. *Nitrate analysis*

The amounts of soil nitrate-N in the extracts were measured *via* a colorimetric assay based on the reduction of nitrate by vanadium(III) combined with detection by the acidic Griess reaction (Miranda et al., 2001). Briefly, vanadium in dilute acid solution was used to reduce nitrate in the extracts to nitric acid, which, when mixed with Griess reagents (sulfanilamide and N-(1-naphthyl)-ethylenediamine), produces a pink-coloured dye. The absorbance was measured in 96-well plates at 540 nm using a spectrophotometer (Multiskan™ GO Microplate, Themo Scientific). The nitrate concentrations in the extracts were calculated from a calibration curve (Figure S1) of absorbance plotted against concentrations, prepared using a set of standard nitrate solutions of known concentrations.

2.5.3. *Determination of EC50 values for soil nitrification*

For each contaminant, dose-response curves were constructed by plotting contaminant concentrations against amount of nitrate produced. The EC50 was

calculated using a spreadsheet tool developed for the purpose (Barnes et al., 2003).

2.6. Soil remediation trial

2.6.1. *Experimental setup*

Uncontaminated control soils (described previously) as well as soils spiked with As, Cd, PFOA, PFOS and 'cocktail' contaminants (at EC50) for the remediation trial were equilibrated for 30 days. For remediation, 20 g (dry weight) subsamples were weighed out in separate 50 mL polypropylene tubes then moistened to 60% MWHC. A 5% weight dose of different adsorbents (GO, FeG, RemB and 1:1 mixture of GO+FeG treatment) were then added to these soils for remediation. Four replicates were prepared for each contaminant and adsorbent combination. Controls where no adsorbent was added were also included in the experiment. Since the GBMs have a low inherent pH (2.6 - 2.8 in aqueous suspension) that may decrease the pH of the soil, lime was applied to GBM-treated soils (i.e., soils with GO, FeG and GO+FeG) as a management step to raise the soil pH. Lime (calcium hydroxide) was added to the soils at the rate of 2.5 g/kg soil, as determined from preliminary tests (Figure S2) to ensure that pH of these soils was in the range of pH 6 - 6.5. The treated soils were incubated for a further 10 days with the adsorbents, before assessing remediation efficacy, as described below.

2.6.2. *Assessment of remediation efficacy*

All uncontaminated, contaminated, and adsorbent-treated samples were subjected to the N-transformation test as described in section 2.4. The amount of soil nitrate in the Day 28 KCl extracts were compared between contaminated and remediated soils. The 'bioaccessible' fraction of the contaminants were determined by $CaCl_2$ extraction (Houba et al., 2000). This procedure involved mixing 7 g subsamples of the soils on an end-over-end shaker with 35 mL of 10 mM $CaCl_2$ solution. After 12 hrs, the samples were centrifuged (3000 g, 30 min) to recover the supernatant. The concentrations of As and Cd in the supernatant were determined by inductively-coupled plasma optical emission spectrometry (ICP-OES). Concentrations of PFOA and PFOS were quantified by liquid chromatography tandem mass spectrometry (LC-MS/MS) (details in SI). A

separate subsample of soil was collected for pH and electrical conductivity (EC) measurements by preparing a 1:5 (soil:water) suspension.

3. Results and Discussion

3.1. Adsorbent properties

The properties of GO, FeG and RemB are summarised in Table 1. Detailed characterisation including SEM and TEM images, EDX spectra, FTIR spectra, XRD spectra as well as surface area and charge properties are provided in the SI (Figures S3 – S8, and Table S2). Briefly, oxidative exfoliation of graphite resulted in the formation of thin GO sheets (Figure S3) containing carboxyl and hydroxyl functional groups (Figure S5). Hydrothermal reduction of GO with Fe^{2+} led to the formation of an Fe-oxide-modified reduced-GO composite, FeG (Figure S3 – S5); the attached Fe was identified to be goethite (α-FeOOH) mineral particles (Figure S6). Elemental (EDX; Table S2 and Figure S4) and structural (XRD; Figure S6) composition highlight the carbonaceous nature of GO, contrasted with the mixed mineral and C-based nature of FeG and RemB as adsorbents. Surface area and charge (zeta potential) properties of a material are known to play an important role in adsorbent-adsorbate interactions. Surface areas of the adsorbents were in the order GO > FeG > RemB (Figure S7). Surface charge for FeG and RemB varied notably with pH (Figure S8). Conversely, GO maintained a highly negative charge across the pH range investigated.

Table 1. Characteristics of adsorbents - graphene oxide (GO), Fe-oxide-modified reduced GO composite (FeG) and RemBind™.

Adsorbent	Elements (EDX)	Surface area (m^2/g)	PZC (pH)	pH (aqueous)	XRD structure
GO	C, O	435	<1.5	2.6 – 2.8	Oriented 'platy' phase with a unit cell of 7.16 Å
FeG	C, O, Fe	242	7.1	2.8 – 3.0	Goethite mineral (α-FeOOH) crystalline phase

RemBind™	C, O, Al, Si	123	5.7	6.2 – 6.7	Dominant amorphous activated-C phase with aluminosilicate clays

Essentially, the GO prepared is a C-based adsorbent with prospects for binding organic contaminants (PFOA and PFOS) through non-specific hydrophobic interactions, as well as for binding cations (Cd^{2+}) electrostatically *via* the negatively charged oxygen-groups. In addition to the inherent C-phase in FeG and RemB, which lend them a capability to bind PFOA and PFOS (similar to GO), they contain added Fe- and Al-based mineral phases, respectively, offering further avenues for binding other contaminants (As-oxyanions).

3.2. Determination of EC50 of As, Cd, PFOA and PFOS towards nitrification

Dose-dependent contaminant effects were observed (Figure S9a – 9d), where soil nitrate levels decreased as contaminant concentrations increased. The EC50 values for effects of As, Cd, PFOA and PFOS on nitrification were 35 mg/kg, 29 mg/kg, 23 mg/kg and 74 mg/kg soil, respectively. These concentrations were used as spiking concentrations in the remediation trial.

3.3. Chemical assessment of remediation efficacy: $CaCl_2$-extractability

To chemically assess remediation efficacy of the adsorbents, first the dilute $CaCl_2$-extractable contaminant fraction (referred to herein as the potentially 'bioaccessible' fraction) of the treated soils was compared with the untreated contaminated soils (Figure 1). In the case of As, PFOA and PFOS-contaminated soils, all adsorbent treatments (i.e. GO, FeG, RemB, and GO+FeG) decreased the bioaccessible contaminant fraction by 36.3 – 98.9% (As), 43.8 – 98.3% (PFOA) and 85.5 – 99.9% (PFOS) (Table S3, and Figure 1). Greater decreases were observed in the soils treated with FeG and RemB, than those treated with GO. However, in Cd-contaminated soils, only the RemB-treatment displayed a reduction (63.3%) in bioaccessibility. All GBM-treated Cd soils displayed an increase in the concentrations of bioaccessible Cd by up to 2 fold. This increase was unexpected, particularly in the case of GO, which has been used successfully for Cd-sorption from water and wastewater (Bian et al., 2015, Sitko et al., 2013), including our own previous research (Lath et al., 2018a). The observed trends for each of the contaminants are further discussed in the following sections.

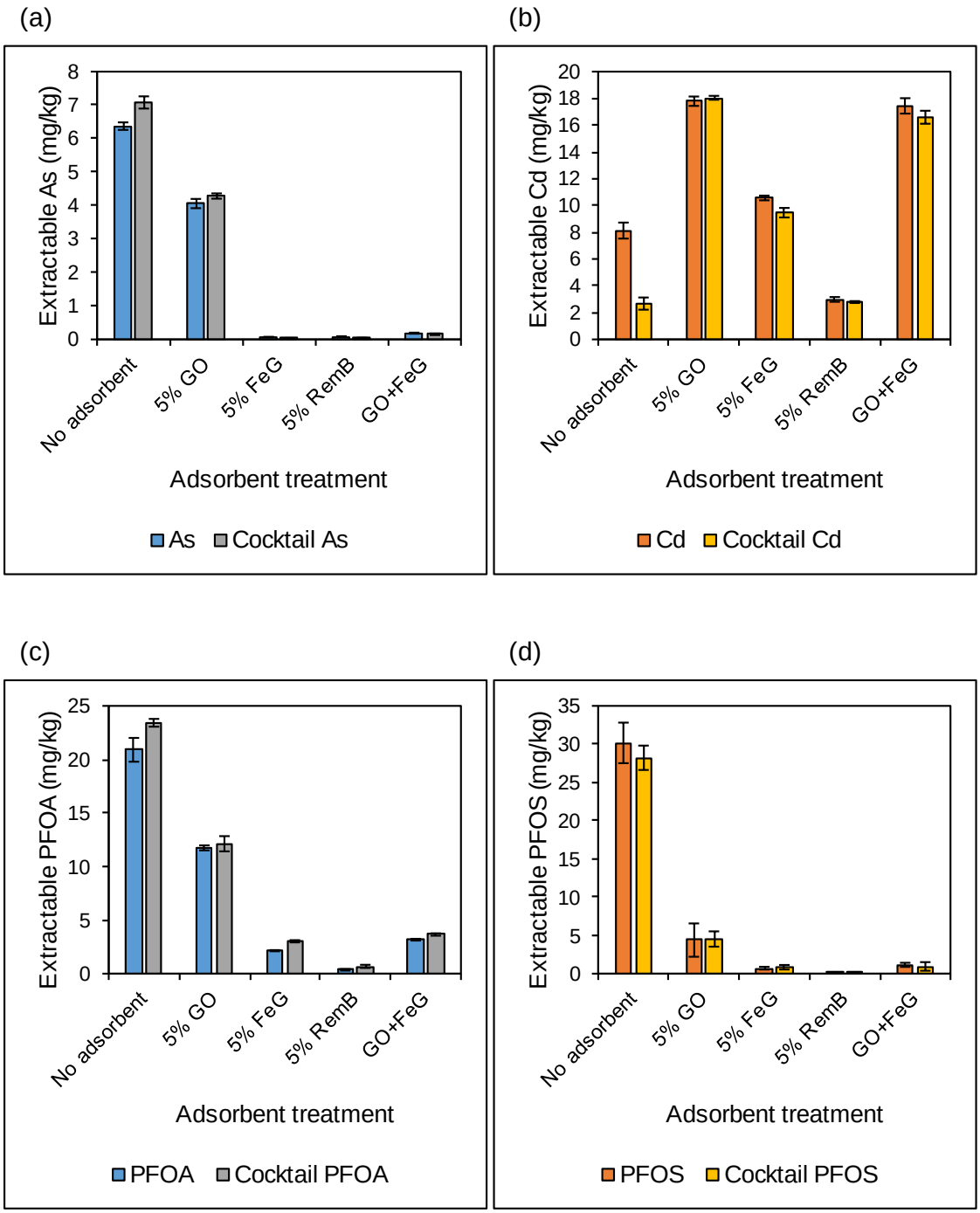

Figure 1. Bioaccessible contaminant-fractions measured in each contaminated soil treated with adsorbents. Contaminated soils include singly-contaminated soils (As, Cd, PFOA and PFOS), as well as a 'cocktail' treatment comprised of the 4 contaminants mixed together. Adsorbents include 5% weight doses of graphene oxide (GO), Fe-oxide-modified reduced GO composite (FeG), RemBind™ (RemB), and a 1:1 GO+FeG treatment. Error bars represent the standard deviation (n = 4).

The pH and EC of the treated and untreated soils measured at the end of the remediation trial are summarised in Figure 2. Despite the addition of lime to the GBM-treated soils as a management step (described in section 2.6 and Figure S2), the pH of these soils was still quite low. The pH decreased from around pH 6.5 at the beginning of the remediation trial (i.e., from the time adsorbents and lime were added) to pH 3.4 - 3.8 for GO, 3.9 - 4.3 for GO+FeG, and 4.7 - 4.9 for FeG-treated soils at the end (38 days later, i.e., 10-day pre-incubation with adsorbents and lime, followed by 28-day nitrification incubation). A similar downward drift of pH has been reported previously by Dimiev et al. (2013) during titration of a GO solution with NaOH, where pH decreased slowly over time, and continued for as long as a few days. This peculiar 'buffering'-like phenomenon was attributed to a gradual generation of protons at the GO/water interface, through reaction with water, due to C-C bond-cleavage (Dimiev et al., 2013). Soils are known to have a certain pH buffering capacity (i.e., capacity to resist pH change) depending on clay, organic matter and carbonate contents (Nelson and Su, 2010). Thus, due to the complexity of soil-matrices, it is possible that such continuous generation of acidification at the GO/moisture interface may occur over an even longer duration of time (weeks), compared to in solution (days). As GO is an intermediate product in the synthesis of FeG, the low pH in FeG-treated soils could also be attributed to similar processes. As a result, the initial pH adjustment with lime was insufficient to neutralise the acidity that was produced by the GBMs over the duration of the incubation.

Overall, soil pH followed the trend: GO < GO+FeG < FeG < No adsorbent < RemB. Correspondingly, treatments with lowered pH displayed higher EC (i.e., GO > GO+FeG > FeG > RemB > No adsorbent). The higher EC in GBM-treated soils is a result of greater concentrations of charged ions present in the extracts. At lower pH, aside from H^+ (from GBMs) and Cd^{2+}, major cations such as Na^+, K^+, Mg^{2+} and Ca^{2+} would be released from soil surfaces, and the concentration of soluble Ca^{2+} ions would have increased due to the dissolution of the added lime, resulting in a 5 – 6 fold increase in EC of extracts from GBM-treated soils, compared to untreated soils. On the other hand, the pH and conductivity of the RemB-treated soils were relatively unaffected, and similar to the soils where no adsorbents were added.

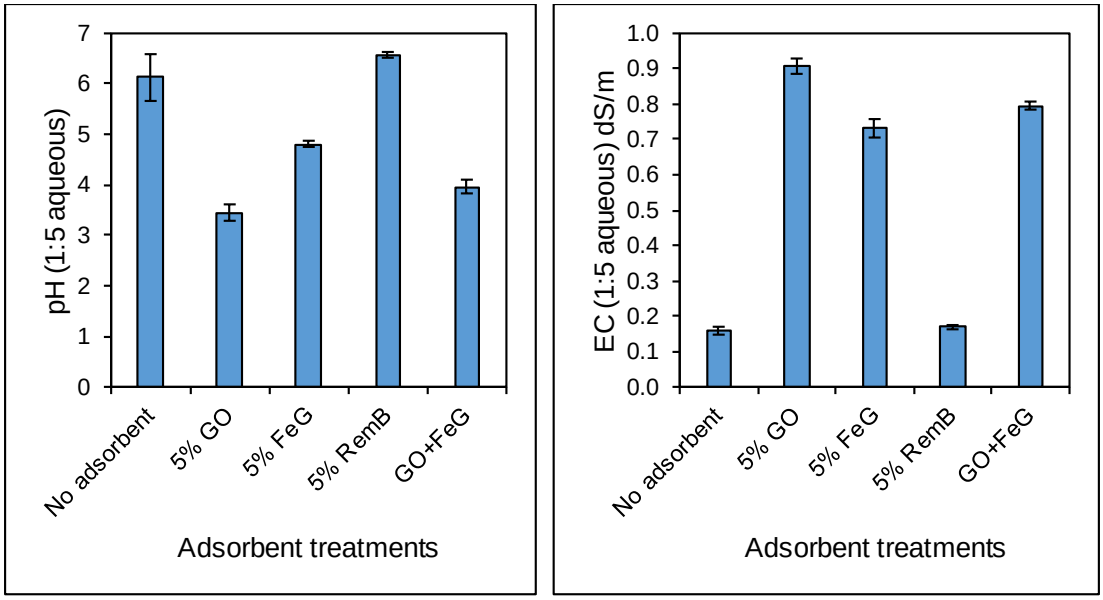

Figure 2. The pH and electrical conductivity of 1:5 (soil:water) aqueous extracts measured for soils treated with different adsorbents, compared to the contaminated control soils where no adsorbent was added. Adsorbents include 5% weight doses of graphene oxide (GO), Fe-oxide-modified reduced GO composite (FeG), RemBind™ (RemB), and a 1:1 GO+FeG treatment. The data for all contaminant-treatments were pooled. Error bars represent the standard deviation (n = 4).

3.3.1. Arsenic bioaccessibility

In As-contaminated soils, all adsorbent treatments resulted in a decrease in bioaccessible-As (Figure 1a). While GO decreased As-bioaccessibility by only ~36%, all other adsorbents reduced As-bioaccessibility by >97%. The mixed mineral and C-based adsorbents in particular (i.e. FeG and RemB) markedly reduced As-solubility. Adsorption of As onto FeG could occur *via* the goethite minerals attached on the FeG-surface. Iron-based minerals, including goethite, are well-known for their ability to bind As-oxyanions through ligand-exchange and complexation mechanisms (Andjelkovic et al., 2015, Manceau, 1995, Warren et al., 2003) and could thus be responsible for As-binding. Similarly, in the case of RemB, the kaolinite (aluminosilicate) and gibbsite components could participate in ligand-exchange between As and the surface-coordinated silicate and hydroxyl ions (Arai et al., 2005). In general, As-sorption is known to be enhanced in low pH conditions; binding sites tend to acquire a greater positive charge at lower pH, facilitating greater sorption of anionic-As (Zhu et al., 2009). However, in FeG and RemB-treated soils, it appears that sorption occurred independent of pH conditions. Both FeG and RemB displayed >98.5% As-sorption, despite the recorded pH being vastly different (i.e., pH 4.8 for FeG-treated soils, and pH 6.6 for

RemB treated soils). For GO-treated soils, the decreased bioaccessibility of As was, at first, unexpected considering the predominantly negative charge on GO (Figure S8). Our previous study using the same GBMs revealed that GO did not adsorb As from aqueous test solutions, even at low pH, due to repulsion between As-oxyanions and the highly negatively-charged GO surface (Lath et al., 2018a). However, in the soil matrix tested here, a reasonable amount of As-sorption (36%) was observed. It is possible that the decrease in soil pH (due to the addition of GO) decreased the net negative charge (or increased positive charge) on soil mineral and organic surfaces, enabling sorption. Moreover, the soluble cations in the soil, particularly the Ca^{2+} ions (from the dissolution of lime at lowered pH) are likely to promote bridging between anionic-As and negatively-charged GO sites, hence, facilitating As-binding. Such cation-induced sorption of As due to bridge-formation has been reported previously in the case of humic substances (Lin et al., 2004), as well as a magnetic GO-based adsorbent (Yang et al., 2017). The levels of reduction in As-bioaccessibility observed due to addition of GO, FeG, RemB and GO+FeG in the 'cocktail'-contaminated soils were similar to those observed in the singly-contaminated soils.

3.3.2. Cadmium bioaccessibility

The increased bioaccessibility of Cd in GBM-treated soils (Figure 1b) can be explained by the observed decreases in pH (and increases in EC) in these samples. Fundamentally, Cd, which mainly occurs in its free cationic form (Cd^{2+}) in the environment, can be retained by the negatively-charged binding sites (e.g. organic matter, clay) in soil. However, low pH conditions can mobilise retained Cd^{2+} ions. Indeed, the levels of bioaccessible Cd increased as pH of the soil decreased from 6.1 (for the control Cd-contaminated soil) to 3.4, 4.7 and 4.3 with the addition of GO, FeG and mixed GO+FeG, respectively.

Graphene-based adsorbents, particularly GO, have previously displayed excellent Cd-adsorption from solution (Sitko et al., 2013), due to electrostatic interactions of Cd^{2+} with the negatively-charged oxygen-functional groups of GO. This has been the case even when solution pH was as low as 3 – 4, as GO maintains a highly negative charge even in these pH conditions (Figure S8) (Bian et al., 2015, Lath et al., 2018a). However this was not reflected in our study with soil. One possible reason for this is the increased EC in GBM-treated soils due to the dissolution of added lime. Divalent cations like Ca^{2+} can bind with the oxygen-groups associated with GO, reducing the binding sites potentially available for Cd-sorption. Additionally, studies have reported that increased concentrations of free Ca^{2+} ions can significantly reduce Cd-retention by soil (Temminghoff et al., 1995). Since both Ca and Cd exist as divalent cations in solution, and have similar charge:radius ratios (Ca^{2+} = 2.02 e/Å, Cd^{2+} = 2.06 e/Å), they can compete for similar binding sites (Choong et al., 2014).

Uwamariya et al. (2016) showed that Ca competed with Cd for sorption sites on Fe-oxide-coated sand, as well as on granular ferric hydroxide. Our previous research also demonstrated that competition by Ca^{2+} strongly suppressed Cd-sorption by GO (Lath et al., 2018a). Such competition may explain why GBMs, through acidification and in combination with lime, did not successfully bind Cd in the soils tested. This was the case in both the singly-contaminated soil, as well as the 'cocktail'-contaminated soil.

It may be suggested that, with appropriate pH adjustment, GO and FeG may potentially become suitable adsorbents for Cd-remediation in contaminated soils. However, given the acidifying properties of GBMs discussed previously, the amount of base required to raise the pH to suitable levels would be substantial. The most commonly favoured amendment in agricultural and soil management practices for this purpose is lime (Lim et al., 2013). However, our results show that addition of lime resulted in a concurrent increase in EC, likely due to increases in Ca^{2+} ions in the soil because of acidification. Any potential benefits conferred due to increased pH (by increased liming) may be diminished by increased competition for binding sites on GBMs, hindering Cd-sorption. Further studies would be required to determine if this is the case.

Unlike GO and FeG, the commercial adsorbent, RemB, was able to reduce bioaccessibility of Cd from 8.1 mg/kg to 3 mg/kg (a 63% reduction) in the Cd-contaminated soil. The pH of RemB-treated soils was measured to be 6.6. Since RemB has a PZC of 5.7 (Figure S8), it possesses a net negative charge at pH > 5.7 and is potentially able to retain cationic Cd on its surfaces (activated-C, or associated clays and minerals). In the case of the 'cocktail'-contaminated soil, the RemB treatment had no effect on Cd-bioaccessibility. This may be attributed to the greater contaminant load, and possible preferential binding for the other co-contaminants, as is apparent from the greater amounts of As, PFOA and PFOS adsorbed (>98%), compared to Cd-sorption (63.3%) (Figure 1, Table S3), when they occur singly.

3.3.3. PFOA and PFOS bioaccessibility

For PFOA and PFOS-contaminated soils, all adsorbent treatments resulted in a decrease in bioaccessible PFOA and PFOS (Figure 1c and 1d). In singly-contaminated soils, PFOA-bioaccessibility was reduced by 43.8, 89.7, 98.3 and 84.8% for the GO, FeG, RemB and GO+FeG treatments, respectively (Table S3). Similarly, PFOS-bioaccessibility was reduced by 85.5% for the GO-treatment, and by >96% for the FeG, RemB and GO+FeG treatments (Table S3). Comparing the different GBM treatments, FeG-treated soils appeared to have adsorbed more PFOA and PFOS than the GO-treated soils. This is consistent with our previous work on remediation of PFAS-contaminated waters where greater sorption was observed by FeG (and RemB) than by GO (Lath et al., 2018b).

The acid dissociation constant, pK_a, of PFOA and PFOS are reportedly low (0.5 – 2.8) (Goss, 2008, Moody and Field, 2000), and hence they exist in their dissociated anionic form in most environmental conditions. Despite the net negative charge on the surfaces of GO (Figure S8), considerable sorption of anionic PFAS was observed, which suggests the role of non-electrostatic binding mechanisms. These could be hydrophobic interactions between the graphitic plane and the hydrophobic tails of the PFAS molecules. A study using hematite revealed that PFOA and PFOS sorbed to Fe-oxide minerals in different ways. PFOA could form inner-sphere Fe-carboxylate complexes *via* ligand-exchange, while the sulphonate group from PFOS forms outer-sphere complexes and hydrogen-bonds at the hematite surface (Gao and Chorover, 2012). The increased sorption in the case of FeG, compared to GO, may be attributed to such interactions at the goethite mineral phase. Similar mechanisms may be observed in the case of RemB, with alumina as the mineral phase (Wang and Shih, 2011). The pH values of FeG-treated soils were 4.8 (Figure 2a), which is below the PZC for FeG of 7.1 (Figure S8). Consequently, in these conditions, FeG had a net positive charge, making it possible for additional electrostatic interactions to be involved.

On comparing the two PFAS-contaminated soils, greater remediation efficacy was detected for PFOS than PFOA. Previous studies have reported that for PFASs with the same perfluorocarbon chain-lengths, PFASs with sulphonate head groups (e.g. PFOS) usually exhibit much greater sorption to minerals and sediments than their counterparts with carboxylate head groups (e.g. PFOA) (Hellsing et al., 2016, Higgins and Luthy, 2006, Lath et al., 2018b). Hence the differences in the efficacy of remediation can be ascribed to the differences in the properties of their charged functional head-groups. In the 'cocktail'-contaminated soils, the extent of remediation achieved was similar to that observed in the singly-contaminated soils, indicating that either sufficient binding surfaces were available, and/or that no competitive sorption was evident.

3.3.4. Outcomes and implications of bioaccessibility-based assessment

Overall, based on the bioaccessible contaminant-fractions, it appears that apart from Cd, other contaminants (As, PFOA and PFOS) in the soils were successfully remediated to varying degrees (> 89%) depending on the adsorbent. In the case of As-contamination, FeG and RemB were equally effective and performed better than GO. In PFAS-contaminated soils, RemB-treatment was the most effective, followed by FeG, then GO. In most cases, the use of GO+FeG generated an outcome that was intermediate between the effect observed for GO and FeG. The mixed mineral and C-based adsorbents in particular (i.e. FeG and RemB) provided excellent outcomes for sorption and bioaccessibility-reduction, which may

be credited to provision of multiple types of binding sites that can participate in binding a variety of contaminants through multiple mechanisms.

In the case of the 'cocktail'-contaminated soil, a remarkable observation was that despite the increase in the total contaminant load in the soil, remediation efficacy was not hindered when compared to the singly contaminated soil, particularly in the case of As, PFOA and PFOS (disregarding Cd). One possibility is that these contaminants are being sorbed onto distinctly separate types of binding sites on the adsorbents' surface, *via* different mechanisms. However, a more plausible explanation may be based on the sorption capacity of the adsorbents and availability of binding sites. The remediation trial was conducted using a single concentration for each contaminant (based on the EC50 values); at these concentrations, the binding sites may not have been saturated. Further isotherm studies using higher concentrations would be required to determine maximum sorption capacities of GO, FeG and RemB towards the As, Cd, PFOA and PFOS in soil, however this was not the current focus of this study.

3.4. Biological assessment of remediation efficacy: soil nitrification response

To determine if remediation was also effective from a biological and soil-health point of view, the impact of the adsorbents on soil nitrification processes was investigated. Nitrate production in remediated soils was compared to that in unremediated contaminated control soils. Considering the dose-dependent effect of the different contaminants on nitrate production (section 3.2), addition of the adsorbents was expected to reduce contaminant bioaccessibility and alleviate the toxic effect, thereby potentially restoring nitrification. Data from the N-transformation tests for each of the treatments from the remediation trial are presented in Figure 3.

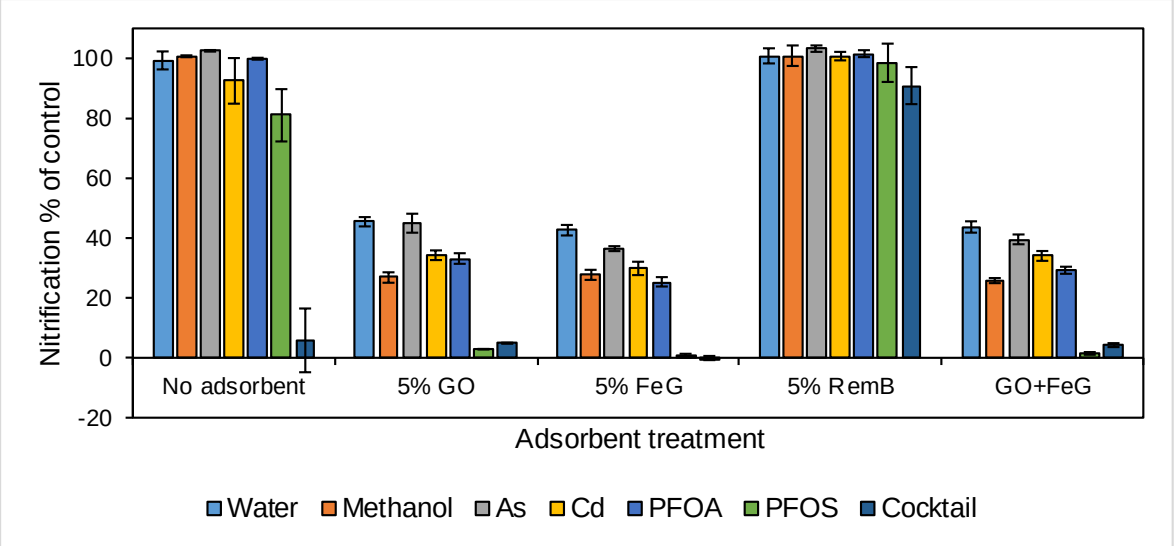

Figure 3. Observed nitrification in contaminated soils, compared with remediated soils. Data are expressed as a percentage of nitrification in uncontaminated controls. Contaminant treatments include singly-contaminated soils (As, Cd, PFOA and PFOS), as well as a 'cocktail' treatment comprised of the 4 contaminants mixed together. Adsorbents include 5% weight doses of graphene oxide (GO), Fe-oxide-modified reduced GO composite (FeG), RemBind™ (RemB), and a 1:1 GO+FeG treatment. Error bars represent the standard deviation (n = 4).

First, when examining the contaminated soils where no adsorbent was added (i.e., no remediation implemented), nitrification in the As, Cd or PFOA-contaminated soils was not significantly different from nitrification in uncontaminated control (water or methanol-spiked) soils ($p = 0.1602$). This was unexpected, since the soils were spiked with pre-determined concentrations of each of the contaminants that had previously displayed a 50% decrease in nitrification (Figures S9a – 9d). Based on the expected *versus* observed levels of nitrification in these 'no adsorbent' contaminated soils (Figure 4), it is apparent that the only soils displaying inhibited nitrification compared to the uncontaminated controls were the PFOS-contaminated soil (18.7% inhibition) and 'cocktail'-contaminated soil (94.2% inhibition). The toxic effects of the As, Cd and PFOA-contaminated soils seem to have been alleviated prior to addition of any adsorbents. This could be attributed to either: 1) potential aging of the contaminants in soil, and/or 2) adaptation of soil microbial communities to the contaminants in the soils. The soils used in the remediation trial were pre-incubated with the contaminants for 30 days, followed by another 10-day incubation after the addition of adsorbents prior to commencing the 28-day soil nitrification test. On the other hand, soils used in the preliminary testing conducted to determine the EC50 concentrations, were only incubated with the

contaminants for 5 days prior to 28-day soil nitrification tests. The >30 days of incubation may have already 'aged' the contaminants in the soil, rendering them less bioaccessible and alleviating their toxic effects. As reported in the literature, ageing can occur over weeks, or even months, depending on soil particle size, organic matter, inorganic constituents, contaminant concentration and microbial activity (Semple et al., 2003). Similarly, adaptation of soil microbes to elevated contaminant concentrations, increasing tolerance (as indicated by the increase in the EC50 towards nitrification over time), is a commonly reported phenomenon (Rusk et al., 2004).

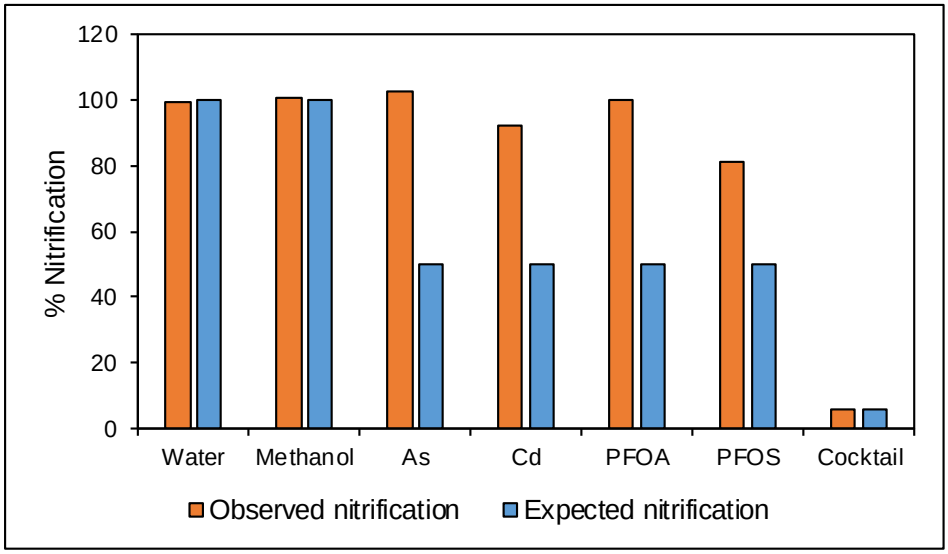

Figure 4. Bar graph comparing the observed nitrification versus expected nitrification in uncontaminated (water and methanol-spiked) soils, and contaminated soils spiked with As, Cd, PFOA and PFOS at 50% effect concentrations (EC50), where no remediation was implemented.

Whether due to ageing of the contaminants in the soil, or due to adaptation of the microbes for increased tolerance towards the contaminants (Rusk et al., 2004), the increased incubation time (from 5 to >30 days) plausibly changed the observed toxicity of the contaminants. Despite this underestimation of the individual toxicity of the contaminants, the incubation time for each of the treatments within the remediation trial were kept consistent, making it possible to, nevertheless, draw comparisons between the remediation efficacy (in terms of nitrification-restoration) of the contaminant-treatments, as well as adsorbent-treatments within the experiment.

A first glance at Figure 3 shows that the addition of all GBM-treatments to the soils led to an inhibition of nitrification, compared to the unremediated (contaminated) control soils,

whereas the RemB-treated soils did not exhibit any inhibition. Our initial assumption was that reduced nitrification would primarily occur as a consequence of contaminant-stress (i.e., due to greater bioaccessible contaminant-concentrations), in situations where the adsorbents failed to bind the contaminants. However, taking into consideration the chemical assessment of remediation discussed previously (section 3.3), it is clear that in the case of As, PFOA and PFOS, the GBMs did in fact bind the contaminants (Figure 1). Thus the reduced nitrification observed in the case of GBMs for As, PFOA and PFOS-contaminated soils is not a consequence of greater bioaccessible contaminant fractions.

As discussed earlier, the pH of the soil solutions in all GBM-treated soils was especially low, ranging from pH 3.5 – 4.8 (Figure 2a). Previous research has demonstrated that pH is significant environmental parameter impacting nitrification response (Quastel and Scholefield, 1951). Based on a variety of studies, the ideal pH conditions that support microbial nitrification are reported to range from pH 5 to 8.5 (Curtin et al., 1998, OECD, 2000, Sauvé et al., 1999), depending on the soil type and constituents. Furthermore, a few studies have demonstrated that the influence of pH can even surpass the influence of high contaminant concentration on nitrification (Sauvé et al., 1999, Smolders et al., 2001). The Cd-contaminated soils were the only soils in the remediation trial where the GBMs did not successfully reduce bioaccessibility. However, biologically, the observed toxicity in terms of inhibition to nitrification was not specifically greater in Cd-soils compared to other contaminated soils. Even in As-, PFOA- and PFOS-contaminated soils, where FeG, for instance, reduced bioaccessibility by ≥90% (alleviating contaminant-induced stress), nitrification was reduced by 63.5%, 74.6% and 99.3%, respectively. It is thus reasonable to infer that that the decreased nitrification observed in soils treated with GBMs is a consequence of lowered pH conditions, rather than contaminant-induced stress. Unlike GBM-treatments, it appears that for singly-contaminated soils, RemB did not hinder the nitrification function (Figure 3). The soil solutions for all RemB-treated soils had an average pH of around 6.6, which was comparable to that of the uncontaminated soils (pH 6.1), and within the pH range suitable for nitrification as suggested in the literature. This corroborates our hypothesis that pH played a greater role in the nitrification outcome. While there were no effects on nitrification for the singly-contaminated soils in this study (Figures 3 and 4), the added stress from the co-occurrence of multiple contaminants in the 'cocktail'-contaminated soil severely inhibited the soil-nitrification response. This response, which is greater than a '50% effect', is not surprising given that the 4 different contaminants were each spiked at their intended EC50-concentrations, making the total level of contamination in this soil vastly greater than in the singly-contaminated soils. Mixtures of contaminants can interact in complex ways; the 'cocktail' of 4 contaminants may have interacted in either an additive or

synergistic manner, increasing the toxic effect on the nitrifying bacteria (Ramakrishnan et al., 2011). However, RemB did manage to alleviate this mixture toxicity and restore nitrification to levels comparable to that observed in the uncontaminated control soils (Figure 3). This positive response could be attributed to reduced bioaccessibility of each of the 4 contaminants in the mixture (as seen in Figure 1); i.e., reduced contaminant-stress.

4. Conclusions

Graphene-based adsorbents showed great promise for *in situ* soil remediation based on large reductions in the solubility of multiple inorganic and organic contaminants in soil. A drawback is the inherent acidity in these products that could impede efforts to reduce the solubility of cationic metal contaminants in soil, and impact soil microbial function. The goethite-based composite, FeG, was superior to GO for immobilising multiple contaminants simultaneously, likely due to the mixed mineral and C-based nature of this material, providing pathways for binding *via* multiple mechanisms – i.e., ligand-exchange and inner-sphere complexation of As with the goethite phase, hydrophobic interactions of PFOA and PFOS at the graphitic plane, as well as ligand-exchange of the carboxylate and sulphonate head groups of PFOA and PFOS. In contrast, interactions with GO are limited to hydrophobic and simple electrostatic interactions. Similar to FeG, the commercial mixed mode sorbent material (RemBind™) was also effective in reducing the solubility and toxicity of multiple contaminants simultaneously and did not suffer from the soil acidification displayed by the GBMs. Hence, while GBMs could reduce the bioaccessibility of As, PFOA and PFOS, their application *in situ* for soil remediation requires that acidity generated by the materials is neutralised.

5. Acknowledgements

We thank Bogumila Tomczak (University of Adelaide) for assistance with ICP-OES analyses, Jun Du (CSIRO) for assistance with LC-MS/MS analyses, and Erinne Stirling for assistance with nitrate analyses. We also thank Ziltek Pty. Ltd. for their support and provision of RemBind™. Financial support from Australian Research Council Discovery Grant DP150101760 is gratefully acknowledged.

6. References

Abollino O, Aceto M, Malandrino M, Sarzanini C, Mentasti E (2003). Adsorption of heavy metals on Na-montmorillonite. Effect of pH and organic substances. *Water Research,* **37,** 1619-1627.

Adriano DC, Wenzel WW, Vangronsveld J, Bolan NS (2004). Role of assisted natural remediation in environmental cleanup. *Geoderma,* **122,** 121-142.

Andjelkovic I, Tran DNH, Kabiri S, Azari S, Markovic M, Losic D (2015). Graphene aerogels decorated with α-FeOOH nanoparticles for efficient adsorption of arsenic from contaminated waters. *ACS Applied Materials & Interfaces,* **7,** 9758-9766.

Arai Y, Sparks DL, Davis JA (2005). Arsenate adsorption mechanisms at the allophane−water interface. *Environmental Science & Technology,* **39,** 2537-2544.

Barnes M, Correll R, Stevens DP (2003). A simple spreadsheet for estimating low-effect concentrations and associated logistic dose response curves. . Christchurch, New Zealand: The Society of Environmental Toxicology and Chemistry Asia/Pacific – Australasian Society of Ecotoxicology: Solutions to Pollution.

Bei Y, Deng S, Du Z, Wang B, Huang J, Yu G (2014). Adsorption of perfluorooctane sulfonate on carbon nanotubes: influence of pH and competitive ions. *Water Science and Technology,* **69,** 1489-95.

Bian Y, Bian Z-Y, Zhang J-X, Ding A-Z, Liu S-L, Wang H (2015). Effect of the oxygen-containing functional group of graphene oxide on the aqueous cadmium ions removal. *Applied Surface Science,* **329,** 269-275.

Chen Z, Li H, Ma W, Fu D, Han K, Wang H, He N, Li Q, Wang Y (2018). Addition of graphene sheets enhances reductive dissolution of arsenic and iron from arsenic contaminated soil. *Land Degradation & Development,* **29,** 572-584.

Choong G, Liu Y, Templeton DM (2014). Interplay of calcium and cadmium in mediating cadmium toxicity. *Chemico-Biological Interactions,* **211,** 54-65.

Curtin D, Campbell CA, Jalil A (1998). Effects of acidity on mineralization: pH-dependence of organic matter mineralization in weakly acidic soils. *Soil Biology and Biochemistry,* **30,** 57-64.

Dimiev AM, Alemany LB, Tour JM (2013). Graphene oxide. Origin of acidity, its instability in water, and a new dynamic structural model. *ACS Nano,* **7,** 576-588.

Dreyer DR, Park S, Bielawski CW, Ruoff RS (2010). The chemistry of graphene oxide. *Chemical Society Reviews,* **39,** 228-240.

Ersan G, Apul OG, Perreault F, Karanfil T (2017). Adsorption of organic contaminants by graphene nanosheets: A review. *Water Research,* **126,** 385-398.

Gao X, Chorover J (2012). Adsorption of perfluorooctanoic acid and perfluorooctanesulfonic acid to iron oxide surfaces as studied by flow-through ATR-FTIR spectroscopy. *Environmental Chemistry,* **9,** 148-157.

Goss K-U (2008). The pKa values of PFOA and other highly fluorinated carboxylic acids. *Environmental Science & Technology,* **42,** 456-458.

Hellsing MS, Josefsson S, Hughes AV, Ahrens L (2016). Sorption of perfluoroalkyl substances to two types of minerals. *Chemosphere,* **159,** 385-391.

Higgins CP, Luthy RG (2006). Sorption of perfluorinated surfactants on sediments. *Environmental Science & Technology,* **40,** 7251-7256.

Houba VJG, Temminghoff EJM, Gaikhorst GA, van Vark W (2000). Soil analysis procedures using 0.01 M calcium chloride as extraction reagent. *Communications in Soil Science and Plant Analysis,* **31,** 1299-1396.

Hughes MF (2002). Arsenic toxicity and potential mechanisms of action. *Toxicology Letters,* **133,** 1-16.

Lath S, Navarro D, Tran D, Kumar A, Losic D, McLaughlin MJ (2018a). Mixed-mode remediation of cadmium and arsenate ions using graphene-based materials. *CLEAN – Soil, Air, Water,* **46,** 1800073.

Lath S, Navarro DA, Losic D, Kumar A, McLaughlin MJ (2018b). Sorptive remediation of perfluorooctanoic acid (PFOA) using mixed mineral and carbon-based materials. *Environmental Chemistry,* **In review**.

Leininger S, Urich T, Schloter M, Schwark L, Qi J, Nicol GW, Prosser JI, Schuster SC, Schleper C (2006). Archaea predominate among ammonia-oxidizing prokaryotes in soils. *Nature,* **442,** 806-9.

Lim JE, Ahmad M, Lee SS, Shope CL, Hashimoto Y, Kim K-R, Usman ARA, Yang JE, Ok YS (2013). Effects of lime-based waste materials on immobilization and phytoavailability of cadmium and lead in contaminated soil. *CLEAN – Soil, Air, Water,* **41,** 1235-1241.

Lin H-T, Wang MC, Li G-C (2004). Complexation of arsenate with humic substance in water extract of compost. *Chemosphere,* **56,** 1105-1112.

Manceau A (1995). The mechanism of anion adsorption on iron oxides: Evidence for the bonding of arsenate tetrahedra on free $Fe(O, OH)_6$ edges. *Geochimica et Cosmochimica Acta,* **59,** 3647-3653.

Miranda KM, Espey MG, Wink DA (2001). A Rapid, simple spectrophotometric method for simultaneous detection of nitrate and nitrite. *Nitric Oxide,* **5,** 62-71.

Moody CA, Field JA (2000). Perfluorinated surfactants and the environmental implications of their use in fire-fighting foams. *Environmental Science & Technology,* **34,** 3864-3870.

Nelson PN, Su N (2010). Soil pH buffering capacity: a descriptive function and its application to some acidic tropical soils. *Soil Research,* **48,** 201-207.

Novoselov KS, Falko VI, Colombo L, Gellert PR, Schwab MG, Kim K (2012). A roadmap for graphene. *Nature,* **490,** 192-200.

O'Day PA, Vlassopoulos D (2010). Mineral-based amendments for remediation. *Elements,* **6,** 375-381.

OECD (2000). OECD Guidelines for the testing of chemicals. Test Guideline 216, Soil microorganisms: nitrogen transformation test. Paris: OECD Publishing.

Paktunc D, Bruggeman K (2010). Solubility of nanocrystalline scorodite and amorphous ferric arsenate: Implications for stabilization of arsenic in mine wastes. *Applied Geochemistry,* **25,** 674-683.

Qi Z, Hou L, Zhu D, Ji R, Chen W (2014). Enhanced transport of phenanthrene and 1-naphthol by colloidal graphene oxide nanoparticles in saturated soil. *Environmental Science & Technology,* **48,** 10136-10144.

Quastel JH, Scholefield PG (1951). Biochemistry of nitrification in soil. *Bacteriological Reviews,* **15,** 1-53.

Rakowska M, Kupryianchyk D, Harmsen J, Grotenhuis T, Koelmans A (2012). In situ remediation of contaminated sediments using carbonaceous materials. *Environmental Toxicology and Chemistry,* **31,** 693-704.

Ramakrishnan B, Megharaj M, Venkateswarlu K, Sethunathan N, Naidu R 2011. Mixtures of environmental pollutants: effects on microorganisms and their activities in soils. *In:* Whitacre, DM (ed.) *Reviews of Environmental Contamination and Toxicology Volume 211.* New York, NY: Springer New York.

Robertson GP, Groffman PM 2015. Nitrogen transformations *In:* Paul, EA (ed.) *Soil microbiology, ecology and biochemistry (Fourth edition).* Boston: Academic Press.

Rusk JA, Hamon RE, Stevens DP, McLaughlin MJ (2004). Adaptation of soil biological nitrification to heavy metals. *Environmental Science & Technology,* **38,** 3092-3097.

Sauvé S, Dumestre A, McBride M, Gillett JW, Berthelin J, Hendershot W (1999). Nitrification potential in field-collected soils contaminated with Pb or Cu. *Applied Soil Ecology,* **12,** 29-39.

Semple KT, Morriss AWJ, Paton GI (2003). Bioavailability of hydrophobic organic contaminants in soils: fundamental concepts and techniques for analysis. *European Journal of Soil Science,* **54,** 809-818.

Semple KT, Doick KJ, Wick LY, Harms H (2007). Microbial interactions with organic contaminants in soil: Definitions, processes and measurement. *Environmental Pollution*, **150**, 166-176.

Sitko R, Turek E, Zawisza B, Malicka E, Talik E, Heimann J, Gagor A, Feist B, Wrzalik R (2013). Adsorption of divalent metal ions from aqueous solutions using graphene oxide. *Dalton Transactions,* **42,** 5682-5689.

Smolders E, Brans K, Coppens F, Merckx R (2001). Potential nitrification rate as a tool for screening toxicity in metal-contaminated soils. *Environmental Toxicology and Chemistry,* **20,** 2469-2474.

Temminghoff EJM, Van Der Zee SEATM, De Haan FAM (1995). Speciation and calcium competition effects on cadmium sorption by sandy soil at various pHs. *European Journal of Soil Science,* **46,** 649-655.

Tofighy MA, Mohammadi T (2011). Adsorption of divalent heavy metal ions from water using carbon nanotube sheets. *Journal of Hazardous Materials,* **185,** 140-147.

Upadhyay RK, Soin N, Roy SS (2014). Role of graphene/metal oxide composites as photocatalysts, adsorbents and disinfectants in water treatment: a review. *RSC Advances,* **4,** 3823-3851.

USEPA (2016). Drinking water health advisory for perfluorooctanoic acid (PFOA). EPA Document Number: 822-R-16-005. Washington, D C.

Uwamariya V, Petrusevski B, Lens PNL, Amy GL (2016). Effect of pH and calcium on the adsorptive removal of cadmium and copper by iron oxide–coated sand and granular ferric hydroxide. *Journal of Environmental Engineering,* **142,** 1-9.

Wang F, Shih K (2011). Adsorption of perfluorooctanesulfonate (PFOS) and perfluorooctanoate (PFOA) on alumina: Influence of solution pH and cations. *Water Research,* **45,** 2925-2930.

Warren GP, Alloway BJ, Lepp NW, Singh B, Bochereau FJM, Penny C (2003). Field trials to assess the uptake of arsenic by vegetables from contaminated soils and soil remediation with iron oxides. *Science of the Total Environment,* **311,** 19-33.

Xiong T, Yuan X, Wang H, Leng L, Li H, Wu Z, Jiang L, Xu R, Zeng G (2018). Implication of graphene oxide in Cd-contaminated soil: A case study of bacterial communities. *Journal of Environmental Management,* **205,** 99-106.

Yang X, Xia L, Song S (2017). Arsenic adsorption from water using graphene-based materials as adsorbents: a critical review. *Surface Review and Letters,* **24,** 1730001.

Zhu H, Jia Y, Wu X, Wang H (2009). Removal of arsenic from water by supported nano zero-valent iron on activated carbon. *Journal of Hazardous Materials,* **172,** 1591-1596.

7. Supporting Information

Mixed-mode mineral, carbon and graphene-based materials for simultaneous remediation of arsenic, cadmium, PFOA and PFOS in soils

Supriya Lath [*, 1], Divina A. Navarro [1, 2], Dusan Losic [3], Michael J. McLaughlin [1, 2]

[1] School of Agriculture Food and Wine, The University of Adelaide, PMB 1 Glen Osmond, SA 5064, Australia.

[2] CSIRO Land and Water, PMB 2 Glen Osmond, SA 5064, Australia.

[3] School of Chemical Engineering, The University of Adelaide, Adelaide, SA 5005, Australia.

* Corresponding author email: supriya.lath@adelaide.edu.au

Text S1. Synthesis of graphene oxide (GO) and Fe-oxide-modified reduced GO composite (FeG).

A top-down approach based on an improved Hummer's method [1] which involves strong oxidative exfoliation of graphite using concentrated H_2SO_4, H_3PO_4 and $KMnO_4$ was used to synthesise GO. Unreacted $KMnO_4$ was reduced using 30% H_2O_2, and multiple wash cycles were performed with 30% HCl and distilled water to remove metal and acid residues. The material was dried (35 °C, 36 hours) to obtain the solid GO product, which was used as flakes. Based on a method reported by Cong et al. [2], GO was further modified by adding $FeSO_4.7H_2O$ to a stable suspension of well-exfoliated GO. After adjusting the pH to 3.5 using ammonia, the suspension was hydrothermally reduced at 90 °C for 6 hrs without stirring until a black 3D hydrogel monolith (FeG) was formed. The hydrogel was then separated, washed, freeze dried and crushed into the powdered FeG product.

Text S2. Sample preparation for characterisation of adsorbents.

SEM-EDAX samples were prepared by applying the dried adsorbents directly onto aluminium stubs covered with adhesive carbon tape. Images were obtained using a spot size of 3, and an accelerating voltage of 10 kV. For TEM, adsorbents were ultra-sonicated in ethanol (20 min), after which the suspensions were drop-casted onto a Lacey copper grid and dried for a few hours before imaging at an accelerating voltage of 100 kV.

FTIR and XRD analyses were performed using powdered adsorbent samples. FTIR spectra were recorded at wavelengths ranging from 400 - 4000 cm^{-1}. XRD spectra were recorded using Fe-filtered Co Kα radiation, automatic divergence slit, 2° anti-scatter slit and fast X'Celerator Si strip detector. The diffraction patterns were recorded from 3 - 80° in steps of 0.017° 2 theta with a 0.5 second counting time per step for an overall counting time of approximately 35 minutes.

Specific surface area (SSA) of adsorbents were measured using the methylene blue (MB) dye absorption method commonly used for carbonaceous materials. 15 mg of each adsorbent was added to 150 mL of 20 mg/L MB solutions and shaken for 60 hrs at 100 rpm to allow the solutions to attain equilibrium and maximum absorption. After centrifugation, supernatants were analysed using UV-visible spectrophotometry (at 664 nm) and compared to controls to determine the amount of MB absorbed. The SSA was then calculated using the following equation:

$$SSA = \frac{N_A . A_{MB} . (C_i - C_e) . V}{M_{MB} . m_s}$$

where, N_A represents Avogadro number (6.023×10^{23} molecules/mole), A_{MB} is the area covered per MB molecule (1.35 nm^2), C_i and C_e are the initial and equilibrium MB concentrations, respectively, V is the volume of MB solution, M_{MB} is the molecular mass of MB, and m_s is the mass of the adsorbent.

Surface charge and PZC of adsorbents were determined by using 0.1 % w/v suspensions in Milli Q water, that were adjusted to pH values ranging from around 2 – 10. The suspensions were placed on a shaker for 48 hrs to equilibriate pH before measuring zeta potential across the pH gradient using dynamic light scattering (Malvern Zetasizer NanoZS).

Table S1. Selected physio-chemical properties of Karoonda sandy soil.

Soil Characteristics	Details
Soil type	Sandy soil (Karoonda, South Australia)
Particle size distribution	96% sand, 0.4% silt, 3% clay
pH	6.4 (1:5 soil:water)
Electrical conductivity	0.04 dS/m (1:5 soil:water)
Total Carbon (C) %	0.78%
Cation exchange capacity	3.4 cmol(+)/kg
ICP major cations, Ca^{2+}	422 mg/kg
ICP major cations, Mg^{2+}	245 mg/kg
ICP major cations, Na^{+}	<40 mg/kg
ICP major cations, K^{+}	438 mg/kg

Figure S1. Standard calibration curve for soil nitrate-N quantification.

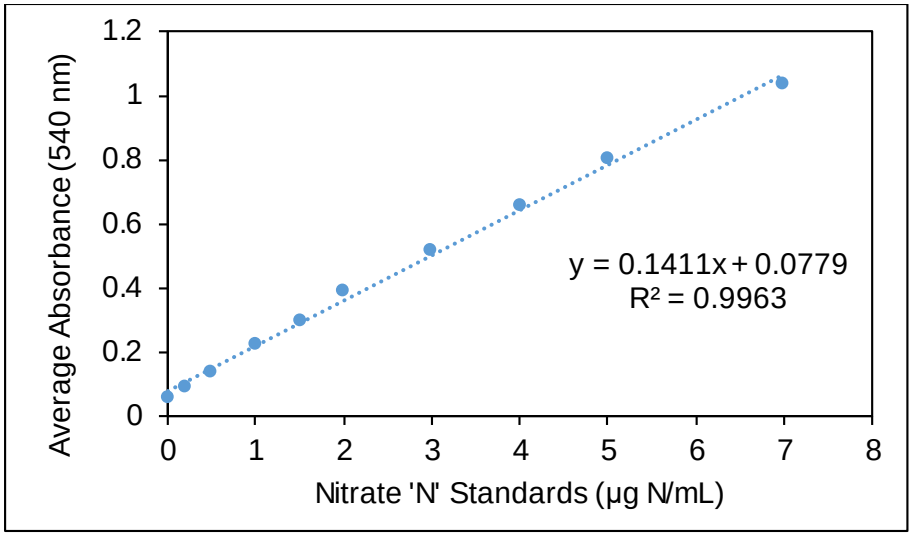

Figure S2. Determining lime-application rate for GBM-treated soils. Curve shows impact of increasing lime dose on pH of soil.

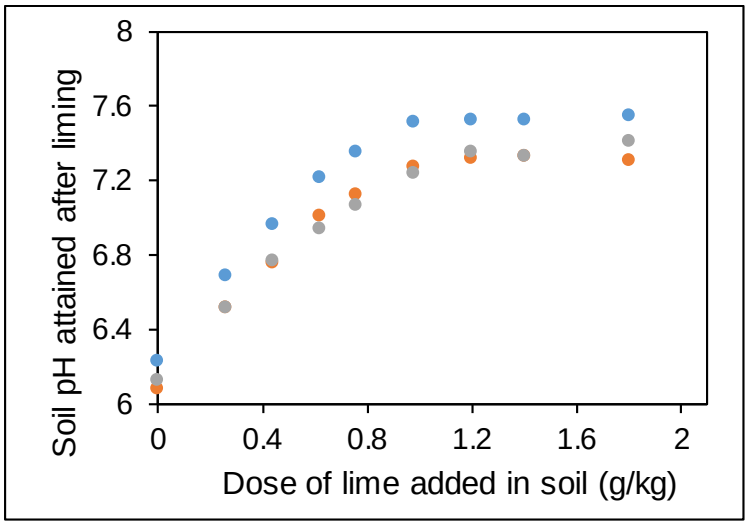

Due to the acidity of GBMs, lime was added to the GBM-treated soils to raise the pH to a range of 6 – 6.5, to match the control (untreated) soils, as well as the RemB-treated soils. Based on the test, a lime dose of 0.26 g/kg soil would suffice to raise the pH to the desired level. To compensate for the capacity of GBMs to slowly 'buffer' down to a lower pH (i.e., around pH 3), as observed in the laboratory through previous experiments, an excess dose of 2.5 g/kg soil (almost 10 fold greater than that calculated as sufficient), was added to the GBM-treated soils. Despite this, the pH recorded for GBM-treated soils at the end of the 28-day nitrification incubation period was in the range of 3.5 – 4.8.

Text S3. Details of liquid chromatography tandem mass spectrometry (LC-MS/MS) analysis for PFOA and PFOS

Analysis of PFAS was performed using a Thermo TSQ Quadrupole Mass Spectrometer (ThermoFisher Scientific, USA) equipped with a Thermo-Finnigan Surveyor Plus high performance liquid chromatography system. A 10 µL aliquot was used for sample injection (autosampler at 10^0C). Separation was achieved on a Thermo Scientific Hypersil Gold PFP column (100 x 2.1 mm, particle size 3 µm) in a 25^0C oven at a flow rate of 250 µL/min. The mobile phase consisted of (A) 5 mM ammonium acetate and (B) methanol. The gradient profile consisted of the following conditions: mobile phase B increased from 0 to 5% within 2 minutes, then ramped to 95% in another 5 minutes. This condition (95% B) was then held isocratically for 4 minutes, after which, conditions were changed to 95% A and held for 5 minutes. The total run time for each injection was 15 min. To prevent the ion source from contamination with matrix components, the first 2.5 min of the flow of each chromatographic run was diverted to waste *via* a 6 port-2-position valve installed post-column.

Sample ionisation for MS detection was achieved through negative mode electrospray operating under the following conditions: spray voltage of 4 kV, sheath gas pressure of 40 a.u., auxiliary gas pressure of 5 a.u. and collision gas pressure of 1.5 mTorr. The analytes were monitored using two product ions in multiple reaction monitoring (MRM). Retention times for PFOA and PFOS were 12.08 and 12.15 min respectively.

Analyte	Parent mass (m/z)	Product mass (m/z)
PFOA	412.9	169
	412.9	369.1
PFOS	498.8	80.17
	498.8	98.73

Method setup as well as data acquisition and data processing were conducted using the Xcalibur 3.0 software. Concentrations were determined from calibration curves (linear range 1 – 100 µg/L PFOA/PFOS in 5% methanol) prepared using a set of standard solutions of known PFOA and PFOS concentrations.

Figure S3. Scanning electron microscopy (SEM) images of (a) graphene oxide (GO), (b) Fe-oxide-modified reduced-GO (FeG), and (c) RemBind™. Transmission electron microscopy (TEM) images of (d) GO, and (e) FeG. Dark spots in 1(e) confirm the attachment of Fe-based nanoparticles (50 - 100 nm).

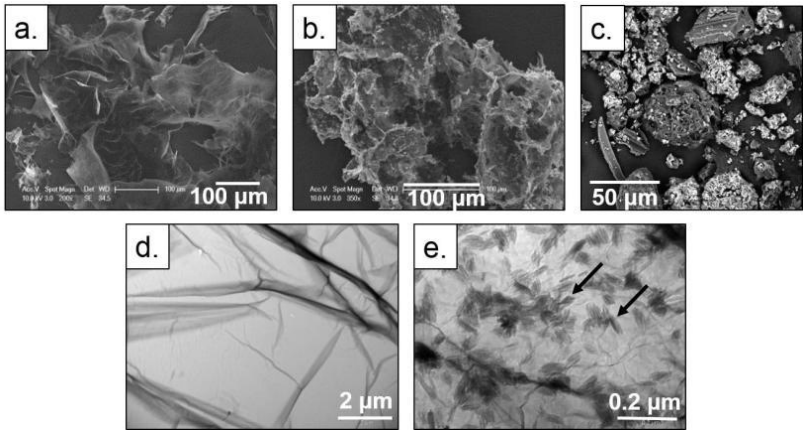

Table S2. Elemental composition of adsorbents graphene oxide (GO), Fe-oxide-modified reduced-GO (FeG) and RemBind™ (RemB), as determined by energy dispersive X-ray (EDX) detector coupled to a scanning electron microscope. See Figure S4 for EDX spectra.

Adsorbent	Element (series)	Weight %	Atomic %
GO	C (K)	65.88	72.01
	O (K)	34.12	27.99
FeG	C (K)	37.19	56.39
	O (K)	28.48	32.42
	Fe (K)	34.34	11.20
RemB	C (K)	22.42	34.37
	O (K)	27.70	31.89
	Si (K)	38.63	26.36
	Al (K)	11.26	7.38

Figure S4. Energy dispersive X-ray (EDX) spectra collected for adsorbents graphene oxide (GO), Fe-oxide-modified reduced-GO (FeG) and RemBind™ (RemB) to elucidate elemental composition. All adsorbents exhibited signals for carbon and oxygen. FeG displayed an additional signal for iron, and RemB displayed additional signals for aluminium and silicon.

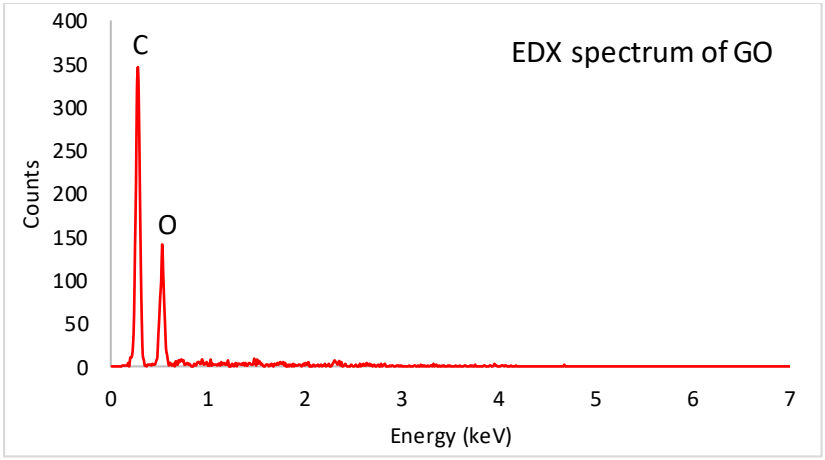

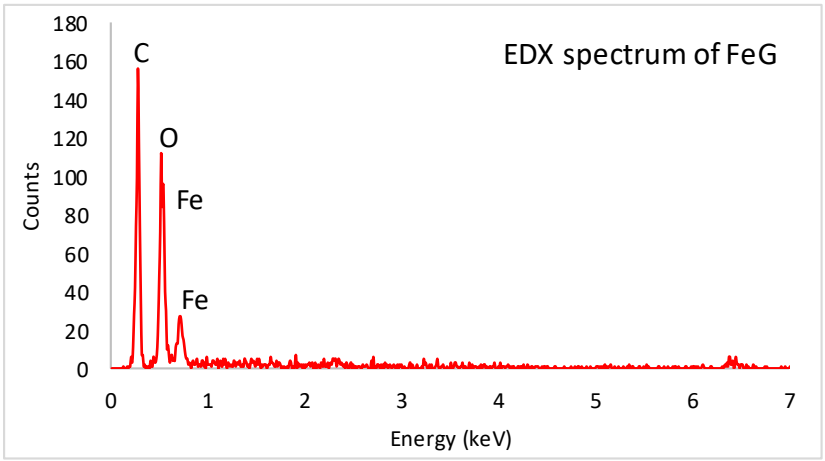

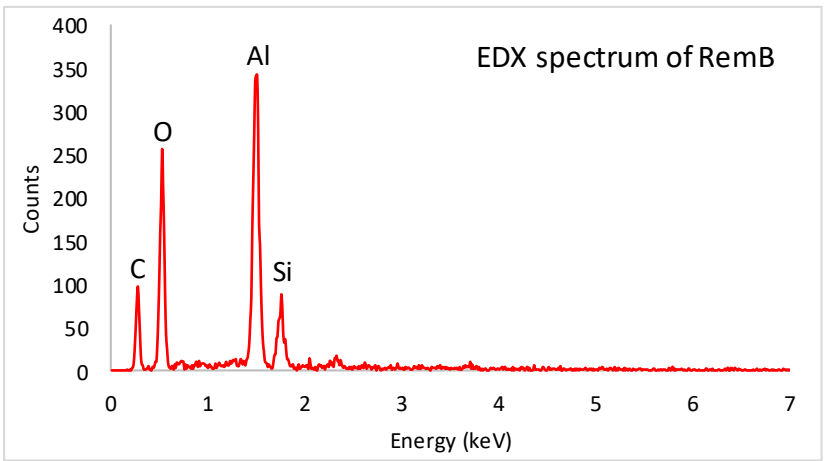

Figure S5. Fourier-transform infrared (FTIR) spectra of adsorbents graphene oxide (GO), Fe-oxide-modified reduced-GO (FeG) and RemBind™ (RemB).

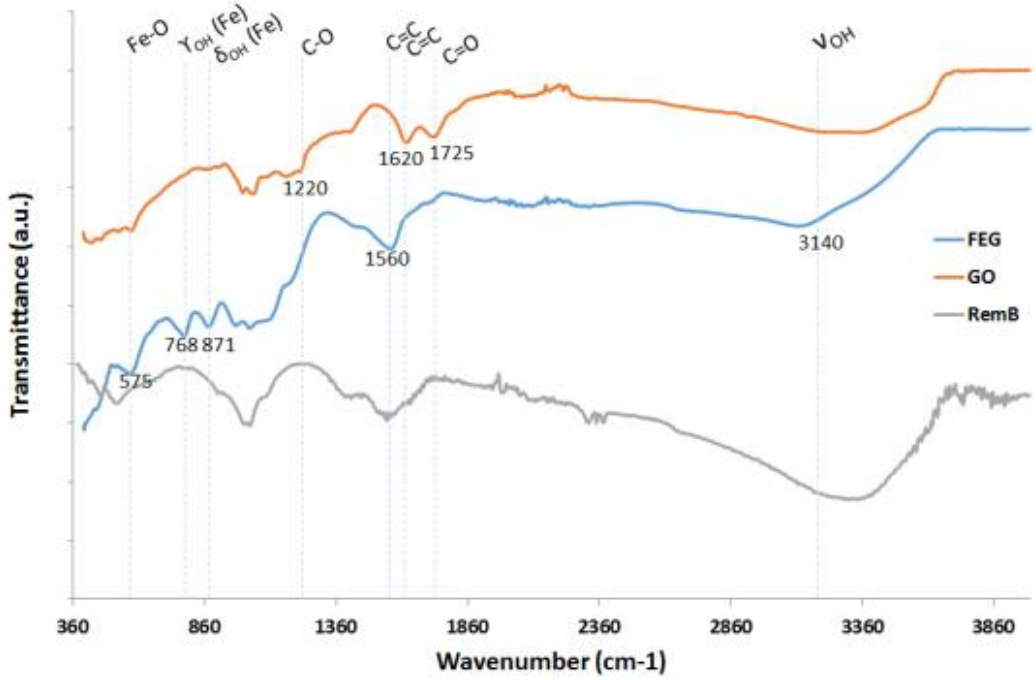

Figure S6. X-ray diffraction (XRD) spectra of adsorbents graphene oxide (GO), Fe-oxide-modified reduced-GO (FeG) and RemBind™ (RemB).

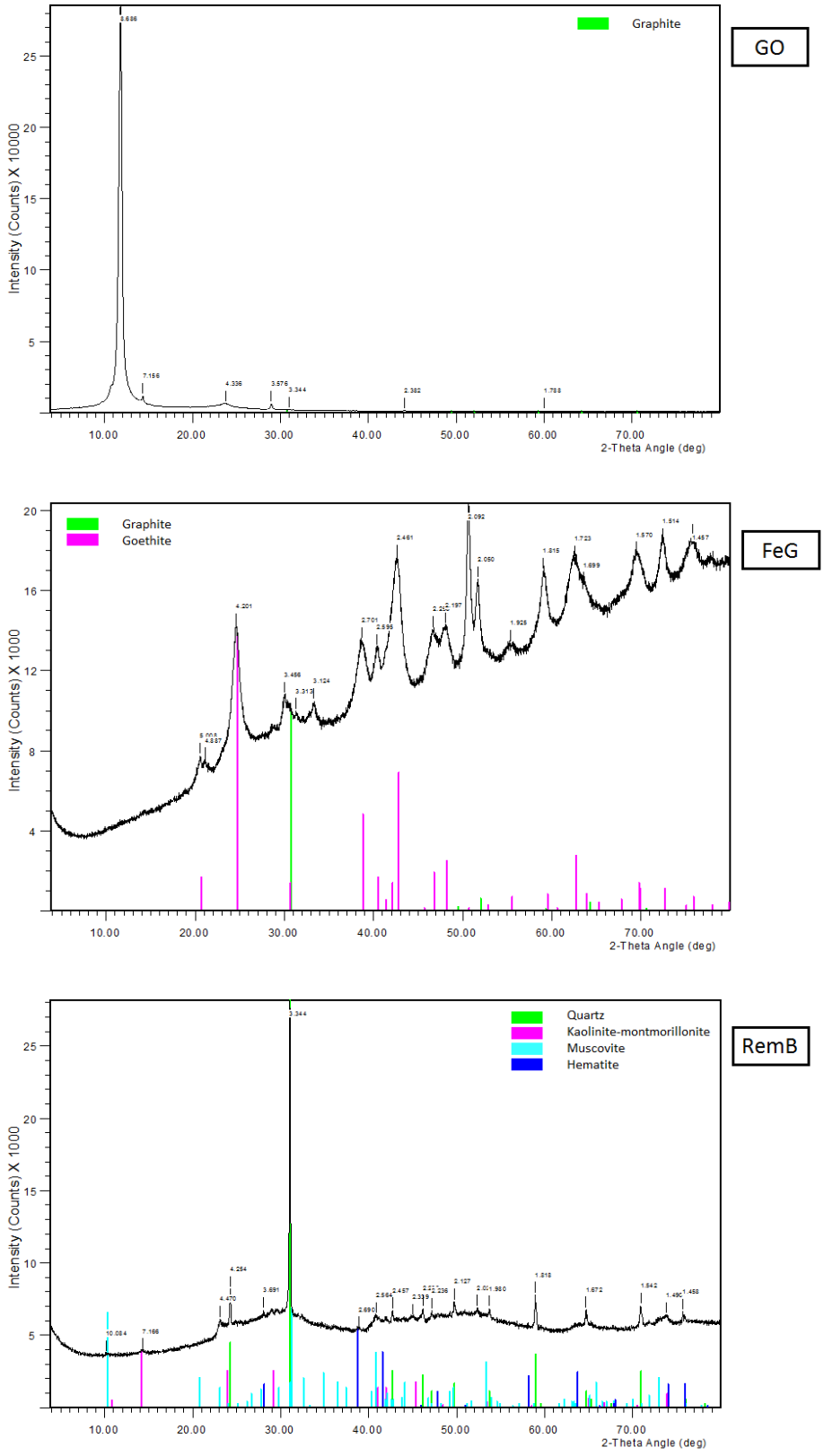

Figure S7. Methylene blue standard calibration curve (664 nm) and sample analysis for measurement of surface areas of adsorbents graphene oxide (GO), Fe-oxide-modified reduced-GO (FeG) and RemBind™ (RemB).

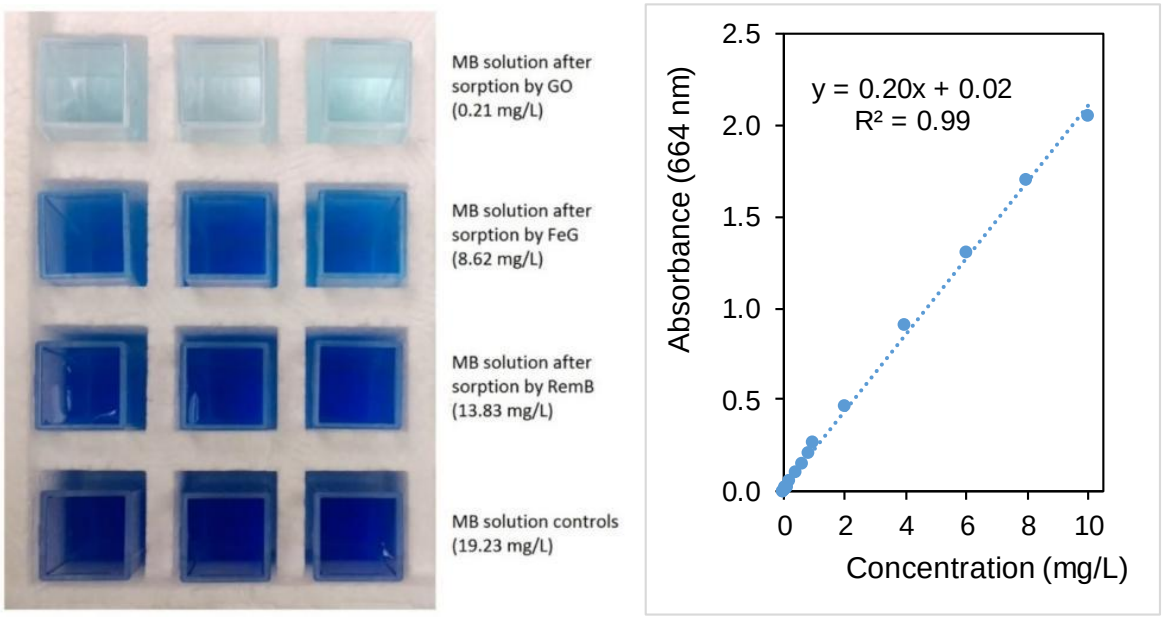

Figure S8. Surface zeta potential measurements of graphene oxide (GO), Fe-oxide-modified reduced-GO (FeG) and a commercial adsorbent, RemBind™ (RemB), as a function of pH (25 °C) to determine point of zero charge (PZC).

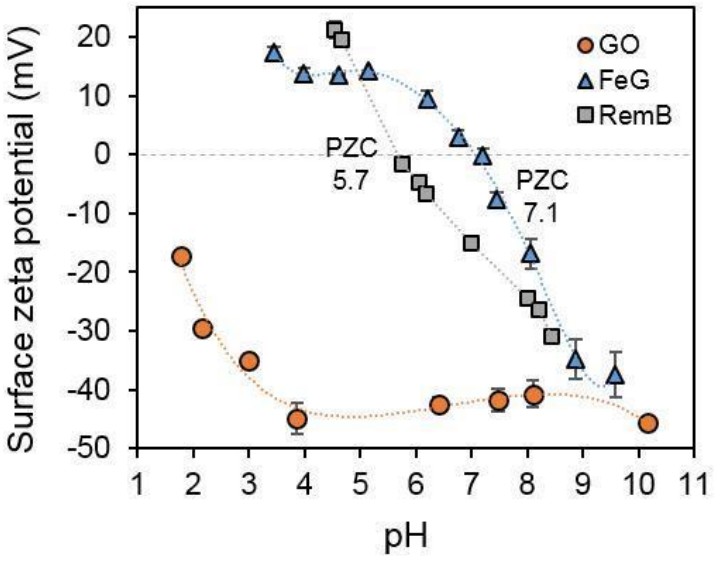

Figure S9. Dose-response curves for soil microbial nitrification in the presence of (a) arsenate at 0.1 - 2500 mg/kg, (b) cadmium at 0.1 - 1000 mg/kg, (c) PFOA at 0.1 - 40 mg/kg and (d) PFOS 0.08 - 224 mg/kg soil. Blue vertical lines show the 50% effect concentration (EC 50).

(a)

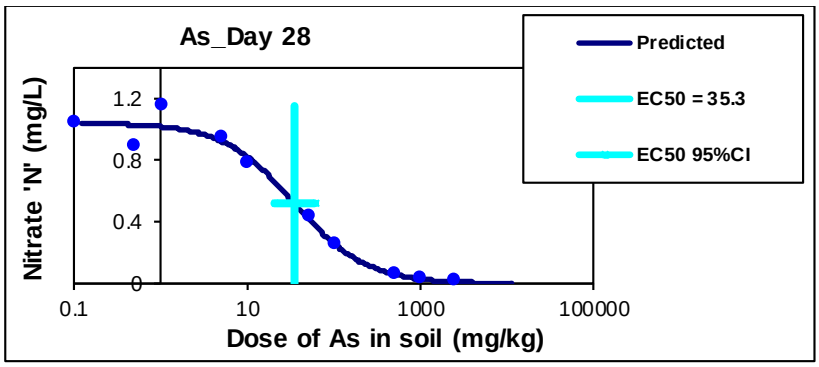

(b)

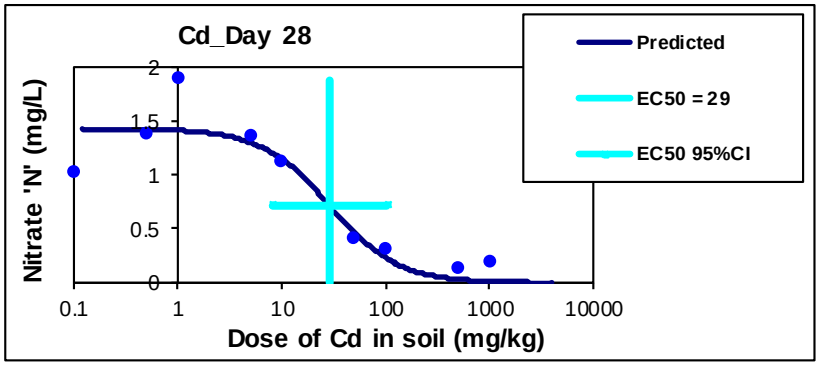

(c)

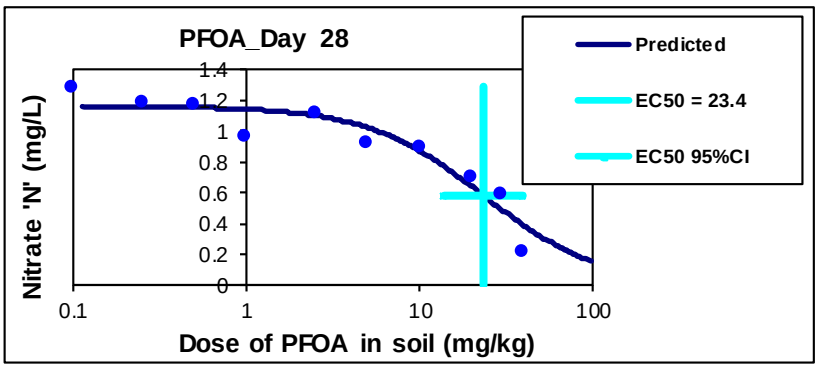

(d)

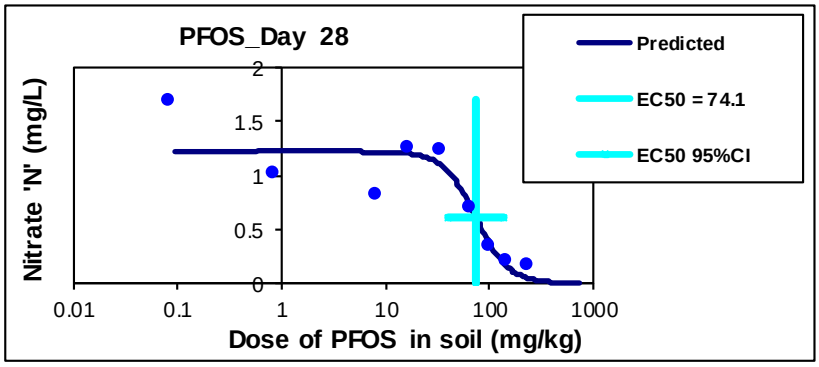

Table S3. Percentage reduction in 'bioaccessible' contaminant-fractions in remediated soil, compared to contaminated control soils. Contaminant-treatments include singly-contaminated soils (As, Cd, PFOA and PFOS), as well as a 'cocktail' treatment comprised of the 4 contaminants mixed together. Adsorbents include 5% weight doses of graphene oxide (GO), Fe-oxide-modified reduced GO composite (FeG), RemBind™ (RemB), and a 1:1 GO+FeG treatment.

Performance was colour-coded as follows:

- Green (bold text) (80 – 100% reduction in bioaccessibility)
- Yellow (underlined text) (0 – 80% reduction in bioaccessibility)
- Red (italicised text) (increased bioaccessibility)
-

Percent (%) reduction in 'bioaccessible' contaminant fractions				
Contaminant	GO	FeG	RemB	GO+FeG
As	<u>36.3</u>	**98.9**	**98.7**	**97.1**
Cd	*-118.9*	*-30.0*	<u>63.3</u>	*-114.6*
PFOA	<u>43.8</u>	**89.7**	**98.3**	**84.8**
PFOS	**85.5**	**97.6**	**99.9**	**96.2**
Cocktail As	<u>39.5</u>	**99.5**	**99.5**	**97.8**
Cocktail Cd	*-575.0*	*-253.9*	*-4.3*	*-520.6*
Cocktail PFOA	<u>48.2</u>	**87.1**	**97.1**	**84.4**
Cocktail PFOS	**83.9**	**97.0**	**99.7**	**96.7**

CHAPTER 7. Summary and Future Research Directions

1. Summary of Thesis Outcomes

Recent and historical development activities have caused an accumulation of various contaminants in the soil environment. While some contaminants degrade, others resist breakdown and persist in the environment. Contaminated sites contain a mix of contaminants (i.e. metals, metalloids, cations, anions, organic contaminants), and a single process may not suffice for adequate remediation of a site. Hence, there is a need to develop technologies that can target multiple contaminant classes simultaneously. Remediation can be achieved through degradation, removal or immobilisation of contaminants. *In situ* processes like adsorption (which rely on lowering contaminant mobility and bioavailability or bioaccessibility to alleviate toxicity) are generally favoured as they are less invasive and less energy intensive. Graphene-based materials (GBMs) have a versatile surface chemistry and are great candidates for development of multi-functional adsorbents. The primary focus of this research was to investigate the use of GBMs for adsorptive remediation of different soil contaminants.

The model contaminants chosen for the work were arsenate (As; an anionic metalloid), cadmium (Cd; a cationic metal) and two perfluorinated alkyl substances (PFASs) of current interest, perfluorooctanoic acid (PFOA) and perfluorooctane sulphonate (PFOS) – each of these are persistent contaminants, resistant to breakdown, and thus are ideal for remediation-testing *via* adsorption.

1.1. Synthesis of GBMs and characterisation of adsorbents successfully completed

Two GBMs were synthesised in the laboratory using raw graphite – graphene oxide (GO; an oxidised derivative of graphene with a myriad of oxygen functional groups), and an iron-modified graphene composite (FeG; a reduced-GO composite containing attached goethite mineral nanoparticles). Due to differences in their surface chemistry and active sorption sites, they were expected to bind different contaminants depending on the mechanisms involved. Performance of the GBMs was benchmarked against a commercial adsorbent, RemBind™ (RemB) which is a powdered mixture of activated carbon, amorphous Al-hydroxide, kaolin clay and other proprietary additives. Due to the mixed mineral and carbonaceous nature of FeG and RemB, they were expected to be more versatile adsorbents compared to GO. The morphology and surface properties of the adsorbents were characterised using a variety of microscopy and spectroscopy-based techniques (summarised in Table 1).

Table 1. Characteristics of adsorbents.

Adsorbent	Elements (EDX)	Surface area (m^2/g)	PZC (pH)	XRD structure
GO	C, O	435	<1.5	Oriented 'platy' phase with a unit cell of 7.16 Å
FeG	C, O, Fe	242	7.1	Goethite mineral (α-FeOOH) crystalline phase
RemBind™	C, O, Al, Si	123	5.7	Dominant amorphous activated-C phase with aluminosilicate clays

1.2. Successful demonstration of multiple sorption of As and Cd using GBMs

Positively-charged FeG showed a strong affinity to bind anionic As, whereas negatively-charged GO showed a strong affinity to bind cationic Cd. At lower As-concentrations (≤ 250 µM), FeG displayed greater As-sorption compared to RemB, while at higher concentrations (≥ 500 µM), sorption by RemB was greater. Amounts of Cd adsorbed by GO were superior to that adsorbed by RemB. Sorption was pH dependent: an increase in pH promoted Cd-sorption and decreased As-sorption. GO displayed excellent Cd sorption even in acidic conditions, which is unlike that observed with typical adsorbents like clays or zeolites that only weakly sorb Cd at low pH values. The maximum amounts of contaminant adsorbed by GO and FeG, were 782 µmol Cd/g and 408 µmol As/g, respectively. At environmentally relevant concentrations, competition by phosphate did not significantly affect As sorption, whereas competition by Ca strongly suppressed Cd sorption. Sorption was influenced by the charge properties and surface functional groups of the adsorbents. In the case of FeG and RemB, As binding was attributed to ligand-exchange mechanisms with hydroxyl groups on the mineral phases of the adsorbents – goethite and alumina, respectively. Below the point of zero charge, electrostatic interactions may also play a role in binding As. In the case of Cd sorption by GO and RemB, electrostatic interactions were identified as the main binding

mechanism. Co-occurrence of As and Cd at a contaminated site would usually require opposing treatment strategies due to their differing physico-chemical properties. A mixture of GO and FeG, however, was successful in simultaneous sorption of Cd and As from co-contaminated model solutions, as well as a natural contaminated dam water sample, with greater sorption than the commercial mixed-mode adsorbent, RemB. The study highlighted the potential application of GBMs in simultaneous management of multiple contaminants (cations and anions).

1.3. Successful demonstration of sorption of PFOA and other PFASs using GBMs

Sorption of PFOA by FeG and RemB (> 90%) was much greater than sorption by GO (60%). Sorption by FeG and RemB were largely unaffected by variations in pH and ionic strength, indicating that binding was predominantly controlled by non-electrostatic forces. In addition to hydrophobic interactions of the carbon-fluorine PFOA chain with the carbonaceous phase of the adsorbents, the role of combined mineral phases in FeG and RemB in binding PFOA *via* ligand exchange mechanisms was apparent. Sorption by GO was hindered at increased pH, which was attributed to an increase in the negative charge of the GO surface, increasing repulsion of the PFOA anion, and reducing scope for hydrophobic interactions. Performance did not correlate with surface area, highlighting the role of surface chemistry. Desorption of adsorbed PFOA was greatest in polar organic solvents like methanol, rather than water, toluene or hexane, providing an indication of binding strength and reversibility from an environmental-partitioning perspective. For instance, precipitation from rainfall events is unlikely to desorb PFOA bound by FeG and RemB, reducing concerns for subsequent leaching into subsurface soils or groundwater. However, at a waste disposal or landfill site, where PFASs may co-occur with polar organic solvent waste from accidental spills, increased PFOA remobilisation is likely, consequently increasing bioavailability to plants and organisms. Treatment of a field water sample contaminated with a variety of PFASs showed that FeG and RemB showed excellent sorption, particularly of PFOS, as well as other sulphonate- and carboxylate-PFASs, and fluorotelomers. A chain-length effect was observed, where greater sorption was detected as chain length increased; increase in the C–F chain length decreases the solubility and increases hydrophobicity of PFASs, allowing stronger hydrophobic interactions with the adsorbents. Successful sorption of a range of PFASs from a contaminated field sample, particularly in the case of FeG and RemB, highlight the potential of using these adsorbents for remediation of PFAS-contaminated waters and soils. Iron-mineral-functionalisation of GO enhanced the amount of PFOA adsorbed (by 30%) as well as binding strength, highlighting the advantage of combining mineral and C-phases in adsorbents to provide multiple modes of binding.

1.4. PFOA sorption-losses observed on laboratory-ware

During experimental work with ^{14}C-PFOA, observations were made relating to the losses of PFOA onto common laboratory ware that were contradictory to those reported in the published literature and in USEPA protocols; i.e., losses observed on polyproplylene (PP) laboratory ware were remarkably higher than on glass. These losses were further explored by testing sorption of ^{14}C-PFOA onto different tube-types (PP, glass, polystyrene and polycarbonate) in varying pH, ionic strength and concentration conditions. In all cases, PP tubes showed significantly lower recoveries compared to other tested materials. Glass tubes showed the best recoveries, contrary to what is implicit in most of the PFAS-related literature. Sorptive losses on a variety of filter-membrane types were also tested. Recoveries of PFOA ranged from 70-75% at best (e.g. PP, regenerated cellulose, glass-fibre and PVDF membranes) to 21% at worst (e.g. nylon membrane), demonstrating that that filtration can be a major source of error, leading to an underestimation of dissolved concentrations. This study drew attention towards potential analytical bias that can occur due to sorptive losses during routine procedures, and highlighted the importance of accounting for such losses and testing the suitability of chosen laboratory ware for specific PFAS-analytes of interest prior to experimental use.

1.5. Successful demonstration of mixed soil remediation of As, PFOA, PFOS

Finally, the remediation efficiency of GBMs was tested for *in situ* application in a soil matrix, using singly-contaminated soils, as well as a mixed/cocktail contaminant treatment containing As, Cd, PFOA and PFOS. Reduction in contaminant bioaccessibility, and effects on microbial soil nitrification were used as indicators of remediation efficacy by comparing treated soils with the unremediated contaminated soils. Particularly, the mixed-mode adsorbents, FeG and RemB greatly reduced bioaccessibility of As, PFOA and PFOS (but not Cd) by 84 – 100% from both singly-contaminated and co-contaminated soils, showing potential for their *in situ* application in soil to reduce soluble contaminant concentrations. Similarly, GO reduced bioaccessibility of As, PFOA and PFOS by 36 – 86%. Sorption of PFOS was greater than PFOA in all cases, as observed in the previous study. In the case of Cd-contaminated soils, while RemB reduced bioaccessibility by 63%, none of the GBMs were successful in binding Cd. In fact, GO increased Cd-bioaccessibility by 2 fold compared to the unremediated control. This was attributed to the reduced soil pH conditions observed in the soils treated with GBMs despite the addition of lime to correct GBM-induced acidification. Low pH mobilised Cd^{2+} ions otherwise retained by negatively-charged binding sites (e.g. organic matter, clay) in soil. Lowered pH may also have led to dissolution of the

added lime, increasing the concentration of soluble Ca^{2+} in the soil, which could compete with Cd^{2+} for sorption sites on the adsorbents' surface, as previously demonstrated.

In singly-contaminated soils, the toxic effects of the contaminants to soil microbial nitrification function were alleviated over the duration of the experiment, either due to ageing of contaminants, or increased tolerance of the microbes. However, the added stress from the co-occurrence of multiple contaminants severely inhibited the nitrification response of the 'cocktail' contaminated soil to only 6% of the nitrification observed in control uncontaminated soils. Considering the dose-dependent effect of contaminants on nitrification, remediation, (i.e. addition of the adsorbents) was expected to restore nitrification due to reduced contaminant bioaccessibility. However, a severe inhibition of soil nitrification ranging from 55 – 99% was observed in all GBM-treated soils, compared to unremediated contaminated soils. This was attributed to lowering of soil pH to levels below those which are ideal for nitrification. While remediation with RemB did not affect nitrification in singly-contaminated soils, it restored nitrification in the 'cocktail' contaminated soil from 6% to 91% of the nitrification in the uncontaminated control soil, due to reduced bioaccessibility of all the contaminants, thus alleviating toxic effects of the contaminant-mixture. RemB did not suffer from the soil acidification displayed by the GBMs. It has been suggested in the published literature that water can react with the C-C bonds in the basal graphene structure, gradually generating protons at the GO/water interface. The inherent acidity of GBMs presents challenges for *in situ* applications unless this acidity can be neutralised.

Overall, the mixed mineral and carbon-based adsorbents – FeG and RemB – showed great promise for *in situ* soil remediation based on large reductions in the solubility of multiple inorganic and organic contaminants in soil, provided acidification induced by the GBMs can be rectified. They provided pathways for binding *via* multiple mechanisms – i.e., ligand exchange and inner-sphere complexation of As with the goethite phase, hydrophobic interactions of PFOA and PFOS at the graphitic plane, as well as ligand-exchange of the carboxylate and sulphonate head groups of PFOA and PFOS. A drawback is the inherent acidity in the GBMs that could impede efforts to reduce the solubility of cationic metal contaminants in soil, and impact soil microbial function. Hence their application *in situ*, for soil remediation, requires that acidity generated by the materials is neutralised.

In summary, in this thesis, the outcomes of research on the development and use of graphene-based adsorbents for adsorptive remediation of multiple contaminants were presented and challenges discussed. Recommendations for future research in this area are provided below.

2. Future Research Recommendations

To further investigate the data and results from this project, address issues raised in the work, and to advance our understanding of the use of GBMs for *in situ* soil remediation, future work in the following areas are recommended:

2.1. Further optimisation of GBMs for improved performance

Further optimisation or functionalisation of the GBMs could be explored to improve sorption performance. For instance, GO displayed a very high sorption capacity for Cd in an aqueous environment, even at extremely low pH, however this was not the case in the soil matrix. The binding of Cd by GO was determined to be weak, controlled simply by charge-based interactions, making it possible for Ca (from lime dissolution) to compete for binding spots on the GO surface, inhibiting Cd-sorption. If the binding of Cd-binding was more specific or covalent, the impacts of Ca-competition may be reduced. Certain thiol or sulfhydryl functional groups can bind Cd more strongly; developing functionalised graphene materials with such groups (e.g., by using mercaptobenzothiazole) may improve the strength of Cd-binding, making them better adsorbents than GO for use in soil. In the case of FeG, by increasing the loading rates of Fe during the synthesis procedure, the amount of goethite minerals attached onto the graphene basal surface can be increased, which could lead to an increase in the amount of As, PFOA or PFOS adsorbed, improving performance of FeG, potentially surpassing the sorption capacity of the commercial adsorbent, RemB.

2.2. Identify specific binding mechanisms through molecular techniques

A greater level of understanding of the binding mechanisms can be gained through sophisticated characterisation techniques of the adsorbent-contaminant complexes. For example, X-ray photoelectron spectroscopy (XPS) can provide information on the chemical and electronic state of the elements comprised in the material, as opposed to merely elemental composition. Synchrotron based techniques like X-ray absorption spectroscopy (XAS) analyses can provide detailed information on electronic structure and symmetry of different elements of interest, as well as types and number of ligands comprised in the structure. For instance, local molecular structural information specifically around the iron (Fe) component from the goethite minerals in FeG can be obtained to ascertain the nature of As-binding. Similarly, closer scrutiny of the binding associated with the negatively charged functional groups of GO could provide insights into how affinity to Cd differs from affinity to Ca or other cations, and its implications for competitive sorption.

2.3. Understand long-term environmental fate of adsorbent-contaminant complexes

Further studies to gain insights into the fate of the adsorbent-contaminant complexes in the soil environment would be useful for their practical applicability *in situ*. Once adsorbed, the contaminants are not considered to be bioaccessible. But in the presence of changing environmental conditions, there is potential for dissociation of the adsorbed contaminants to occur, causing re-mobilisation of the contaminants; bioaccessibility may increase gradually over a long period of time. After sorption, the adsorbent-contaminant complex in soil could be exposed to 'ageing' conditions to simulate its fate in the environment by exposing to a day/night photoperiod and temperature conditions. Measurement of soluble contaminant concentrations over various periods of time ranging from a few months to a couple of years could be made to monitor contaminant desorption. Some additional variables may include different soil-types and exposure to a range of temperature and UV radiation conditions.

2.4. Assessment of remediation using other soil ecological endpoints

Soil-based experiments using additional soil ecological and ecotoxicological endpoints could be conducted as a means of further assessing the possibility of using novel GBMs *in situ* in soil for remediation, and identifying any risks involved. These could involve plant germination experiments, or plant-uptake experiments, where phytoavailability of contaminants and bio-concentration factor may be measured before and after soil remediation. Soil respiration, soil microbial diversity, and a variety of soil microbial processes may also be evaluated. Soil invertebrates such as *Caenorhabditis elegans* or *Eisenia fetida* may be used as additional indicators of efficacy of soil remediation; endpoints measured would include growth, mortality, as well as feeding and reproductive behaviour. The use of such biological indicators, in addition to physiochemical measurements, will provide a more rounded outlook on the potential of using GBMs successfully for *in situ* soil remediation.